

**EUROLINK S.C.P.A**

Sub-test 1 Section Model Tests for the  
Messina Strait Bridge

FORCE 110-25465 Rev. 1/2010-06-25



**Project No. and Title of Report:**

**FORCE 110-25465**  
**Sub-test 1 Section Model Tests for the**  
**Messina Strait Bridge**

**Client:**  
EUROLINK S.C.P.A

**Client's Ref.:**  
Allan Larsen, COWI A/S

**Author(s):**  
Søren V. Larsen

**Date:** 2010-06-25

**Approved by:** 

Revision	Description	By	Checked	Approved	Date
1	Client's comments included	SVL	SQE	CRS	2010-06-10
A	Issued for Client's Comments (PDF version)	SVL	AaD/SGe	CRS	2010-06-10

**Keywords:**

Suspension Bridge.  
 Section Model Tests.  
 Static Load Coefficients.  
 Stability Tests.  
 Vortex Shedding Tests.

**Classification:**

- Open  
 Internal  
 Confidential

**LIST OF CONTENTS:**

- 1. Introduction ..... 1
- 2. Summary and Conclusions ..... 2
- 3. Model Design ..... 6
  - 3.1 Prototype Structure ..... 6
  - 3.2 Scaling Parameters ..... 7
  - 3.3 Section Model Design ..... 7
    - 3.3.1 Configurations ..... 8
    - 3.3.2 Verification of Pressure Loss Coefficients ..... 10
- 4. Wind Tunnel and Flow Conditions ..... 12
- 5. Wind-Tunnel Test Programme ..... 14
- 6. Static Tests ..... 15
  - 6.1 Static Force Coefficients Definition ..... 15
  - 6.2 Results ..... 17
- 7. Dynamic Tests ..... 24
  - 7.1 Model Configuration ..... 24
  - 7.2 Stability Tests ..... 25
  - 7.3 Damping Tests ..... 29
  - 7.4 Vortex Shedding Tests ..... 30
- 8. References ..... 32

**APPENDICES:**

- Appendix A : Drawings.
- Appendix B : The Boundary-Layer Wind Tunnel II.
- Appendix C : Damping Documentation.
- Appendix D : Stability Tests – Response Plots.
- Appendix E : Vortex Shedding Tests – Response Plots.

## 1. Introduction

FORCE Technology was commissioned by EUROLINK S.C.P.A to conduct an investigation of the wind effects on the bridge deck of the Messina Strait Bridge. COWI A/S acted as the Client's representative. The present section model tests are referred to as Sub-test 1.

The Messina Strait Crossing is a suspension bridge with a main span of 3300 m. The deck is 3666 m long, including the two suspension side spans, and approximately 60 m wide. The structure is composed of three box sections - two lateral ones for the roadway deck and a central one for the railway tracks. The deck's roadway section has three 3.75 m wide lanes in each direction. The railway section has two tracks and two lateral pedestrian sidewalks.

The height of the two towers is 383 m to allow for a navigation clearance with a minimum height of 65 m. The bridge's suspension system consists of two pairs of steel cables each with a diameter of 1.24 m and the total length between the anchor blocks is 5300 m.

The present report describes the section model tests performed to assess the static load coefficients and the aerodynamic stability for the bridge deck for 7 geometrical configurations of the road deck. The 7 configurations were investigated in a group of tests referred to as *Optimisation of Configuration* or *Optimisation Tests*. Based on these initial tests, an optimum configuration was selected and this configuration was tested in a group of tests referred to as *Verification of Optimum Configuration* or *Verification Tests*.

The section model tests were performed on a 1:80-scale section model of the bridge deck in FORCE Technology's 2.6 m wide boundary-layer wind tunnel. The tests were conducted at FORCE Technology in May 2010.

The work was performed according to the Agreement between FORCE Technology and Eurolink s.c.p.a. (with reference to FORCE Technology's quotation 110-25465 dated 2010-04-21).

## 2. Summary and Conclusions

This report presents the results of the wind-tunnel tests conducted to establish aerodynamic data for various configurations of the bridge girder for the Messina Strait Bridge. A 2.55 m long section model built at a geometric scale of 1:80 for previous investigations was rebuilt for the present tests. The model was tested in smooth flow (a few verification tests were conducted in turbulent flow) in FORCE Technology's 2.6 m wide Boundary-Layer Wind Tunnel.

The tests were grouped into two:

- 1) Optimisation of configuration (optimisation tests)
- 2) Verification of optimum configuration (verification tests)

All tests in this series were conducted with the road girders having 2% outward slope.

For the optimisation tests, the model represented the main aerodynamic features of the deck cross-section with the following configurations:

- C1 Deck without safety screens, with solid railway screens and without rail walkway soffit plates
- C2 Deck without safety screens, with solid railway screens, with rail walkway porous soffit plates
- C3 Deck without safety screens, with solid railway screens, with rail walkway solid soffit plates
- C4 Deck with inner safety screens, with solid railway screens, with rail walkway soffit plates (porous)
- C5 Deck with inner and outer safety screens, with solid railway screens, with rail walkway soffit plates (porous)
- C6 As C4 but without solid railway screens
- C7 As C2 but without solid railway screens

Wind screens, roadway crash barriers and railway side platforms were present in all configurations.

For these 7 configurations, the static wind load coefficients and their variations with angle of wind incidence were established from  $-10^\circ$  to  $+10^\circ$  in steps of  $1^\circ$ . Further, the aerodynamic stability of deck was determined at  $0^\circ$ . All these tests conducted for the optimisation of the section, were conducted in smooth flow.

Based on the tests described above, configuration C5 was chosen as the optimum configuration by the Client's representatives. The aerodynamic characteristics of the optimum configuration was verified through stability and damping tests ( $-4^\circ$ ,  $0^\circ$  and  $+4^\circ$ ), static coefficients from  $-10^\circ$  to  $+10^\circ$  in steps of  $1^\circ$  at three wind speeds and vortex shedding tests at  $0^\circ$ . All verification tests were conducted in both smooth and turbulent flow.

The main findings are summarised in the following. The various configurations are shown in Section 3.1.

**Static Tests**

The static force coefficients at 0° and their variations with angle of wind incidence (first derivatives) are shown in Table 2.1 and Table 2.2. Figure 6.3 through Figure 6.6 show plots of all the determined coefficients for the various configurations and test conditions, with the drag and lift coefficients,  $C_d$  and  $C_l$ , being fixed in a wind coordinate system, and  $C_x$  and  $C_z$  being body fixed coefficients, see Section 6.

The static coefficients from the optimisation tests are listed in the following table.

		<b>C1</b>	<b>C2</b>	<b>C3</b>	<b>C4</b>	<b>C5</b>	<b>C6</b>	<b>C7</b>
$C_d$	(0°)	0.105	0.104	0.104	0.106	0.105	0.105	0.101
$C_l$	(0°)	-0.059	-0.053	-0.039	-0.113	-0.082	-0.133	-0.084
$C_m$	(0°)	0.010	0.011	0.013	-0.008	0.005	-0.009	0.013
$\frac{dC_d}{d\alpha}$	(-1° to +1°)	-0.03	0.01	0.01	0.00	-0.05	0.02	0.00
$\frac{dC_l}{d\alpha}$	(-1° to +1°)	-0.06	0.02	0.11	0.30	0.36	0.55	0.69
$\frac{dC_m}{d\alpha}$	(-1° to +1°)	0.20	0.19	0.19	0.32	0.17	0.31	0.23

Table 2.1. Static aerodynamic force coefficients and their slopes (based on a deck width of B= 60.74 m) configurations 1 to 7.

In the verification tests, the static coefficients were established at three wind speeds (12 m/s, 15 m/s and 18m/s, model scale). The static coefficients from the verification tests are listed in the following table.

		Smooth U=12m/s	Smooth U=15m/s	Smooth U=18m/s	Turbulent U=12m/s	Turbulent U=15m/s	Turbulent U=18m/s
$C_d$	(0°)	0.105	0.105	0.106	0.118	0.119	0.119
$C_l$	(0°)	-0.082	-0.083	-0.084	-0.090	-0.091	-0.091
$C_m$	(0°)	0.005	0.005	0.005	0.005	0.004	0.004
$\frac{dC_d}{d\alpha}$	(-1° to +1°)	-0.05	-0.01	0.00	-0.04	-0.04	-0.06
$\frac{dC_l}{d\alpha}$	(-1° to +1°)	0.36	0.37	0.43	1.07	1.09	1.13
$\frac{dC_m}{d\alpha}$	(-1° to +1°)	0.17	0.19	0.20	0.17	0.19	0.20

Table 2.2. Static aerodynamic force coefficients and their slopes (based on a deck width of B= 60.74 m) for the optimum configuration – C5.

### Stability Tests

For the optimisation tests, the aerodynamic stability of the bridge girder was investigated for an angle of wind incidence of 0° in smooth flow. Following this, the aerodynamic stability of the optimum configuration (C5) was investigated for angles of wind incidence of -4°, 0° and +4° in smooth and turbulent flow. The estimated critical wind speeds for onset of aerodynamic instability are listed in the following table.

Configuration	Flow	Angle	$U_{red,cr}$ [ $U_{cr}/(f_t \cdot B)$ ]	$U_{cr}$ [m/s]
C1	Smooth	0°	>24.1	>122
C2	Smooth	0°	23	116
C3	Smooth	0°	23	116
C4	Smooth	0°	17.8	90
C5	Smooth	0°	>24.5	>124
C6	Smooth	0°	18.6	94
C7	Smooth	0°	22.6	114
C5	Smooth	-4°	>22.4	>113
		0°	>24.4	>123
		+4°	>24.5	>124
C5	Turbulent	-4°	>15*	>76*
		0°	>24.5	>124
		+4°	>24.2	>122

Table 2.3. Estimated aerodynamic stability limits as reduced wind speed [ $U_{cr}/(f_t \cdot B)$ ] and full-scale wind speed [m/s].

\*For the configuration C5 in turbulent flow at -4°, the measured displacement and rotation are contaminated by the model hitting the wind tunnel wall from  $U_{red} = U/(f_t \cdot B) = 15$  and higher. This was caused by the large negative displacement in combination with the buffeting response.

In connection with stability tests, the aerodynamic damping was measured at two wind speeds corresponding to 54 m/s and 75 m/s, full-scale, see Section 7.3.

### Vortex Shedding Tests

Finally, the vortex induced response has been investigated in smooth and turbulent flow for the optimum configuration – C5. In smooth flow a small torsional response peak was observed at a reduced wind speed ( $U/(B \cdot f_t)$ ) of approximately 1.0. The recorded response peak had an rms amplitude of 0.075°. Vertical vortex-induced oscillations were not observed in smooth flow. In turbulent, no vertical or torsional vortex induced response was detected.



### 3. Model Design

#### 3.1 Prototype Structure

The Messina Strait Crossing comprises a suspended main span of 3300 m. The total length of the bridge is 3666 m. The bridge deck comprises three closed box girders and the overall deck width is approximately 60 m.

An elevation of the prototype structure is shown in Figure 3.1.

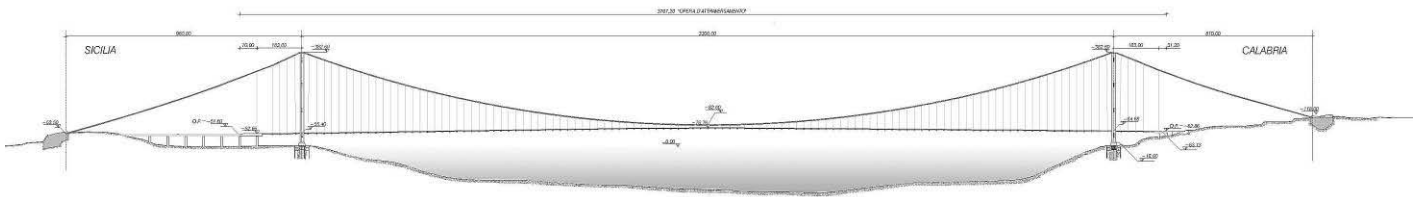


Figure 3.1 Elevation of the Messina Strait Crossing.

Figure 3.1 shows the cross section of the prototype bridge deck and its main dimensions.

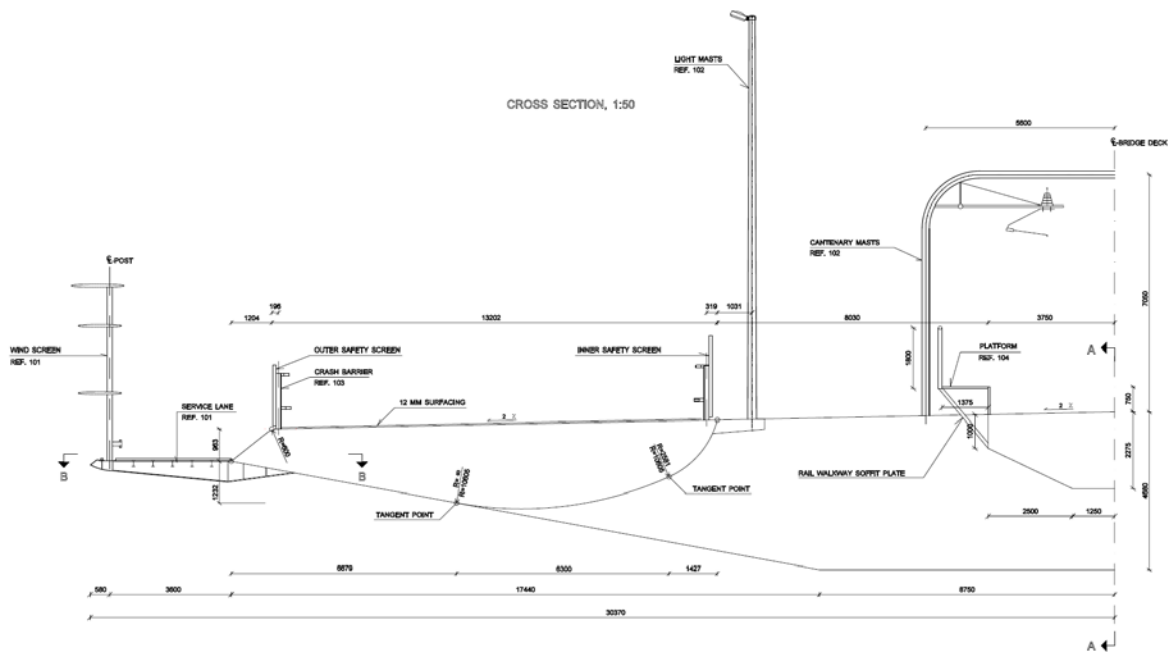


Figure 3.2. Cross-section of prototype bridge deck.

In the tests, the effect of the outer safety screens, inner safety screens, railway soffit plate and a solid railway screens was investigated in various combinations.

### 3.2 Scaling Parameters

A combination of geometrical, mass and stiffness considerations resulted in the selection of a 1:80 geometrical scale for the section model of the Messina Strait Bridge deck, see [1].

### 3.3 Section Model Design

The 1:80 geometrical scale section model of the bridge deck was built with the properly scaled outer shape of the prototype structure.

The model used for the present tests was built of partly the same components as those used in earlier tests in December 2009 and January 2010, see [3]. The actual road box girder cross section had been marginally modified since the earlier design, but it was decided, in agreement with the Client's representative, to re-use these model parts. New cross beams were manufactured to provide the 2% outward slope. Figure 3.3 shows the comparison between the actual bridge deck cross section (blue) and that represented in the model (red). Completely new deck equipment (wind screens, crash barriers, safety screens, soffit plated and walkway screens) were manufactured to match the new design.

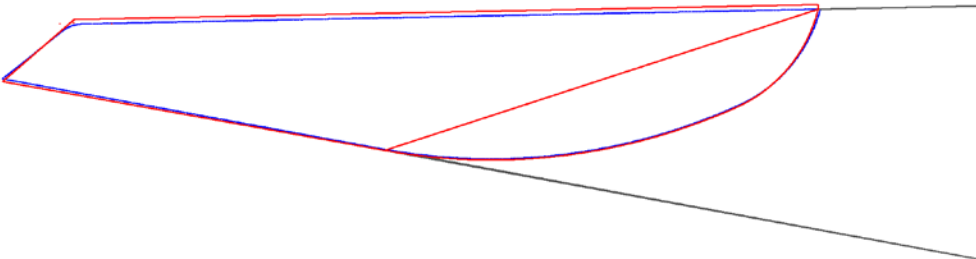


Figure 3.3 Comparison between the actual bridge roadway beam (blue) and the one represented in the model (red).

All the details present on the bridge deck and the wind screens have been produced by means of rapid prototyping. The design of all these elements reproduce the main full-scale characteristics and maintain the drag force acting on the cylinders and the pressure loss coefficient through porous screens, see section 3.3.1.

### 3.3.1 Configurations

For the optimisation tests, the model represented the main aerodynamic features of the deck cross-section with the configurations summarized in the table below:

#	Inner Safety Screens (2.4m)	Outer Safety Screens (1.8m)	Soffit Plate	Solid Railway Screen
C1	off	off	off	on
C2	off	off	porous	on
C3	off	off	solid	on
C4	on	off	porous	on
C5	on	on	porous	on
C6	on	off	porous	off
C7	off	off	porous	off

Table 3.1. Summary of Configurations.

The positions of the relevant screens and plates are illustrated in the following figure.

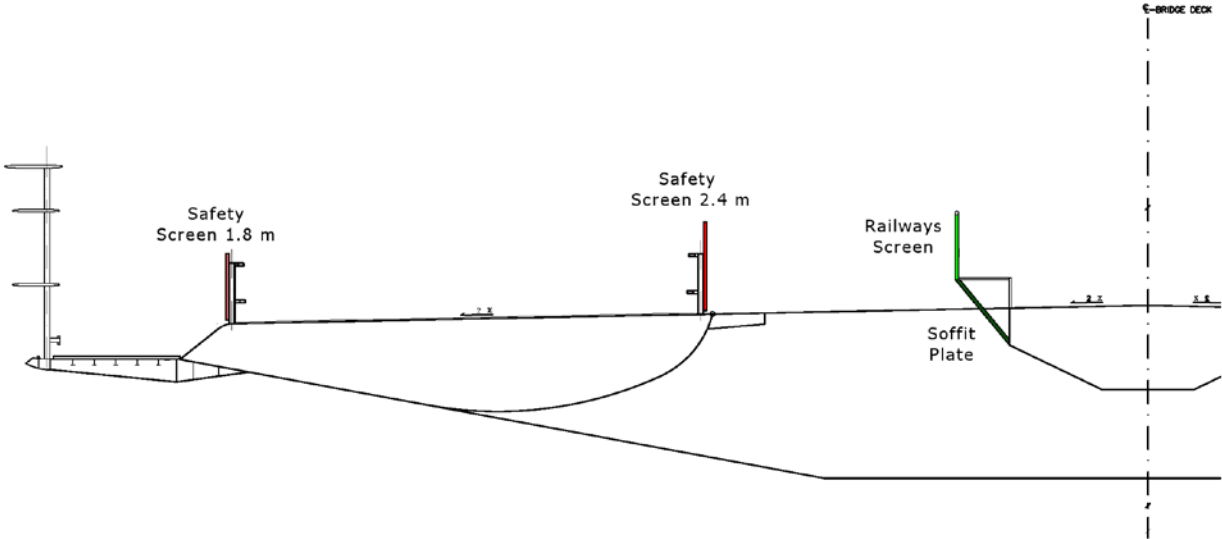


Figure 3.4. Cross-section of prototype bridge deck.

Wind screens, crash barriers and railways platforms were present throughout the tests. In the following the design of various appendages is described.

#### Crash Barrier

The full-scale crash barrier has two horizontal cylinders with a rectangular cross section (160x80 mm) and vertical posts made of HEA 160 profiles with a centre-to-centre spacing of about 1.2 m.

The crash barrier was scaled to preserve the total drag force on the element, i.e. the product of the drag coefficient and the projected area. Manufacturing considerations limit the minimum dimension of each component. Thus, the model crash barrier was designed by lumping the two rectangular cylinders into one with a 1.8x1.8 mm<sup>2</sup> square cross section, placed 14 mm above the

model deck. The number of vertical posts was also reduced in the model, lumping two full-scale posts into one 4 mm wide.

## **Safety Screens**

The full-scale safety screens have the same design of the wind screen, with a net porosity of 55%, and therefore they were scaled assuming the same target provided by the Client for the wind screens, i.e. a loss coefficient equal to 2.7. The target loss coefficient was obtained in model scale with a perforated plate with a porosity of 47% and the diameter of the holes equal to 5.2 mm. In order to match the position of the crash barrier's post, two screen's vertical posts were also lumped into one.

According to the full-scale prototypes, the model screens have different heights for the outer (22.5 mm) and inner (30 mm) plate. The model screen design also included hooks to connect them to the crash barrier's posts at the right positions above the bridge deck. This allowed for an easy and fast change of configuration during the tests.

## **Railway Platform**

The full-scale railway platform comprises a railing, with eleven smaller horizontal circular cylinders and a larger top rail, placed on the edge of an aluminium grating with 80% porosity. In order to maintain the total drag force acting on the railing, it was modelled with a top circular cylinder with a diameter of 1.8 mm and a lower one with a diameter of 1.3 mm. The railing posts number was reduced, lumping three posts into one with a square cross section 2x2 mm.

The scaling principle for the grating was to maintain the full-scale loss coefficient as calculated according to Idelchik [4]. This was obtained by a model grid with a porosity of 77%.

Some of the tested bridge deck configurations included a solid railway screen and a railway soffit plate, either solid or porous. The solid railway screen was produced as a solid fence with the geometrically scaled dimensions and a longitudinal fastener to firmly connect it to the railing.

The soffit plate was modelled to maintain the full-scale loss coefficient of the porous option as calculated according to Idelchik [4]. This scaling procedure lead to a model perforated plate with a porosity of 28% and hole's diameter equal to 5 mm. The solid soffit plate was obtained simply covering the porous option with tape.

## **Wind Screens**

The full-scale wind screen has a complex geometry, with three airfoils separating three strips of net. The vertical posts are supported by an edge beam connected to the bridge deck through steel brackets. The brackets are equally spaced with a centre-to-centre distance of 3.75 m. A horizontal grating with an 80% porosity lean on the brackets. Steel profiles IPE 180 connect the brackets and provide a stable support for the above grating.

The model wind screens outer geometry was scaled according to the drawings provided by the Client. The porosity of the model fence was determined through an experimental analysis (see section 3.3.2 below) to verify that the selected model screen matched the target loss coefficient of 2.7, as required by the Client's specification. According to the scaling approach used in the previous model, the grating was omitted and its porosity was included in the model increasing the dimension of the along-bridge bars.

### 3.3.2 Verification of Pressure Loss Coefficients

The pressure loss coefficient of the perforated panels of the wind screens and safety screens was experimentally documented using a model screen 250 mm x 250 mm, 1 mm thick, with 5.5 mm diameter holes in a square pattern giving approximately 53% porosity, corresponding to the screens used in earlier tests of the Messina Bridge. The test screen was produced by the same rapid prototyping technique and material as the one planned for the model parts, thereby presumably having the same rounding of the edges of the holes, which is a very important parameter.

The test screen was placed in a 250 mm x 250 mm channel, and air was blown through this channel at varying air speed up to 15 m/s in the full channel cross section in order to check the dependency of the pressure drop coefficient with Reynolds Number. The static pressure differential across the screen was measured and normalised by the dynamic velocity pressure measured by Pitot tube to yield the pressure drop coefficient  $C_p$ . Tests were conducted with the screen as produced and with three and four rows of holes blocked such that the measurements represented 53.4%, 49.2% and 47.8% porosity, respectively.

Figure 3.5 shows the measured variation of  $C_p$  with wind speed for the three screens and Figure 3.6 shows  $C_p$  as function of screen porosity at a wind speed of 12 m/s, which is close to the design wind speed in the section model tests.

By extrapolating the results, the porosity of the model screens was chosen at 47%. It should be noted that the screen resistance coefficient is very sensitive to the degree of porosity and the shape of the holes. The model screens have been produced by the same technique as the test screen used for the experimental documentation of the resistance coefficient. However, it has not been possible to accurately verify that the model screens have exactly the same characteristics as the test screen.

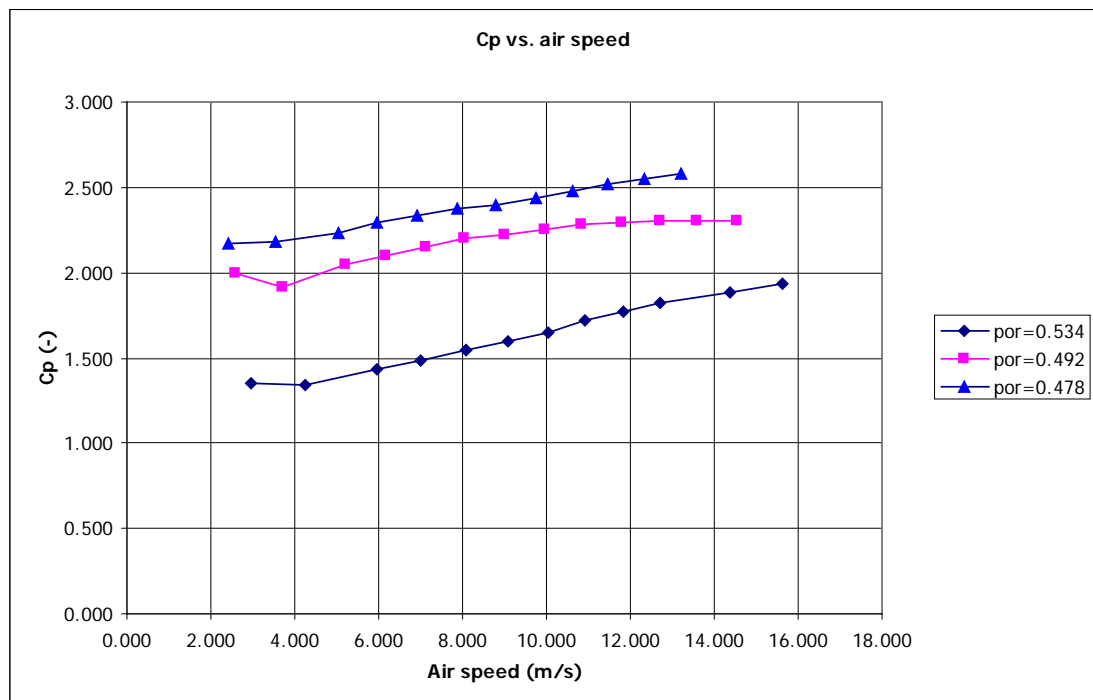


Figure 3.5 Variation of  $C_p$  with wind speed.

The following figure shows the measured values of  $C_p$  for a screen porosity of 53.4%, 49.2% and 47.8%. Since the experimental results showed that the pressure coefficient varies linearly with the screen porosity, the porosity target of 47% was extrapolated from the measurements as corresponding to the required value of  $C_p$  (2.7).

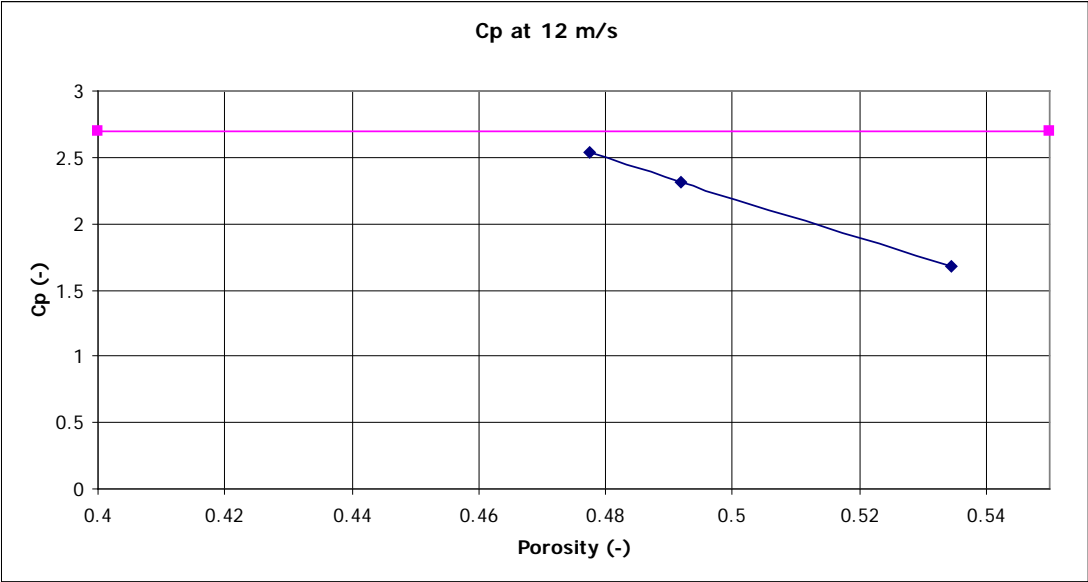


Figure 3.6  $C_p$  as function of screen porosity for  $U=12m/s$ .

## 4. Wind Tunnel and Flow Conditions

The section model tests were conducted in FORCE Technology's 2.6 m wide x 1.8 m high x 21 m long Boundary-Layer Wind Tunnel II. The model was placed 14.5 m downstream of the inlet at the mid height of the wind tunnel. The ceiling of the wind tunnel was adjusted so that it was horizontal throughout the length of the wind tunnel.

The wind-tunnel tests were performed in smooth flow and turbulent flow.

The smooth flow condition corresponds to an empty tunnel (i.e., without exposure upwind of the model). The smooth flow condition has a turbulence intensity ( $I_{u,w}$ ) of approximately 0.5%.

The turbulent exposure was obtained by three spires mounted 1.1 m from the wind tunnel inlet. The spires were 1.8 m high with a tapered width: 0.32 m at the floor to 0.18 m at the wind tunnel ceiling. This exposure resulted in turbulence intensities of approximately 7.5% for  $I_u$  and 7.4% for  $I_w$ . The exposure is shown in Figure 4.1.



Figure 4.1. Turbulence generating spires in the wind tunnel up-wind of the model.

The spectral density function (SDF) of the velocity fluctuation was derived from a long time series recorded at centre position (wind-tunnel centre line), see Figure 4.2 and Figure 4.3.

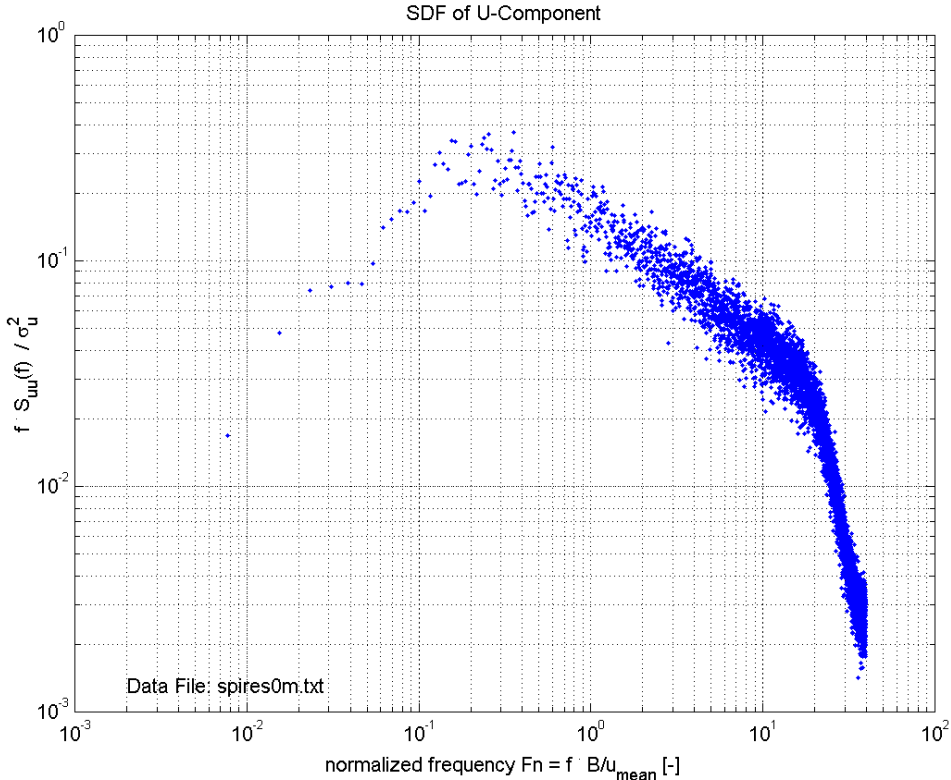


Figure 4.2 U-Component Spectra at Bridge Location (and wind tunnel centre line).

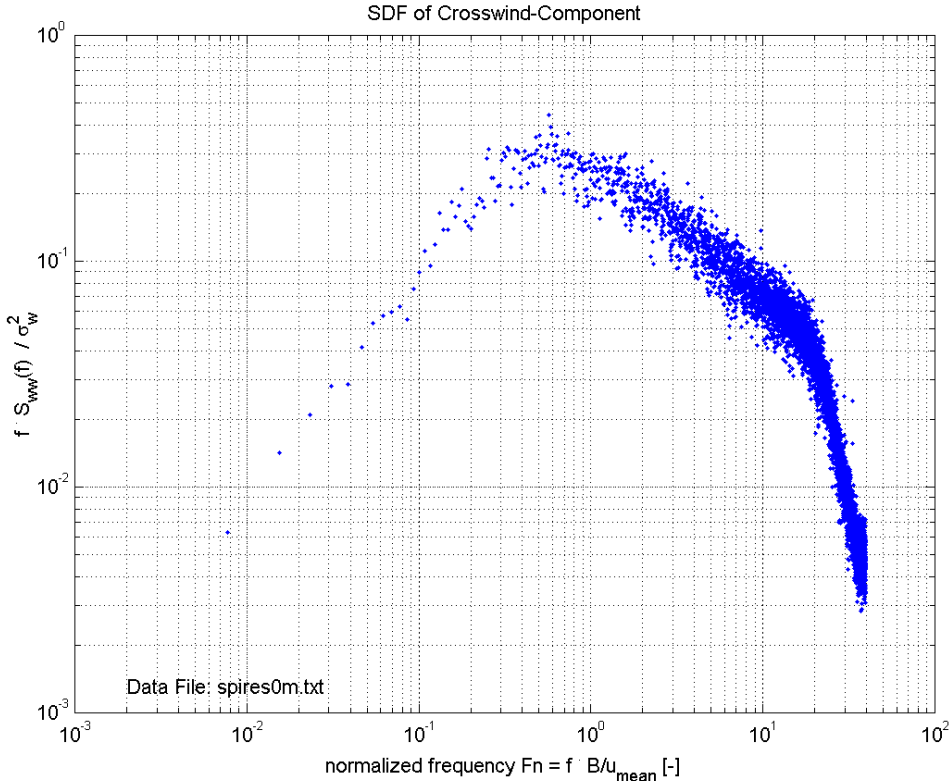


Figure 4.3 W-Component Spectra at Bridge Location (and wind tunnel centre line).



## 5. Wind-Tunnel Test Programme

The test programme consisted of static and dynamic section model tests, the objective being to determine the static wind loads and the critical wind speed for onset of aerodynamic instability. Further, the aerodynamic damping for the selected configuration was estimated based on decays tests performed at two wind speeds. Finally, the susceptibility to vortex shedding induced vibrations was investigated for the selected configuration.

The detailed test programme for the 7 deck configurations is outlined in Table 5.1.

#	Configuration	Test	Flow	Angle(s)	Comment
<b>Optimisation of configuration</b>					
1	C1	Reynolds test	Smooth	0°	
1	C1	Static force coefficient	Smooth	-10° to +10°, Δ1°	
2	C2	Static force coefficient	Smooth	-10° to +10°, Δ1°	
3	C3	Static force coefficient	Smooth	-10° to +10°, Δ1°	
4	C4	Static force coefficient	Smooth	-10° to +10°, Δ1°	
5	C5	Static force coefficient	Smooth	-10° to +10°, Δ1°	
6	C6	Static force coefficient	Smooth	-10° to +10°, Δ1°	
7	C7	Static force coefficient	Smooth	-10° to +10°, Δ1°	
8	C1	Aerodynamic stability	Smooth	0°	
9	C2	Aerodynamic stability	Smooth	0°	
10	C3	Aerodynamic stability	Smooth	0°	
11	C4	Aerodynamic stability	Smooth	0°	
12	C5	Aerodynamic stability	Smooth	0°	
13	C6	Aerodynamic stability	Smooth	0°	
14	C7	Aerodynamic stability	Smooth	0°	
<b>Verification of optimum configuration</b>					
15	C5	Static force coefficient	Smooth	-10° to +10°, Δ1°	3 wind speeds
16	C5	Static force coefficient	Turbulent	-10° to +10°, Δ1°	3 wind speeds
15	C5	Aerodynamic stability	Smooth	-4°, 0°, +4°	Damping at 2 wind speeds
16	C5	Aerodynamic stability	Turbulent	-4°, 0°, +4°	Damping at 2 wind speeds
17	C5	Vortex shedding	Smooth	0°	
18	C5	Vortex shedding	Turbulent	0°	

Table 5.1. Test programme for section model tests.

## 6. Static Tests

### 6.1 Static Force Coefficients Definition

The static aerodynamic force coefficients for the deck of the Messina Strait Bridge were determined based on wind-tunnel tests on a 1:80 geometrical scale model of a section of the deck in smooth flow. The verification tests were also conducted in turbulent flow.

A typical force coefficient is defined as follows:

$$C_{x,z,l,d} = \frac{\bar{F}_{x,z,l,d}}{\bar{q} BL} \quad (6.1a)$$

$$C_m = \frac{\bar{M}}{\bar{q} B^2 L} \quad (6.1b)$$

Where:

- $C$  = Aerodynamic coefficient
- $\bar{F}$  = Time-averaged (mean) aerodynamic force
- $\bar{M}$  = Mean overturning moment (torque)
- $B$  = The bridge deck width (60.74 m in the present case)
- $L$  = The model span length
- $\bar{q}$  = The mean wind velocity pressure<sup>1</sup> at deck level;  $\bar{q} = \frac{1}{2} \rho \bar{V}^2$  where:
- $\rho$  = Air density [kg/m<sup>3</sup>]
- $\bar{V}$  = Mean wind velocity at deck level in [m/s]

The subscripts  $x, z, l, d$  and  $m$  refer to the x and z body-force components, lift, drag and overturning moment, respectively.

The procedure for the determination of the static coefficients consists of mounting the 2.55 m long section model of the bridge in a static rig equipped with two 3-component force balances. The force balances measure the vertical, lateral and torsional reactions at the extremities of the model. The reactions are combined to obtain:  $\bar{F}_l, \bar{F}_d$  and  $\bar{M}$ , respectively.

These quantities are subsequently normalized according to the equations above. This procedure is repeated for several angles of attack of the model (from  $-10^\circ$  to  $+10^\circ$  in increments of  $1^\circ$ , measured from the horizontal plane).

<sup>1</sup> The mean velocity pressure is measured directly (by micro manometers), consequently the value of the air density and the mean wind velocity are not determined explicitly.

The rate of change (or slope) of the coefficients with angle of attack  $\alpha$  in radians is evaluated from these tests in the vicinity of zero degrees (between  $-1^\circ$  and  $+1^\circ$ ).

The drag and lift coefficients,  $C_d$  and  $C_l$ , are defined in the global coordinate system in relation to the wind. The body force coefficients,  $C_x$  and  $C_z$ , defined in the local coordinate system, are linked to the drag and lift coefficients by the following relationships:

$$C_x(\alpha) = C_d(\alpha)\cos\alpha - C_l(\alpha)\sin\alpha \tag{6.2a}$$

$$C_z(\alpha) = C_d(\alpha)\sin\alpha + C_l(\alpha)\cos\alpha \tag{6.2b}$$

A bridge deck width,  $B$ , of 60.74 m (full-scale) was used in the determination of the coefficients. The centre of measurement of the forces and moment was set at the shear centre of the section, 1.33 m (in full-scale) above the bottom of the bottom plate of the railway girder.

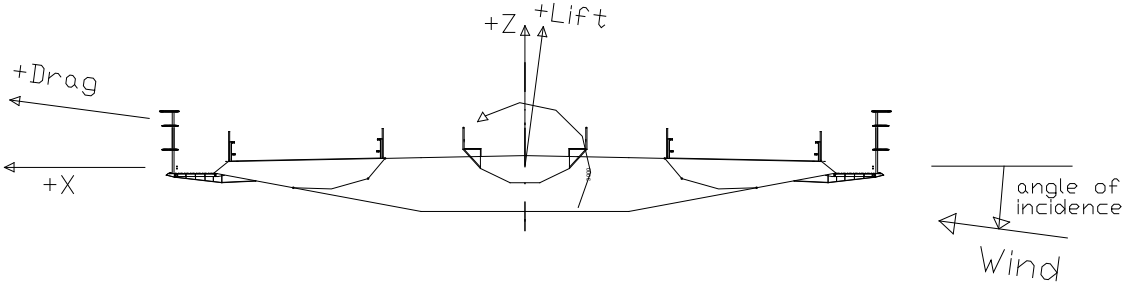


Figure 6.1. Sign convention for the static section model tests.

## 6.2 Results

For the optimisation tests, static tests were conducted in smooth flow and the test wind speed was determined on the basis of the Reynolds number tests for configuration C1, see Figure 6.2.

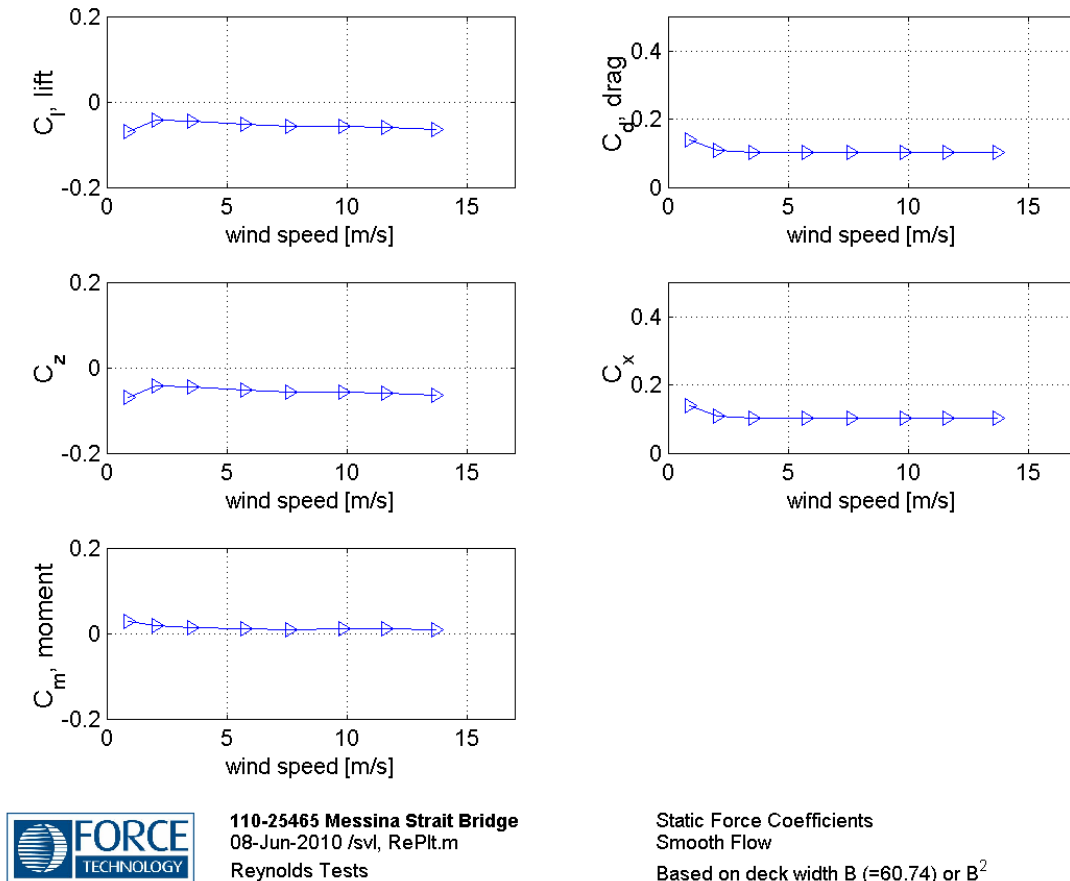


Figure 6.2. Results of Reynolds number tests.

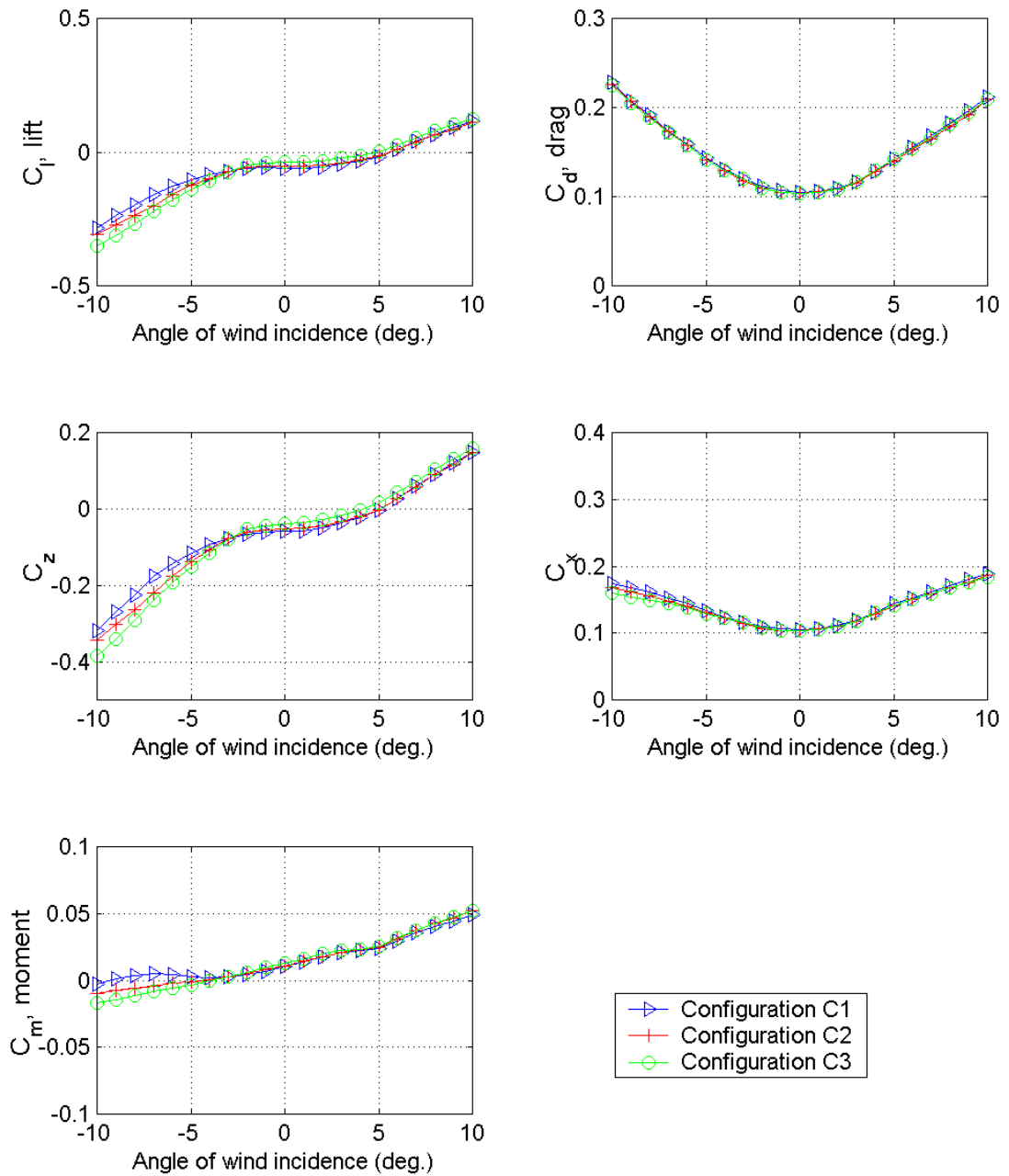
The optimisation tests were conducted at model-scale wind speeds of typically about 12 m/s. The verification tests were conducted at three wind speeds: 12 m/s, 15 m/s and 18 m/s.

Figure 6.3 through Figure 6.6 present the variations of the coefficients with angle of wind incidence,  $\alpha$ , for the bridge deck. Configuration numbers in these plots refer to Table 3.1.

A summary of the main static coefficients is given in Table 2.1 and Table 2.2 of Section 2. The rate of change (slope) of the coefficients around  $0^\circ$  was calculated based on the values at  $-1^\circ$  and  $+1^\circ$ , see also the tables in Section 2.

The measured coefficients have been corrected for the effect of blockage according to ESDU<sup>2</sup>. The blockage correction was in the order of 3-7% depending on the deck inclination.

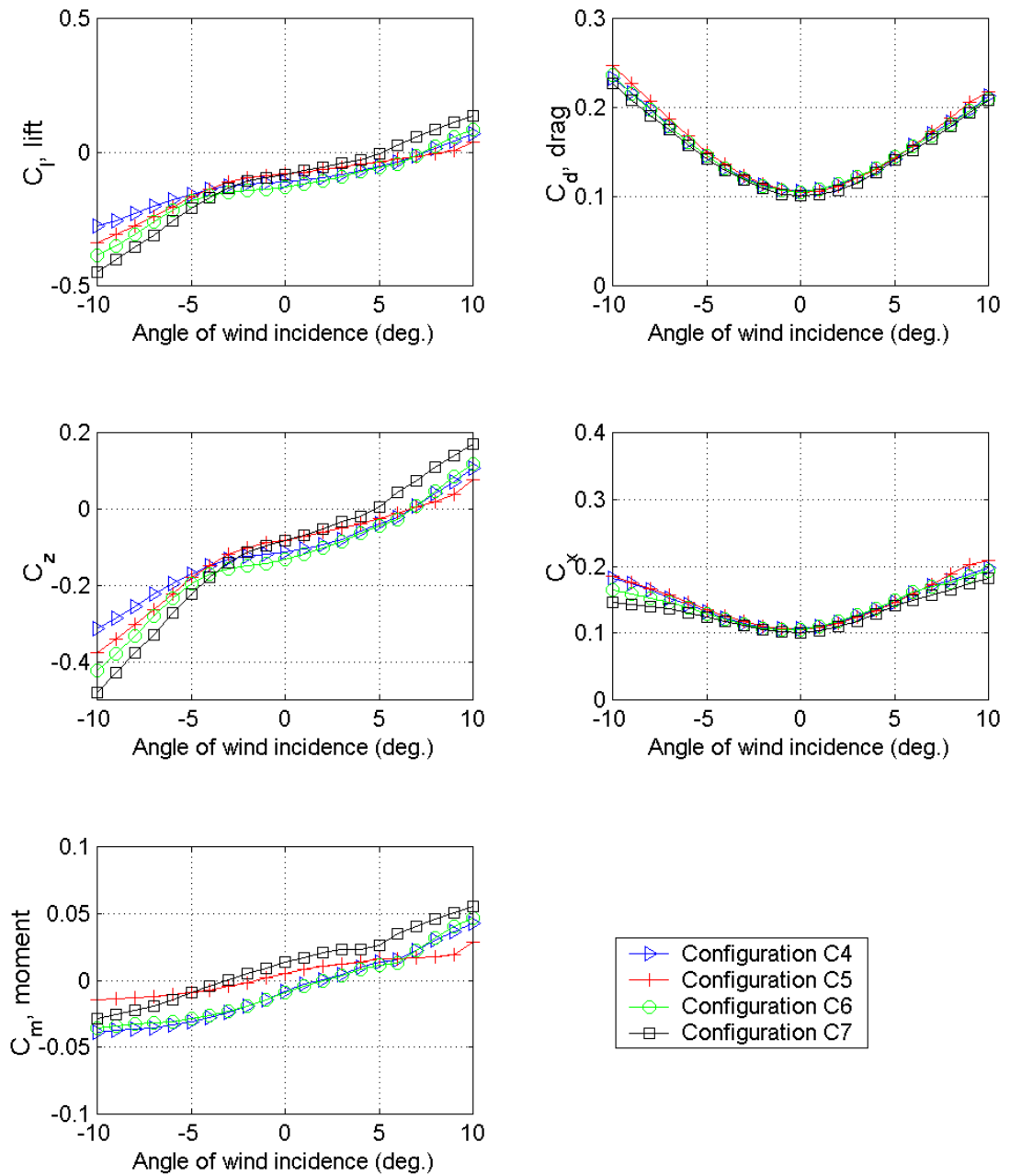
<sup>2</sup> Engineering Sciences Data Unit Item 80024: "Blockage correction for bluff bodies in confined flows", Nov. 1980.



110-25465 Messina Strait Bridge  
 09-Jun-2010 /svl, StatPlt.m  
 Static Load Tests

Static Force Coefficients - Smooth Flow  
 Configurations 1 - 3  
 Based on deck width  $B (=60.74)$  or  $B^2$

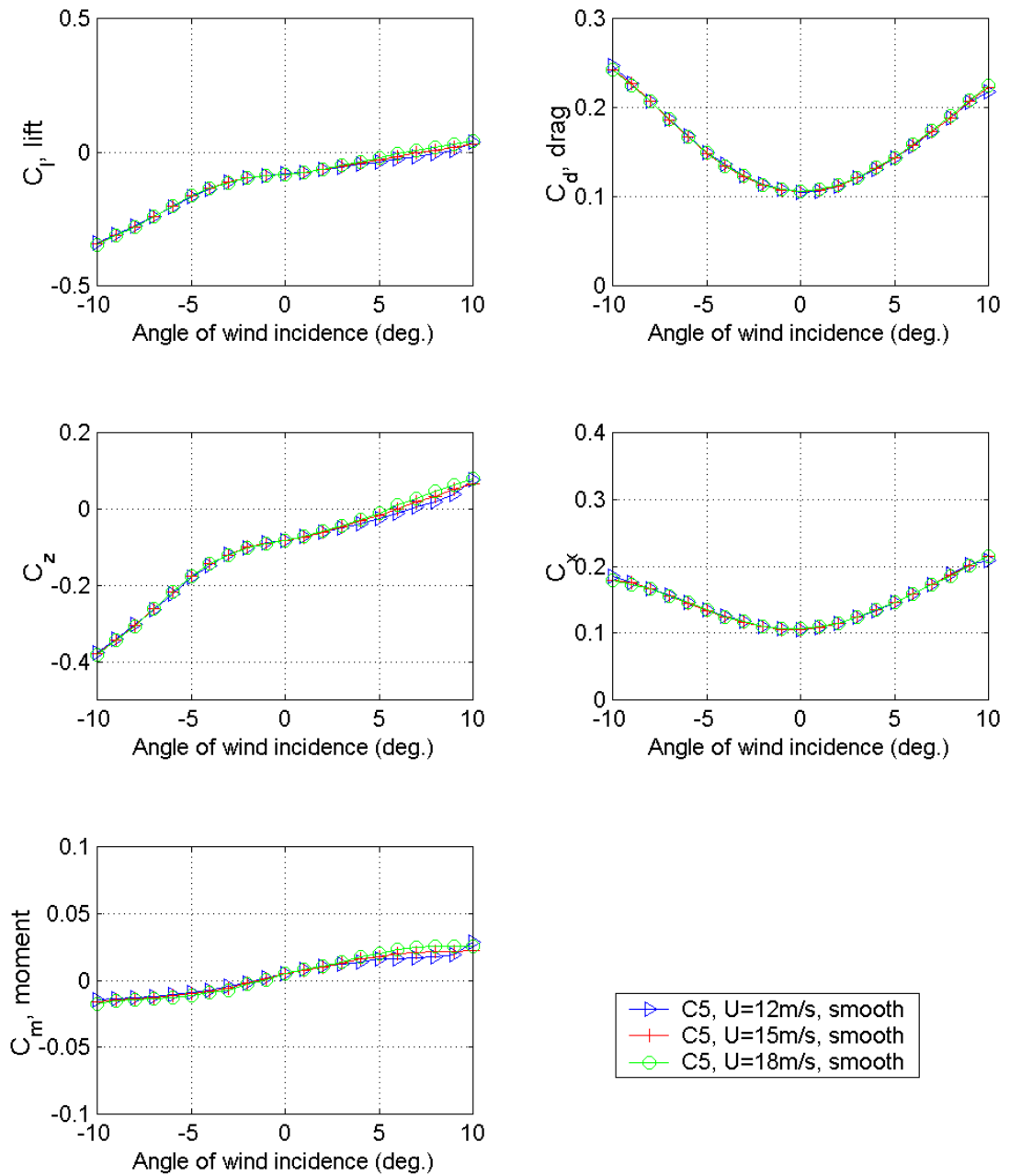
Figure 6.3. Variations of the static force coefficients for configurations 1 to 3.



110-25465 Messina Strait Bridge  
 09-Jun-2010 /svl, StatPlt.m  
 Static Load Tests

Static Force Coefficients - Smooth Flow  
 Configurations 4 - 7  
 Based on deck width  $B$  ( $=60.74$ ) or  $B^2$

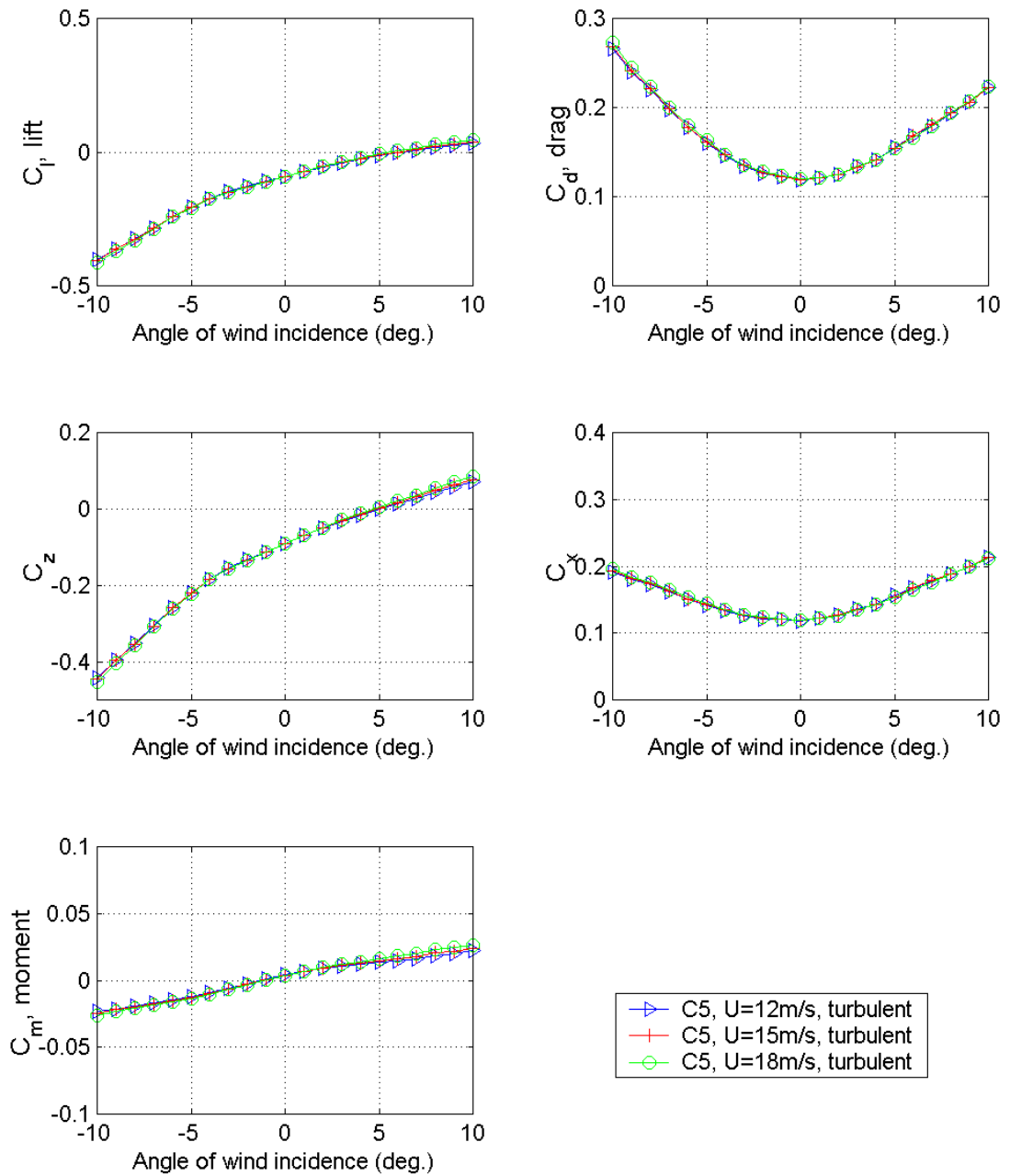
Figure 6.4. Variations of the static force coefficients for configurations 4 to 7.



110-25465 Messina Strait Bridge  
 09-Jun-2010 /svl, StatPlt.m  
 Static Load Tests

Static Force Coefficients - C5  
 Smooth flow  
 Based on deck width B (=60.74) or B<sup>2</sup>

Figure 6.5. Variations of the static force coefficients for the optimum configuration (C5) – smooth flow.



110-25465 Messina Strait Bridge  
 24-Jun-2010 /svl, StatPlt.m  
 Static Load Tests

Static Force Coefficients - C5  
 Turbulent flow  
 Based on deck width B (=60.74) or B<sup>2</sup>

Figure 6.6. Variations of the static force coefficients for the optimum configuration (C5) – turbulent flow.



	Configuration C1			Configuration C2			Configuration C3			Configuration C4		
$\alpha$ [°]	$C_d$	$C_l$	$C_m$	$C_d$	$C_l$	$C_m$	$C_d$	$C_l$	$C_m$	$C_d$	$C_l$	$C_m$
-10	0.228	-0.285	-0.003	0.225	-0.308	-0.010	0.224	-0.350	-0.017	0.233	-0.278	-0.038
-9	0.207	-0.239	0.001	0.207	-0.273	-0.007	0.205	-0.314	-0.015	0.217	-0.256	-0.038
-8	0.191	-0.200	0.004	0.190	-0.239	-0.006	0.188	-0.269	-0.011	0.199	-0.231	-0.037
-7	0.173	-0.157	0.005	0.173	-0.200	-0.004	0.172	-0.220	-0.008	0.178	-0.203	-0.035
-6	0.158	-0.128	0.004	0.157	-0.160	-0.002	0.157	-0.177	-0.006	0.162	-0.180	-0.033
-5	0.143	-0.103	0.003	0.142	-0.125	-0.001	0.142	-0.139	-0.004	0.146	-0.159	-0.031
-4	0.131	-0.085	0.002	0.130	-0.099	0.000	0.129	-0.107	-0.001	0.132	-0.140	-0.027
-3	0.120	-0.071	0.003	0.118	-0.071	0.003	0.119	-0.075	0.003	0.121	-0.127	-0.024
-2	0.112	-0.062	0.004	0.109	-0.057	0.005	0.109	-0.050	0.006	0.113	-0.119	-0.019
-1	0.107	-0.058	0.007	0.105	-0.053	0.008	0.105	-0.041	0.010	0.108	-0.116	-0.014
0	0.105	-0.059	0.010	0.104	-0.053	0.011	0.104	-0.039	0.013	0.106	-0.113	-0.008
+1	0.106	-0.060	0.014	0.105	-0.052	0.014	0.105	-0.037	0.016	0.108	-0.106	-0.003
+2	0.109	-0.055	0.018	0.109	-0.048	0.018	0.109	-0.032	0.020	0.113	-0.098	0.001
+3	0.117	-0.044	0.021	0.115	-0.039	0.021	0.117	-0.023	0.022	0.121	-0.086	0.005
+4	0.129	-0.032	0.022	0.128	-0.028	0.023	0.129	-0.013	0.023	0.131	-0.068	0.010
+5	0.143	-0.016	0.024	0.141	-0.014	0.025	0.142	0.003	0.026	0.143	-0.052	0.013
+6	0.155	0.011	0.029	0.153	0.012	0.031	0.154	0.026	0.032	0.157	-0.038	0.016
+7	0.168	0.041	0.036	0.164	0.037	0.037	0.166	0.051	0.037	0.170	-0.012	0.022
+8	0.182	0.066	0.040	0.179	0.065	0.042	0.181	0.079	0.043	0.183	0.016	0.030
+9	0.196	0.091	0.044	0.191	0.086	0.046	0.195	0.102	0.047	0.197	0.042	0.036
+10	0.212	0.114	0.049	0.210	0.113	0.052	0.209	0.124	0.052	0.213	0.069	0.043
	Configuration C5			Configuration C6			Configuration C7					
$\alpha$ [°]	$C_d$	$C_l$	$C_m$	$C_d$	$C_l$	$C_m$	$C_d$	$C_l$	$C_m$			
-10	0.247	-0.338	-0.015	0.236	-0.387	-0.036	0.228	-0.448	-0.029			
-9	0.227	-0.309	-0.014	0.215	-0.349	-0.034	0.208	-0.401	-0.025			
-8	0.207	-0.277	-0.013	0.197	-0.308	-0.033	0.190	-0.354	-0.022			
-7	0.187	-0.242	-0.012	0.179	-0.260	-0.032	0.175	-0.310	-0.019			
-6	0.168	-0.205	-0.011	0.162	-0.217	-0.031	0.157	-0.257	-0.015			
-5	0.149	-0.166	-0.009	0.146	-0.184	-0.029	0.142	-0.210	-0.009			
-4	0.136	-0.138	-0.007	0.132	-0.163	-0.026	0.130	-0.169	-0.004			
-3	0.123	-0.113	-0.005	0.121	-0.150	-0.023	0.119	-0.136	0.000			
-2	0.114	-0.098	-0.002	0.112	-0.144	-0.019	0.109	-0.109	0.005			
-1	0.108	-0.087	0.002	0.107	-0.141	-0.015	0.103	-0.094	0.009			
0	0.105	-0.082	0.005	0.105	-0.133	-0.009	0.101	-0.084	0.013			
+1	0.106	-0.075	0.008	0.108	-0.121	-0.004	0.103	-0.070	0.017			
+2	0.112	-0.065	0.010	0.115	-0.107	0.000	0.107	-0.055	0.020			
+3	0.121	-0.055	0.012	0.122	-0.092	0.004	0.116	-0.041	0.023			
+4	0.131	-0.047	0.014	0.132	-0.074	0.008	0.127	-0.029	0.023			
+5	0.143	-0.037	0.016	0.144	-0.058	0.011	0.141	-0.007	0.026			
+6	0.157	-0.027	0.016	0.157	-0.045	0.013	0.152	0.026	0.035			
+7	0.172	-0.017	0.017	0.168	-0.013	0.022	0.165	0.055	0.040			
+8	0.189	-0.007	0.018	0.181	0.021	0.031	0.179	0.084	0.046			
+9	0.206	0.006	0.019	0.197	0.056	0.040	0.194	0.111	0.050			
+10	0.218	0.039	0.029	0.210	0.083	0.047	0.209	0.136	0.055			

Table 6.1. The static force coefficients with angle of incidence for configurations C1- C7, smooth flow.

$\alpha$ [°]	C5, 12 m/s, smooth			C5, 15 m/s, smooth			C5, 18 m/s, smooth		
	$C_d$	$C_l$	$C_m$	$C_d$	$C_l$	$C_m$	$C_d$	$C_l$	$C_m$
-10	0.247	-0.338	-0.015	0.242	-0.342	-0.016	0.243	-0.346	-0.018
-9	0.227	-0.309	-0.014	0.226	-0.311	-0.015	0.225	-0.312	-0.016
-8	0.207	-0.277	-0.013	0.207	-0.280	-0.014	0.207	-0.281	-0.014
-7	0.187	-0.242	-0.012	0.186	-0.240	-0.013	0.187	-0.240	-0.014
-6	0.168	-0.205	-0.011	0.167	-0.202	-0.012	0.167	-0.201	-0.013
-5	0.149	-0.166	-0.009	0.149	-0.163	-0.010	0.149	-0.164	-0.011
-4	0.136	-0.138	-0.007	0.134	-0.134	-0.008	0.134	-0.134	-0.009
-3	0.123	-0.113	-0.005	0.123	-0.114	-0.006	0.123	-0.115	-0.007
-2	0.114	-0.098	-0.002	0.113	-0.096	-0.002	0.113	-0.098	-0.003
-1	0.108	-0.087	0.002	0.107	-0.088	0.001	0.108	-0.090	0.001
0	0.105	-0.082	0.005	0.105	-0.083	0.005	0.106	-0.084	0.005
+1	0.106	-0.075	0.008	0.107	-0.075	0.008	0.108	-0.075	0.008
+2	0.112	-0.065	0.010	0.112	-0.065	0.010	0.113	-0.063	0.011
+3	0.121	-0.055	0.012	0.121	-0.053	0.013	0.122	-0.050	0.014
+4	0.131	-0.047	0.014	0.132	-0.041	0.016	0.133	-0.036	0.018
+5	0.143	-0.037	0.016	0.144	-0.029	0.018	0.144	-0.023	0.020
+6	0.157	-0.027	0.016	0.158	-0.016	0.020	0.159	-0.006	0.023
+7	0.172	-0.017	0.017	0.173	-0.004	0.021	0.174	0.007	0.025
+8	0.189	-0.007	0.018	0.189	0.008	0.021	0.190	0.019	0.025
+9	0.206	0.006	0.019	0.207	0.019	0.022	0.208	0.029	0.025
+10	0.218	0.039	0.029	0.223	0.029	0.022	0.225	0.040	0.026
$\alpha$ [°]	C5, 12 m/s, turbulent			C5, 15 m/s, turbulent			C5, 18 m/s, turbulent		
	$C_d$	$C_l$	$C_m$	$C_d$	$C_l$	$C_m$	$C_d$	$C_l$	$C_m$
-10	0.266	-0.404	-0.023	0.268	-0.406	-0.025	0.273	-0.414	-0.026
-9	0.241	-0.364	-0.021	0.241	-0.364	-0.022	0.245	-0.369	-0.023
-8	0.220	-0.325	-0.019	0.221	-0.327	-0.020	0.223	-0.330	-0.021
-7	0.197	-0.283	-0.017	0.199	-0.285	-0.018	0.201	-0.287	-0.019
-6	0.177	-0.242	-0.015	0.177	-0.241	-0.015	0.179	-0.243	-0.016
-5	0.161	-0.207	-0.012	0.162	-0.207	-0.013	0.163	-0.209	-0.014
-4	0.146	-0.174	-0.009	0.147	-0.175	-0.010	0.147	-0.175	-0.011
-3	0.134	-0.148	-0.006	0.135	-0.150	-0.006	0.135	-0.149	-0.007
-2	0.125	-0.127	-0.003	0.127	-0.130	-0.003	0.128	-0.130	-0.004
-1	0.122	-0.110	0.001	0.122	-0.110	0.000	0.123	-0.110	0.000
0	0.118	-0.090	0.005	0.119	-0.091	0.004	0.119	-0.091	0.004
+1	0.121	-0.072	0.007	0.121	-0.072	0.007	0.121	-0.071	0.007
+2	0.125	-0.055	0.009	0.125	-0.055	0.009	0.124	-0.053	0.010
+3	0.134	-0.040	0.011	0.133	-0.038	0.011	0.134	-0.036	0.012
+4	0.141	-0.027	0.012	0.142	-0.024	0.013	0.142	-0.022	0.014
+5	0.155	-0.015	0.013	0.154	-0.011	0.014	0.154	-0.008	0.016
+6	0.168	-0.003	0.015	0.168	0.000	0.016	0.166	0.004	0.018
+7	0.179	0.005	0.016	0.181	0.010	0.017	0.179	0.014	0.020
+8	0.192	0.016	0.018	0.194	0.022	0.021	0.195	0.028	0.023
+9	0.206	0.026	0.020	0.206	0.031	0.022	0.207	0.038	0.025
+10	0.222	0.033	0.022	0.223	0.038	0.024	0.224	0.046	0.026

Table 6.2. The static force coefficients with angle of incidence for configuration C5 – various test conditions.

## 7. Dynamic Tests

### 7.1 Model Configuration

The 2.55 m long section model was mounted in the dynamic rig, consisting of relatively soft springs, allowing the simulation of the vertical and torsional oscillations of a section of the deck. The stiffness of the dynamic rig was adjusted to reproduce the frequency ratio between the first symmetric torsional mode of the deck and the first symmetric vertical mode. The model was ballasted with additional mass to represent the dynamically scaled mass and mass moment of inertia of the deck.

Two dynamic rigs were used in the tests. These are referred to as Soft Rig and Stiff Rig, respectively.

The dynamic properties of the prototype structure, provided by the Client, are compared to the section model properties in Table 6.1. The dynamic properties of the prototype structure, provided as the values in vacuum by the Client, were converted to model-scale in-air properties. Because the determination of eigen-frequencies are performed in still air, it is necessary to calculate a set of target values for the “in-air” condition, which includes theoretical values for “added mass”.

The main cross-sectional dimensions of the bridge deck are illustrated in Figure 6.1 below. Here,  $B_k$  is the aerodynamic width of the bridge deck sub-sections and  $y$  the distance from centre line to the geometric centre of the outer sub-section.

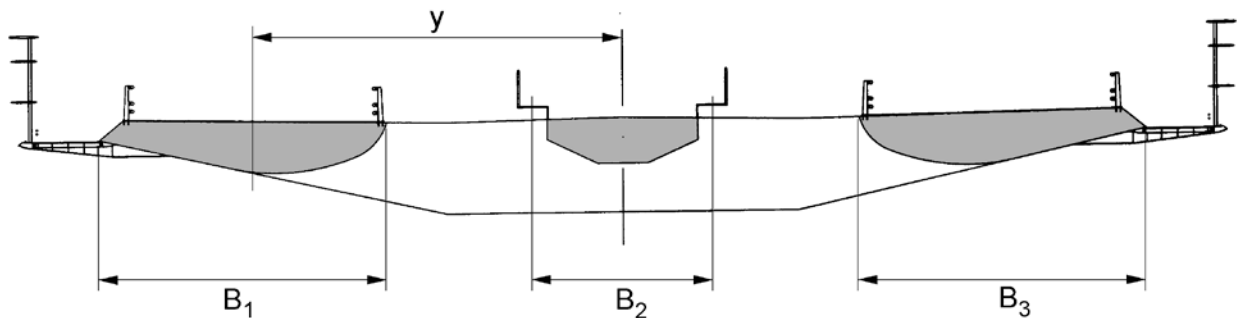


Figure 7.1. Main geometric parameters of the bridge deck.

Due to symmetry  $B_1 = B_3 = 14.4\text{m}$  and  $B_2 = 8.8\text{m}$ . Lateral distance between centre line and outer sub-section centre is  $y = 19.2\text{m}$ . Under vibration, the bridge deck displaced air of a certain mass, which adds to the initial mass of the bridge and affects the moment of inertia. The initial quantities are determined as if the structure would be in vacuum. The effective values for mass and moment of inertia for vibration in air are obtained by determining the additional terms. The effective mass in air  ${}^a m$  results from equation 1:

$${}^a m = {}^v m + \frac{\pi}{4} \cdot \rho_{air} \cdot (B_1^2 + B_2^2 + B_3^2) \quad [\text{kg/m}] \quad (1)$$

Where  ${}^v m$  is the initial mass per unit length in vacuum. The effective moment of inertia in air  ${}^a I$  is defined by equation 2.

$${}^a I = {}^v I + \frac{\pi}{4} \cdot \rho_{air} \cdot 2 \cdot B_1^2 \cdot y^2 \quad [\text{kg m}^2/\text{m}] \quad (2)$$

With  $\rho_{air} = 1.25 \text{ kg/m}^3$  the effective values in air are:

$$^a m = 53,200 + 483 = 53,683 \text{ kg/m}$$

$$^a I = 26,500,000 + 150,092 = 26,650,092 \text{ kg m}^2/\text{m}$$

Hence, the masses are higher in the “in-air” condition and the eigen-frequencies are lower

The resulting velocity scaling for the vertical and torsional response in the Soft Rig was approximately 1:6.5, 1 m/s in the wind tunnel corresponding to 6.5 m/s in full-scale. For the Stiff Rig, the velocity scaling was 1:2.2.

	Prototype		Section Model Soft Rig		Section Model Stiff Rig	
	“Vacuum”	“In-Air”	Target	Obtained	Target	Obtained
$f_{vertical}$ (Hz)	0.0645	0.064	0.797	0.79	2.359	2.41
$f_{torsional}$ (Hz)	0.0831	0.083	1.031	1.00	3.050	3.08
Ratio: $f_{torsional} / f_{vertical}$	1.29	1.29	1.29	1.27	1.29	1.28
Mass per unit length (kg/m)	53,200	53,683	8.388	8.57	8.388	8.31
Mass moment of inertia per unit length (kg·m <sup>2</sup> /m)	26,500,000	26,650,092	0.651	0.645	0.651	0.647

Table 7.1. Dynamic properties of prototype structure and section model.

The model was restrained in the lateral direction, the horizontal motions of the deck having no significant influence on the stability of the deck, which is the normal assumption for section model tests.

In the dynamic rigs (both soft rig and stiff rig) the damping for vertical motion was approximately 0.3% of critical and for torsional motion it was about 0.2% of critical. Decay plots with damping estimates are included in Appendix C.

## 7.2 Stability Tests

The dynamic section model tests for the optimisation tests aimed at defining the aerodynamic stability limit of the deck in smooth flow for an angle of wind incidence of 0°. In the verification tests, the stability limit was investigated in smooth and turbulent flow for angles of wind incidence of -4°, 0° and +4°.

Variations of the mean and root-mean-square (rms) responses with reduced mean wind speeds at deck level are presented in the form of mean and rms vertical displacement normalised by the deck height (4.68 m full-scale). The pitch response is simply presented as the deck rotation in degrees. This section presents summary plots of the results obtained in the dynamic section model tests.

A summary of the main findings is given in Section 2. The detailed presentation given in Appendix D includes plots of the peak factor. The definition of the peak factor is given below.

$$\text{peak factor} = \frac{d_{\max} - d_{\min}}{2 \cdot \text{rms}} \quad (7.2)$$

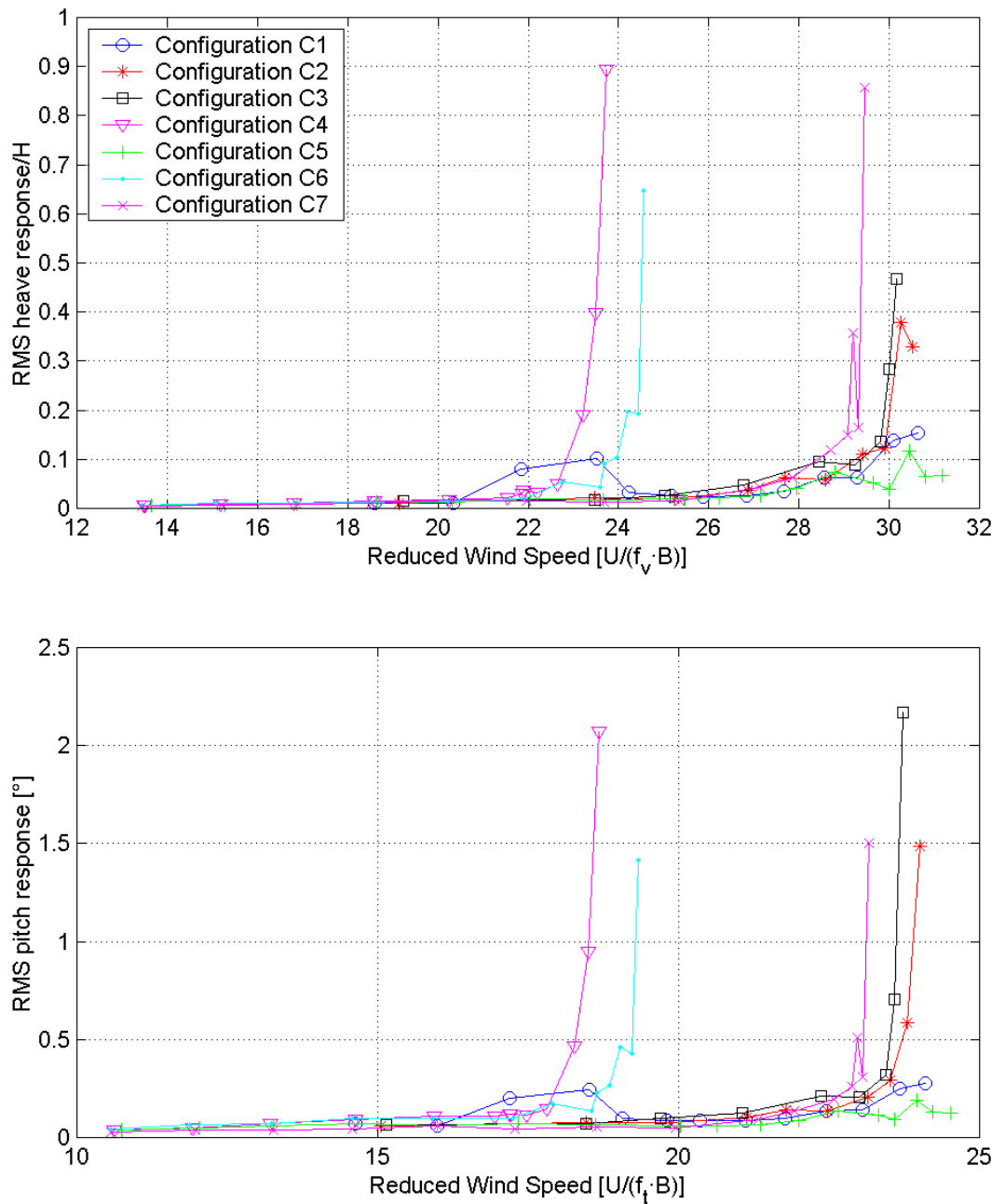
$d_{\max}$  and  $d_{\min}$  are the maximum and minimum values (e.g., deflection) of a given time series, respectively, and rms is the root-mean-square of the time series.

Each of the data points (except from the last point, where instability starts) on the response plots results from the measurements of stable, limited amplitude motion (as opposed to a negative total damping case where the amplitude continues to grow in magnitude for the same wind speed). The peak factor can be used to see whether the motion is in a "locked-in" state of sinusoidal motion or a random type motion.

The onset of an "instability" is defined as when the character of the response changes from a random type motion to that of a regular, sinusoidal motion, involving either pure torsional, pure vertical or a coupled vertical-torsional vibration. This can often be identified through an examination of the peak factor. A random signal has peak factors in the 3-4 range, while a pure sinusoid has a peak factor of  $\sqrt{2}$  or 1.41. Alternatively, a torsional rms response of  $0.5^\circ$  can be chosen as the governing criteria.

However, in the present tests the identification of instability has been difficult in some cases due to the large buffeting response. It was not possible to obtain time series of the response where the harmonic response of starting instability could be observed in the peak factors. Consequently the test speed was gradually increased (and the response measured) until the self excited motion was observed or the test had to be stopped due to large response in order to safeguard the model and the rig.

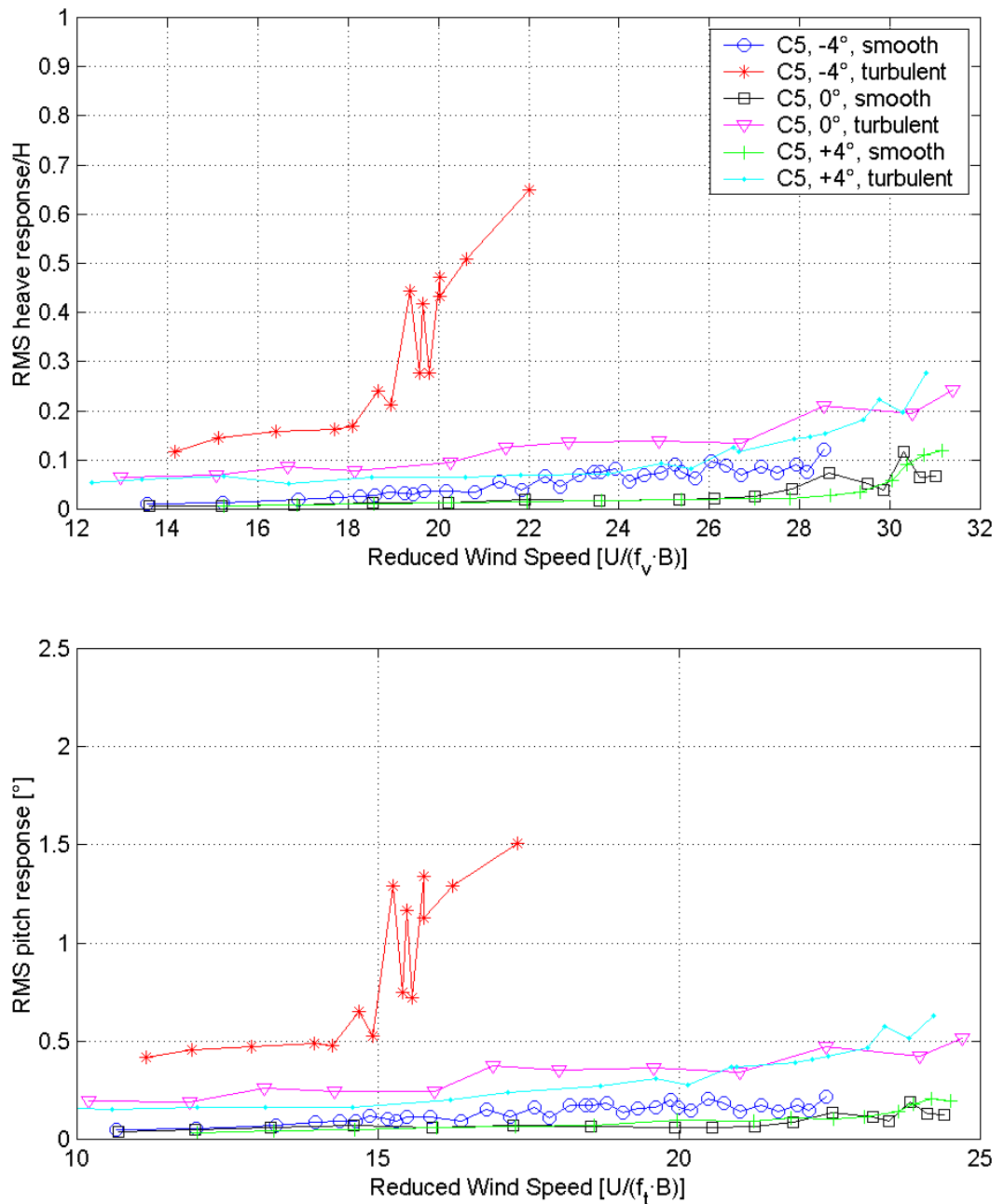
Figure 7.2 and Figure 7.3 show results from the stability tests in terms of rms response.



110-25465 Messina Strait Bridge  
 24-Jun-2010 /svl, stab.m  
 Stability tests

Aerodynamic response  
 RMS vertical and torsional response  
 Smooth flow,  $\alpha = 0^\circ$

Figure 7.2. Response in stability tests smooth,  $\alpha = 0^\circ$ , configurations C1 – C7.



110-25465 Messina Strait Bridge  
 24-Jun-2010 /svl, stabfinal.m  
 Stability tests

Aerodynamic response  
 RMS vertical and torsional response  
 Smooth & turbulent flow,  $\alpha = -4^\circ, 0^\circ, +4^\circ$

Figure 7.3. Response in stability tests, optimum configuration C5.

For the configuration C5 in turbulent flow at  $-4^\circ$ , the measured displacement and rotation is contaminated by the model hitting the wind tunnel wall from.  $U_{red} = U/(f_t \cdot B) = 15$  and higher. This was caused by the large negative displacement in combination with the buffeting response.

### 7.3 Damping Tests

The damping level (i.e., the sum of the aerodynamic and structural damping) has been estimated in connection with the stability tests. At wind speeds corresponding to 54 m/s and 75 m/s (full-scale), respectively, the model was given a combined displacement in torsional and vertical direction (pitch and heave). Subsequently the model was released and the decay signals were recorded. Based on the decay signals the damping levels have been estimated. It should be noted that in some cases - especially at the higher wind speed – the damping was high and therefore for these cases the damping has been estimated based on a limited number of cycles of motion and consequently the damping estimation is a rough approximation. In many cases, the obtained decay signals exhibited damping level that was strongly amplitude dependent.

The vertical damping is presented for amplitudes up to 20 – 40 mm and the torsional damping is presented for an amplitude of approximately 1° - 2°.

The tests results are summarized in the following table.



U [m/s]	flow	angle [°]	vertical damping [% crit]	torsional damping [% crit]
54	smooth	-4	2.2	1.9
75	smooth	-4	1.6	1.3
54	turbulent	-4	3.0	3.8
75	turbulent	-4	6.7	3.4
54	smooth	0	3.1	3.6
75	smooth	0	3.2	2.6
54	turbulent	0	4.0	3.2
75	turbulent	0	3.9	2.8
54	smooth	+4	4.9	4.3
75	smooth	+4	4.2	4.3
54	turbulent	+4	4.2	3.1
75	turbulent	+4	8.1	6.4

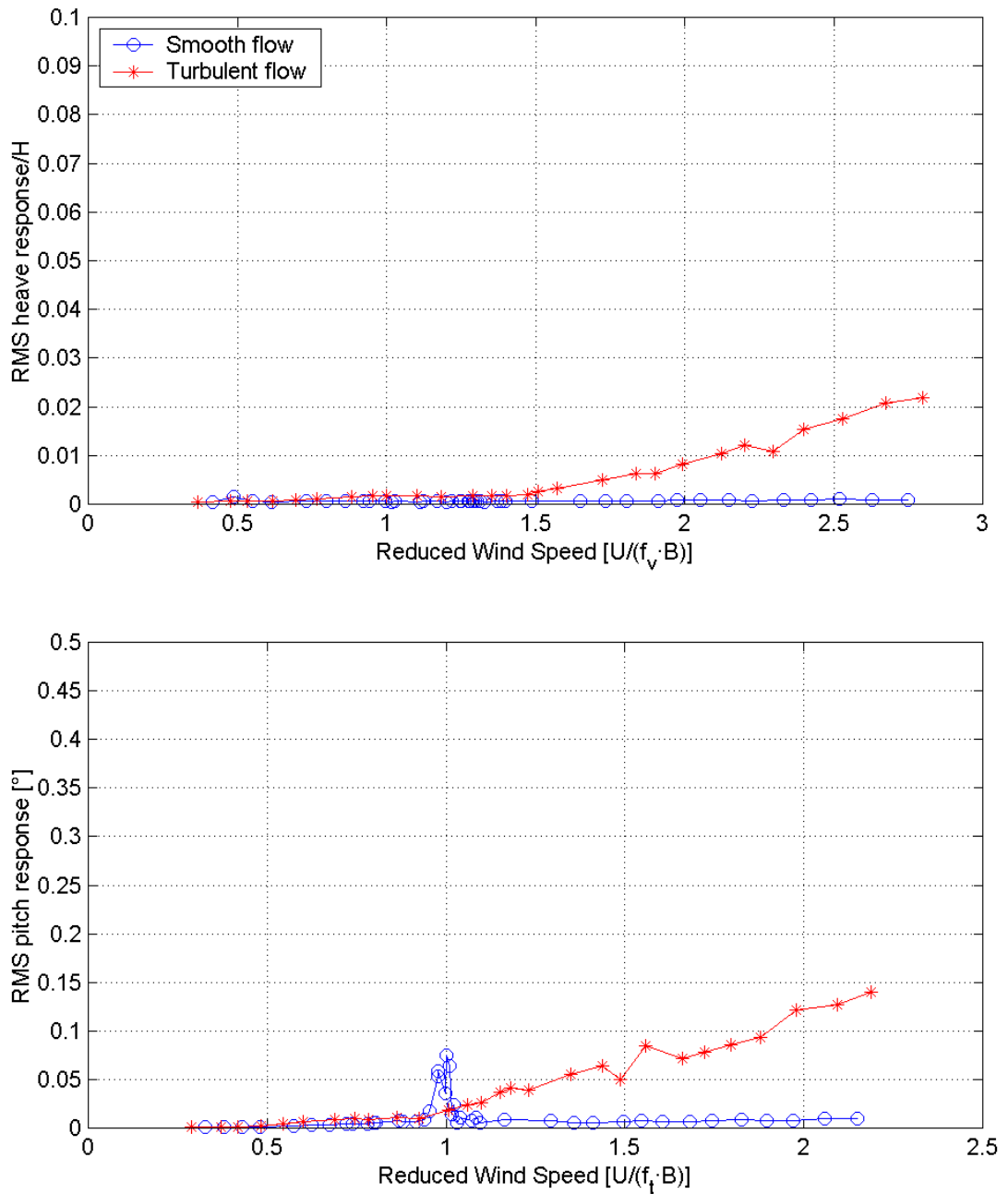
Table 7.2 Estimated Damping Level (in % of Critical) for configuration C5.

### 7.4 Vortex Shedding Tests

Vortex-shedding induced oscillations of configuration C5 were investigated in the Stiff Rig. The tests were conducted for a wind incidence of 0°, and in smooth and turbulent flow. The results are presented in this section.

In smooth flow a small torsional response peak was observed at a reduced wind speed ( $U/(B \cdot f_i)$ ) of approximately 1.0. The recorded response peak had an rms amplitude of 0.075°. Vertical vortex-induced oscillations were not observed in smooth flow. In turbulent, no vertical or torsional vortex induced response was detected.

The results of the tests are presented in Figure 7.4 as rotation and normalised vertical displacement, respectively, as function of reduced wind speed. Detailed plots are located in Appendix E.



110-25465 Messina Strait Bridge  
 24-Jun-2010 /svl, vortex.m  
 Vortex Shedding Tests

Aerodynamic response  
 RMS vertical and torsional response  
 Smooth & turbulent flow,  $\alpha = 0^\circ$

Figure 7.4. Results of vortex-shedding tests for configuration C5.

## 8. References

- [1] "Section Model Tests for the Messina Strait Crossing, Italy"  
FORCE 2005011 rev. 3.1, 2005-04-18
- [2] "Stability Tests for Modified Deck for the Messina Strait Crossing, Italy"  
FORCE 2005263 rev. A, 2005-12-22
- [3] "Static section model tests the Messina Strait Bridge"  
FORCE 109-28238 rev. 1, 2010-01-13
- [4] "Handbook of Hydraulic Resistance"  
I.E. Idelchik

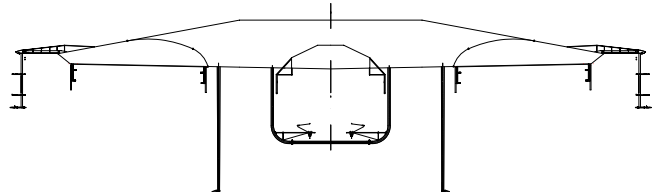
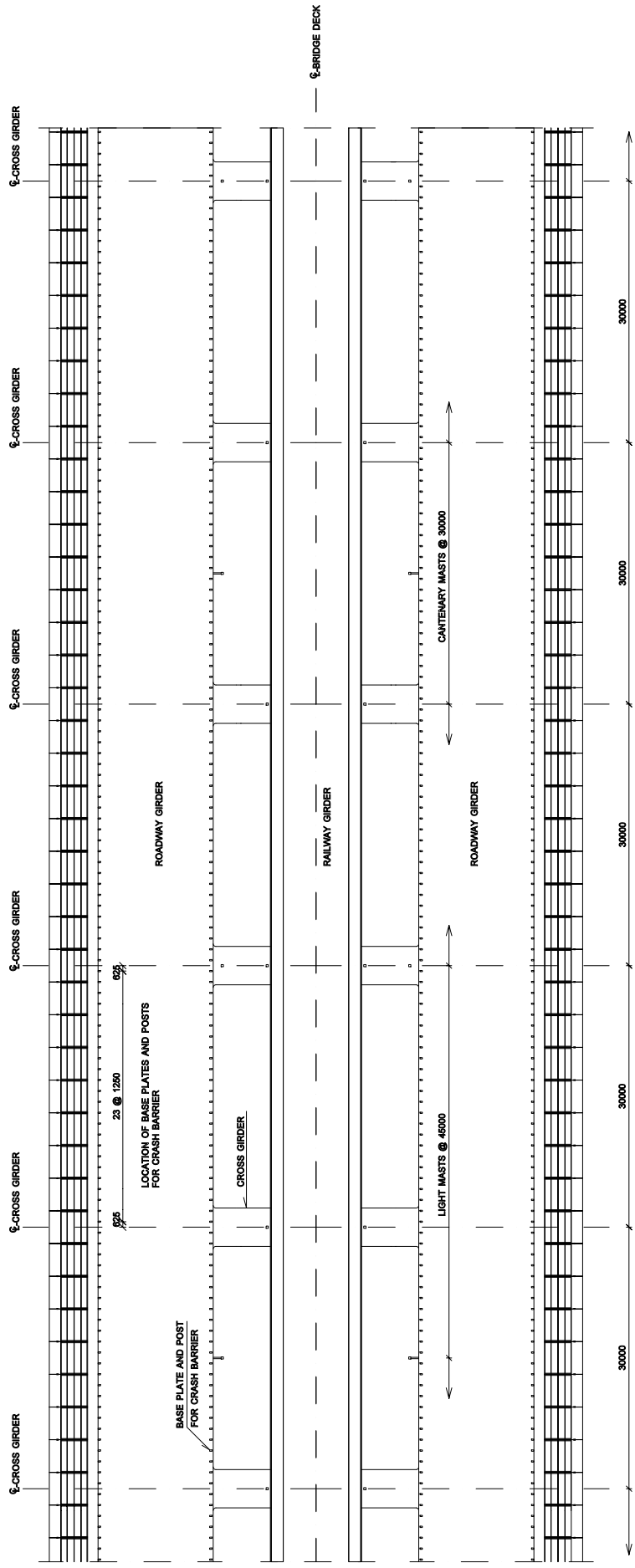
## APPENDIX A

### Drawings

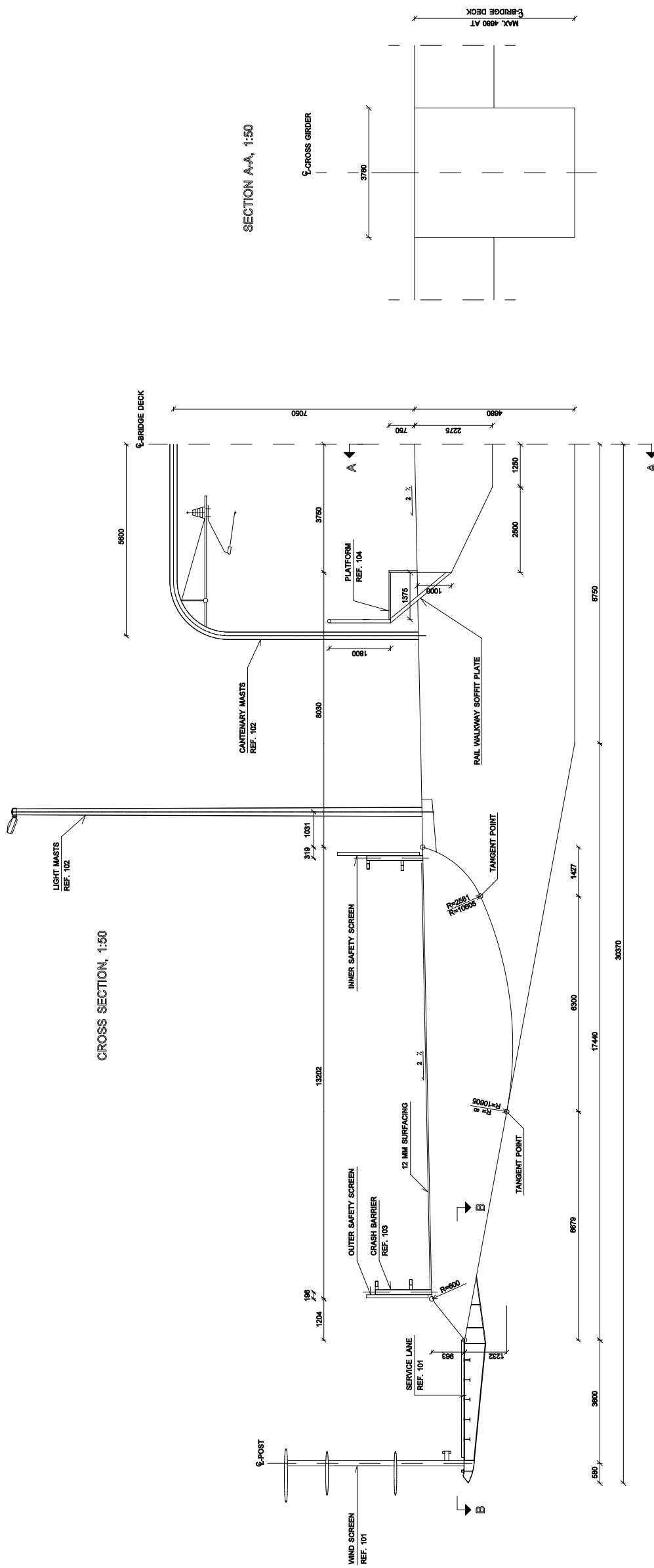
NOTE GENERALI

DIMENSIONS:  
ALL DIMENSIONS ARE IN MILLIMETRES UNLESS OTHERWISE STATED.

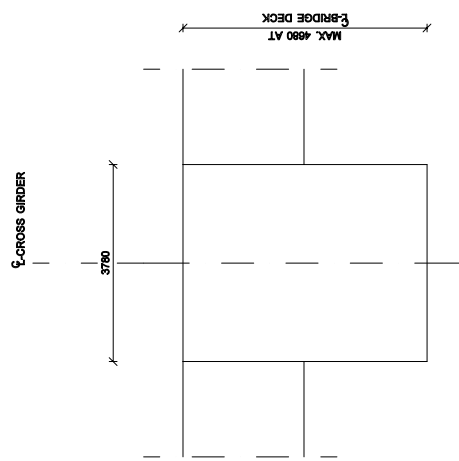
PLAN, 1:250



CROSS SECTION, 1:50



SECTION A-A, 1:50



Rev.	Date	Description	Designed	Checked	Approved

**STRETTO DI MESSINA  
BRIDGE OVER THE MESSINA STRAIGHT**

Project No.	
Designed	HEAE
Checked	IPD
Approved	AN / L.S.J.
Date	2010/04/20
Project No.	100
Scale	100

DESCRIPTION: CROSS SECTION FOR WIND TUNNEL TEST  
 COMPANY: COWI  
 ADDRESS: P.O. Box 10, DK-2800 Kongens Lyngby, Denmark  
 TEL: +45 45 99 22 12  
 WWW: www.cowi.dk

DIMENSIONS:  
ALL DIMENSIONS ARE IN MILLIMETRES UNLESS OTHERWISE STATED.

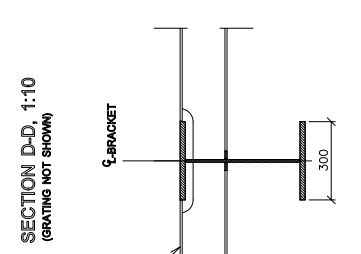
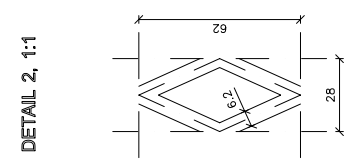
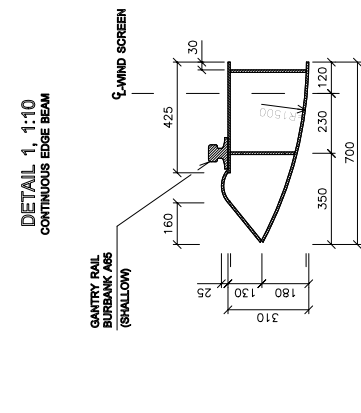
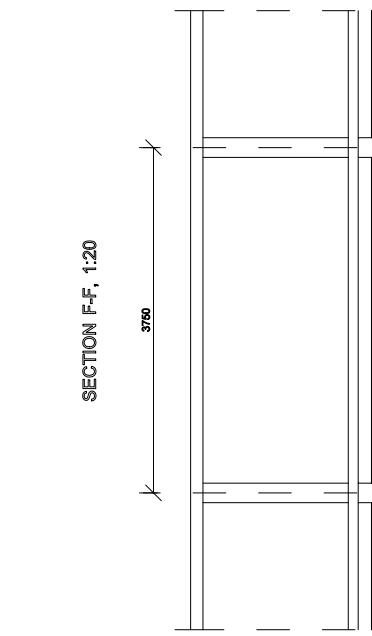
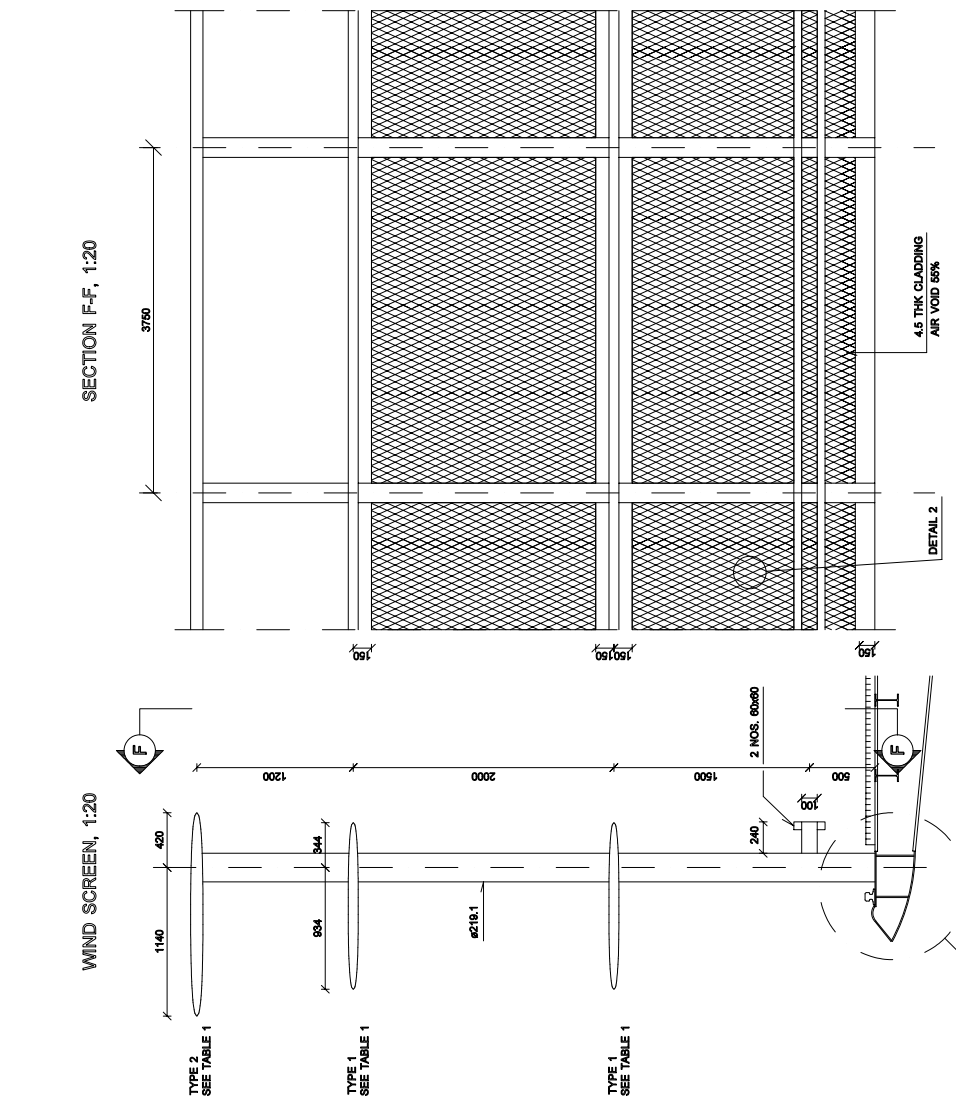
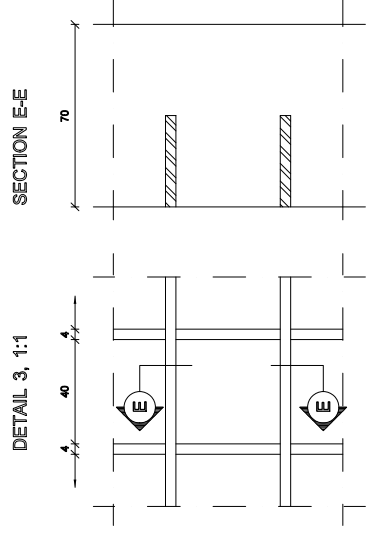
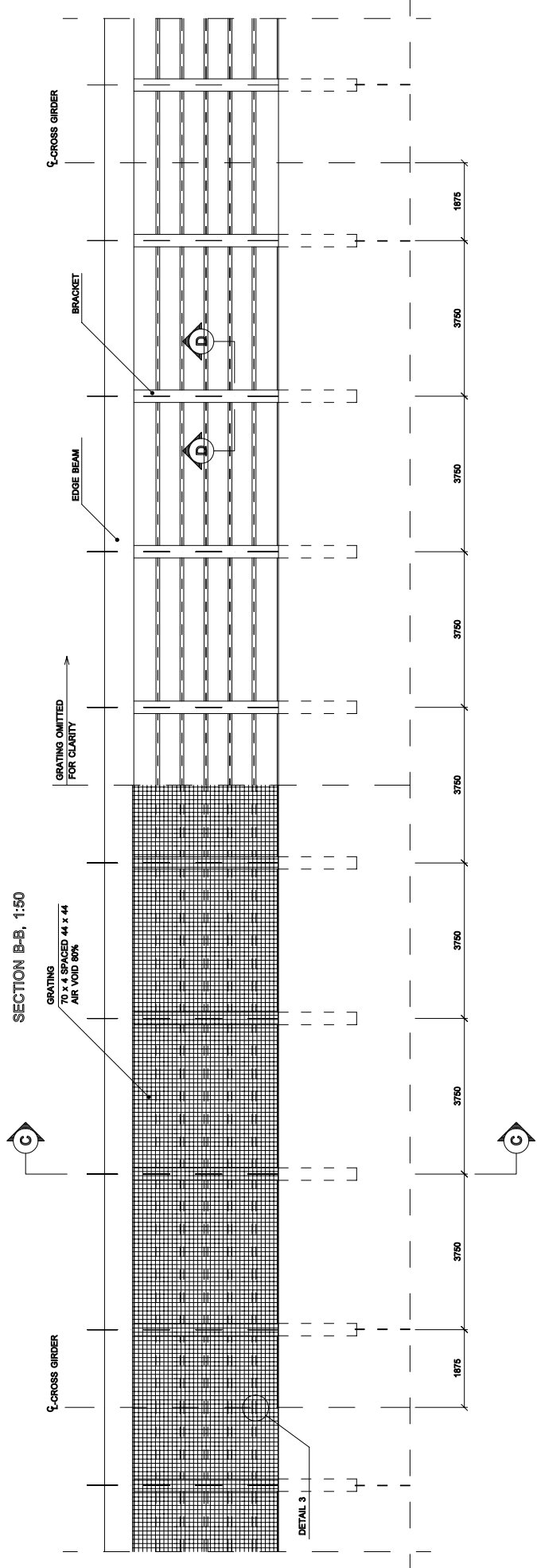
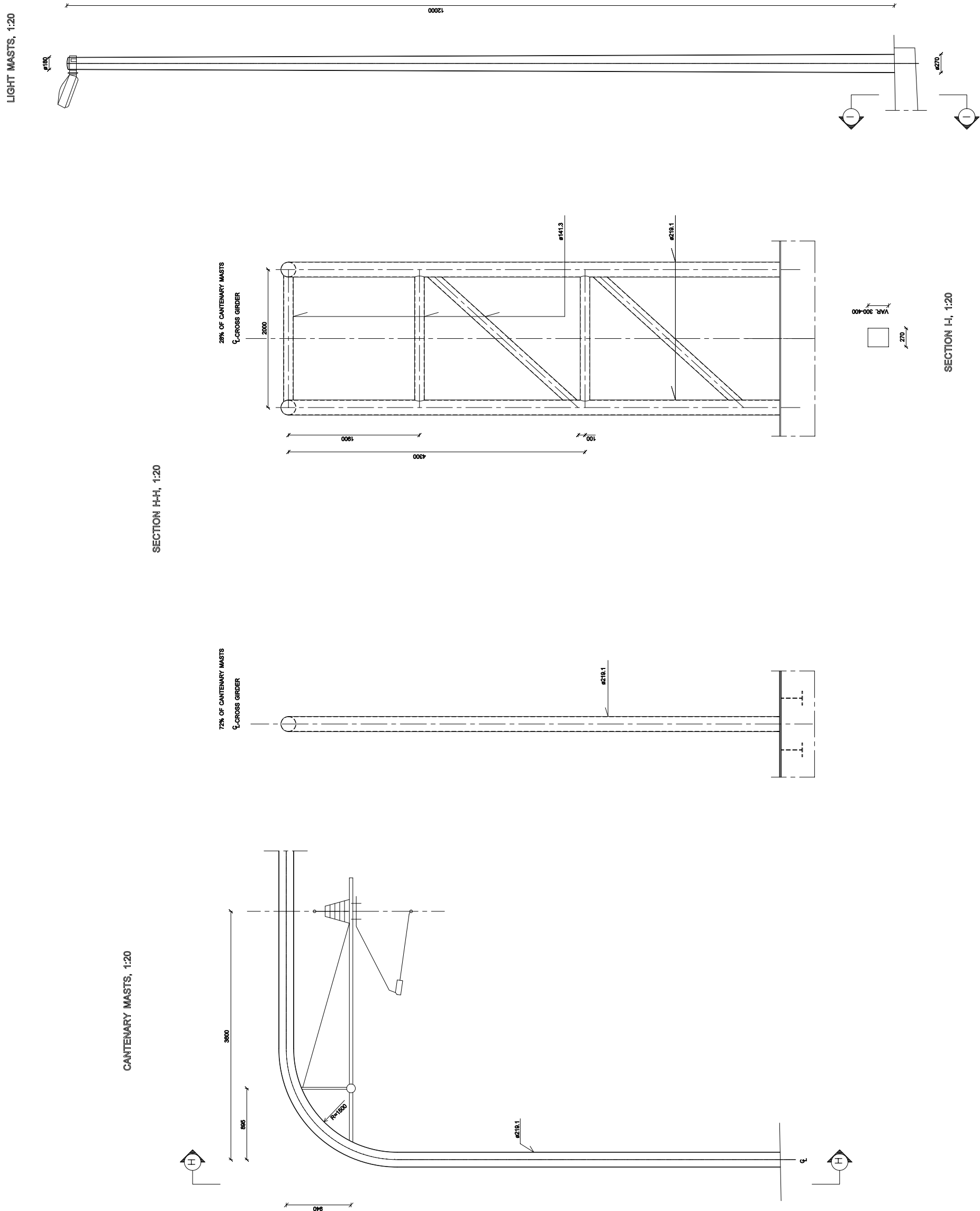


TABLE 1

TYPE 1		TYPE 2	
X (mm)	Y (mm)	X (mm)	Y (mm)
0	0	0	0
16	12	20	14
32	16	39	19
64	21	78	25
96	24	117	30
128	27	159	33
160	31	204	38
192	34	251	41
224	37	299	45
256	38	348	47
288	38	398	47
320	38	448	47

DIMENSIONS:  
ALL DIMENSIONS ARE IN MILLIMETRES UNLESS OTHERWISE STATED.

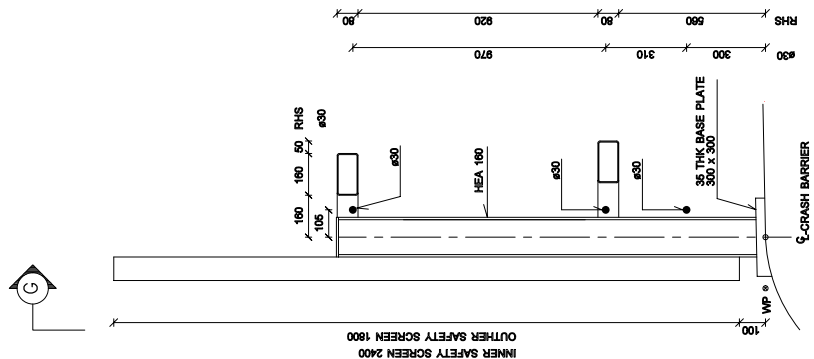


No.	Date	Description	Designer	Checked	Approved
<b>STRETTO DI MESSINA</b>					
<b>BRIDGE OVER THE MESSINA STRAIGHT</b>					
Project No.					
Designed: HEAL					
Checked: IPID					
Approved: A.M. / L.S.J.					
Scale:					
Date:					
Drawing No.:					
Sheet No.:					
Description:					
DRAWING FOR WIND TUNNEL TEST					
COMPILE 2					
DATE: 09/09/2011					
TIME: 14:45:52					
USER: 102					
DRAWING: 102					
SCALE: 1:20					
SHEET NO.: 00					

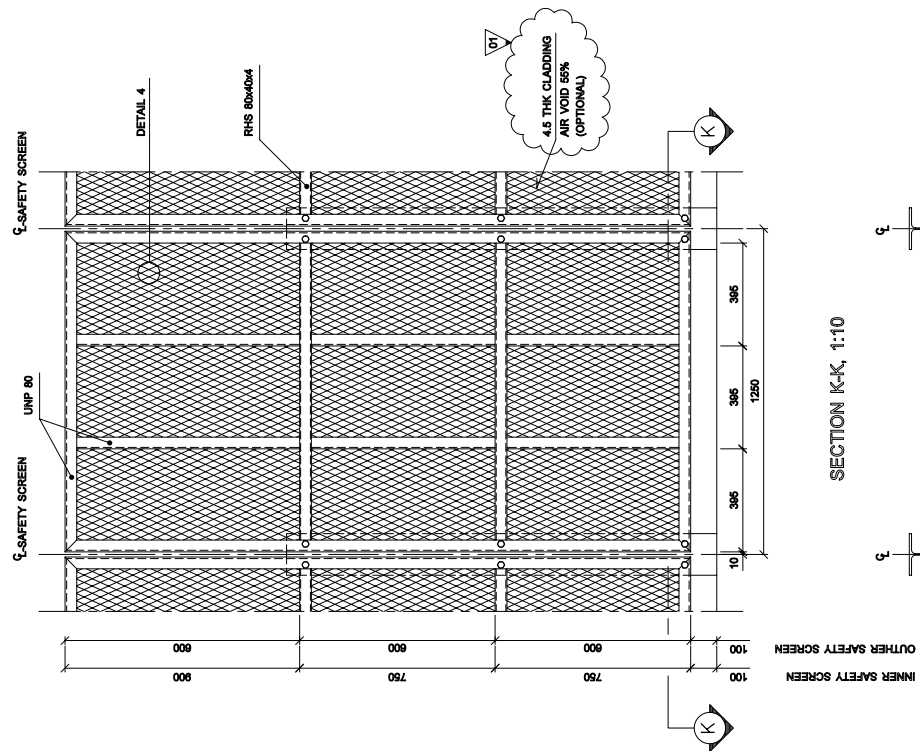
NOTE GENERALI

DIMENSIONS:  
ALL DIMENSIONS ARE IN MILLIMETRES UNLESS OTHERWISE STATED.

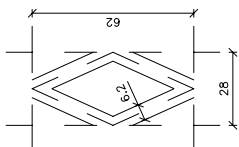
CRASH BARRIER, 1:10



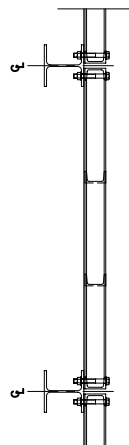
SECTION G-G, 1:10



DETAIL 4, 1:1



SECTION K-K, 1:10



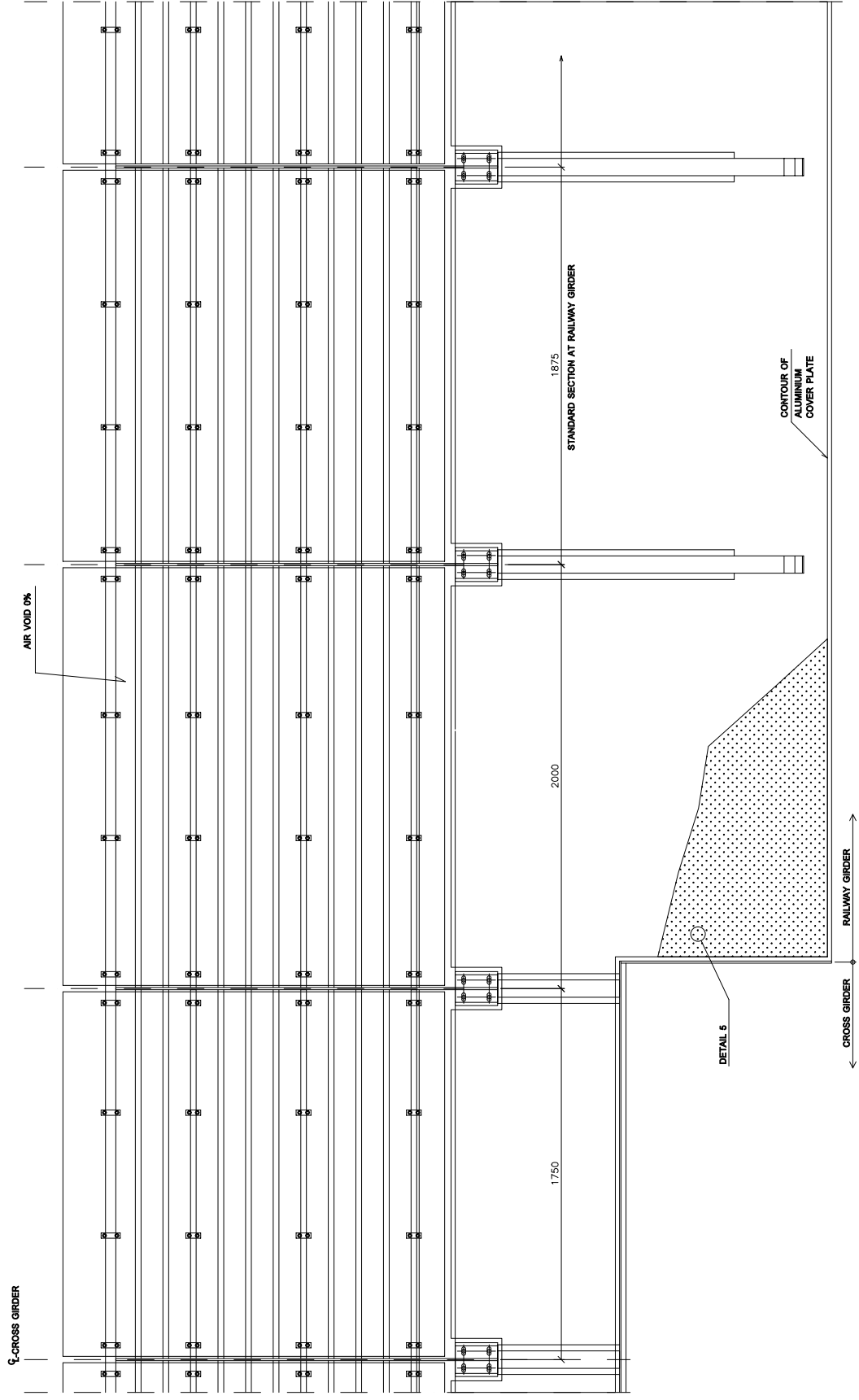
ST.	2019/04/27	ADDITIONAL INFO ADDED	HEAE	HPD	ALN
Rev.	1.00	Description	Designed	Checked	Approved

STRETTO DI MESSINA  
BRIDGE OVER THE MESSINA STRAIGHT

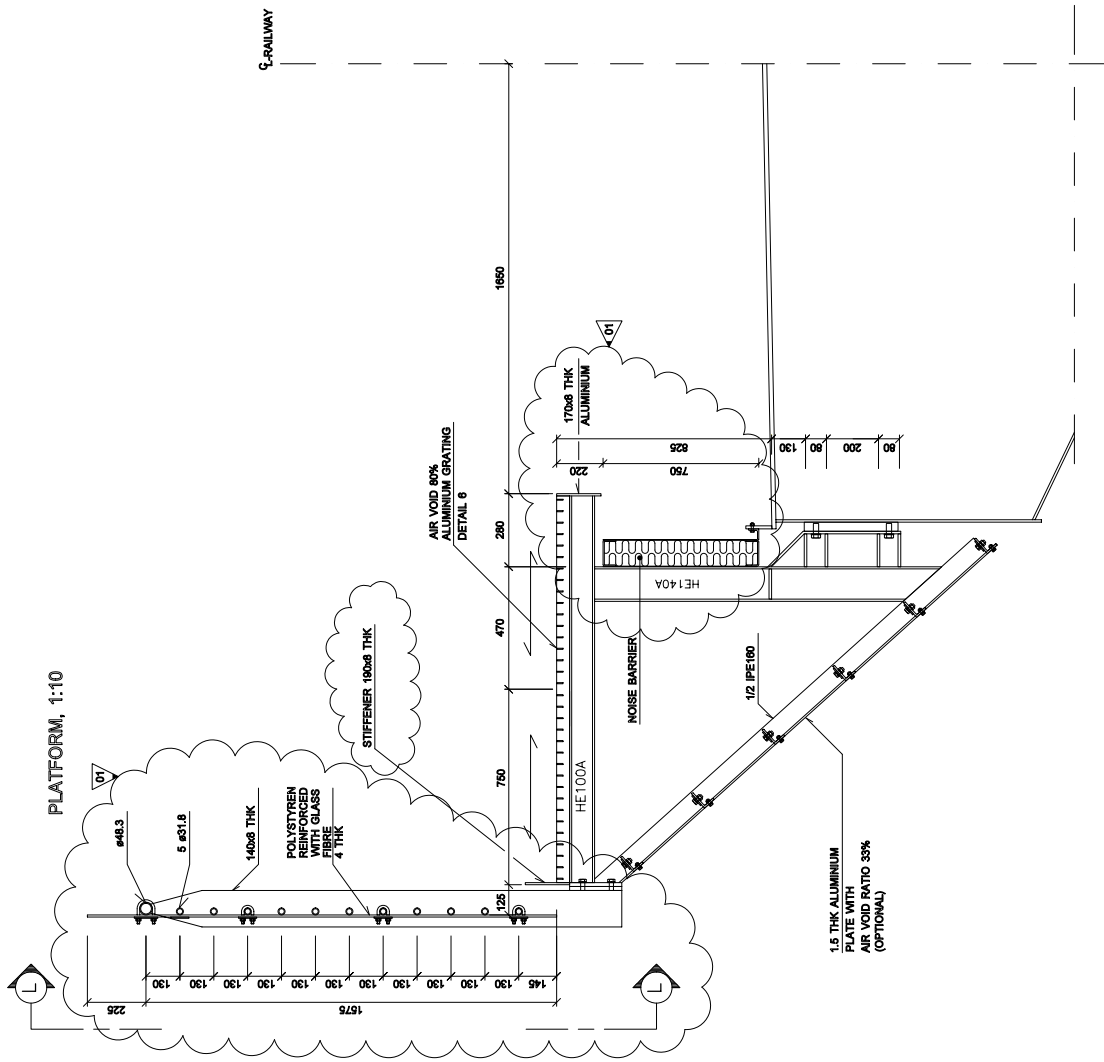
DESCRIPTION	SECTION FOR WIND TUNNEL TEST	Project No.	HEAE
DATE	2019/04/27	Designed	HPD
CLIENT	COMUNE DI MESSINA	Checked	ALN / L.S.J.
PROJECT NO.	103	Approved	ALN / L.S.J.
DATE	2019/04/27	Drawn	ALN / L.S.J.
PROJECT NO.	103	Scale	1:10
DATE	2019/04/27	Client No.	103
PROJECT NO.	103	Client Name	COMUNE DI MESSINA
DATE	2019/04/27	Client Address	Strada 2
PROJECT NO.	103	Client Phone	Tel. +39 09 67 21 12
DATE	2019/04/27	Client Email	info@comune.messina.it
PROJECT NO.	103	Client Website	www.comune.messina.it



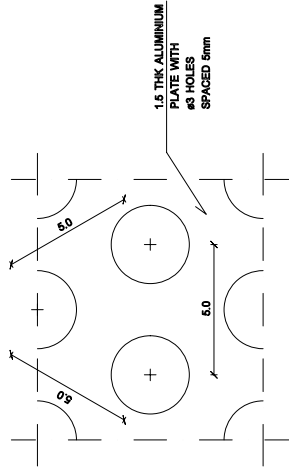
SECTION L-L, 1:10



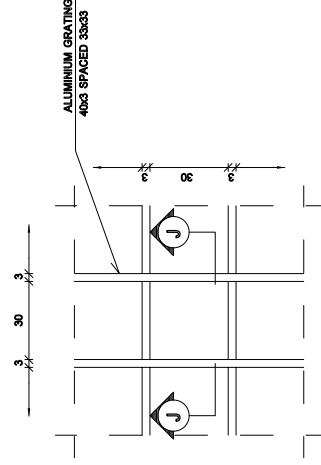
PLATFORM, 1:10



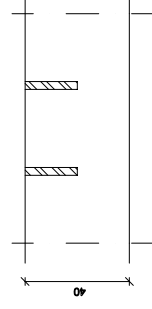
DETAIL 5



DETAIL 6, 1:1



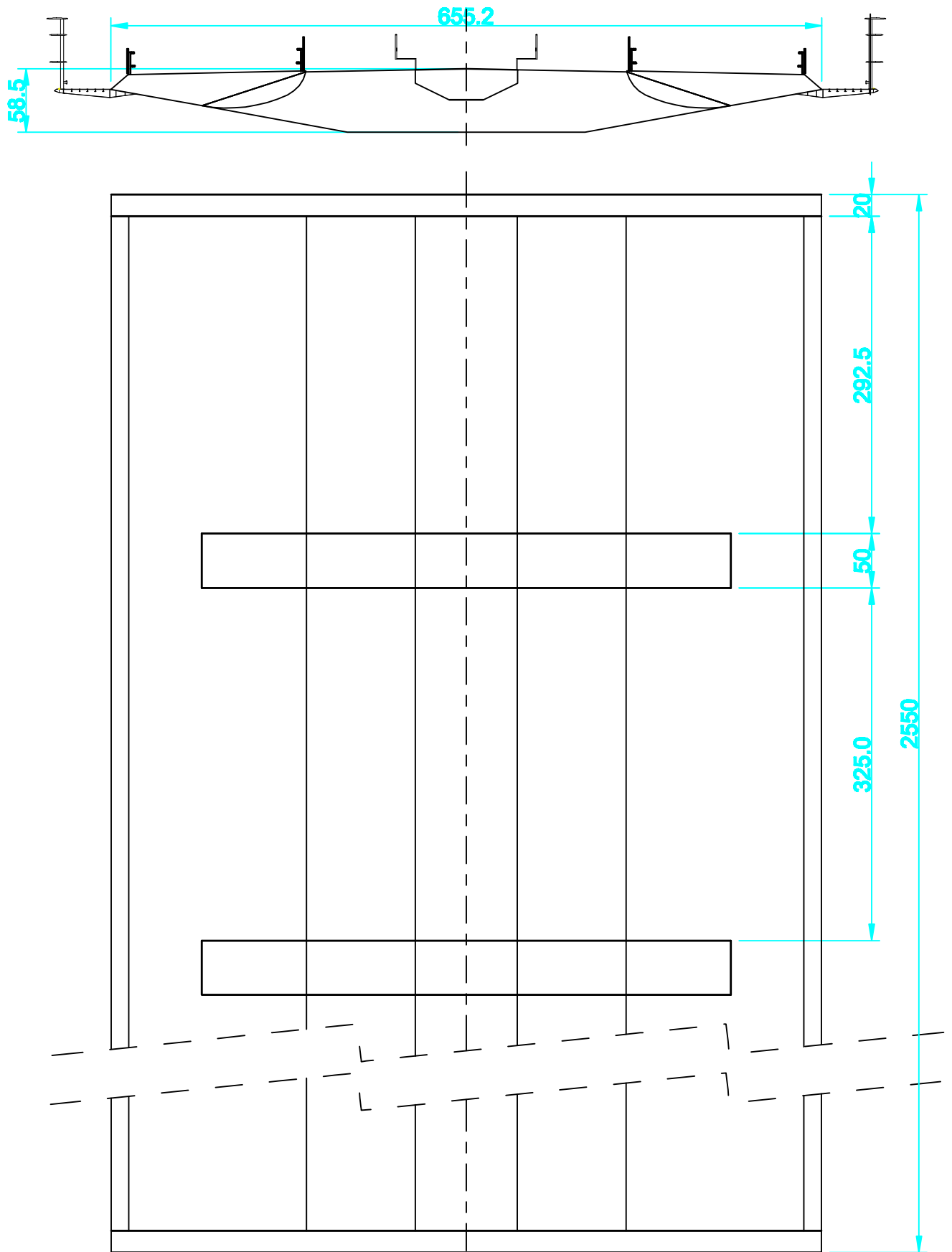
SECTION J-J



Project No.	HE/AL
Design No.	HE/AL
Checked	HE/AL
Approved	HE/AL
Date	HE/AL
Issue No.	HE/AL
Scale	HE/AL
Project Name	HE/AL
Client	HE/AL
Contract No.	HE/AL
Project No.	HE/AL
Design No.	HE/AL
Checked	HE/AL
Approved	HE/AL
Date	HE/AL
Issue No.	HE/AL
Scale	HE/AL
Project Name	HE/AL
Client	HE/AL
Contract No.	HE/AL

STRETTO DI MESSINA  
 BRIDGE OVER THE MESSINA STRAIGHT  
 Project No. HE/AL  
 Design No. HE/AL  
 Checked HE/AL  
 Approved HE/AL  
 Date HE/AL  
 Issue No. HE/AL  
 Scale HE/AL  
 Project Name HE/AL  
 Client HE/AL  
 Contract No. HE/AL

104



- Division for Maritime Industry

SCALE	DRAWN BY	TITLE	CHECKED BY	TITLE	ACCEPTED BY
	TER				
	DATE	DIP	GENERAL DRAWING		
	2010-05-08		P---		

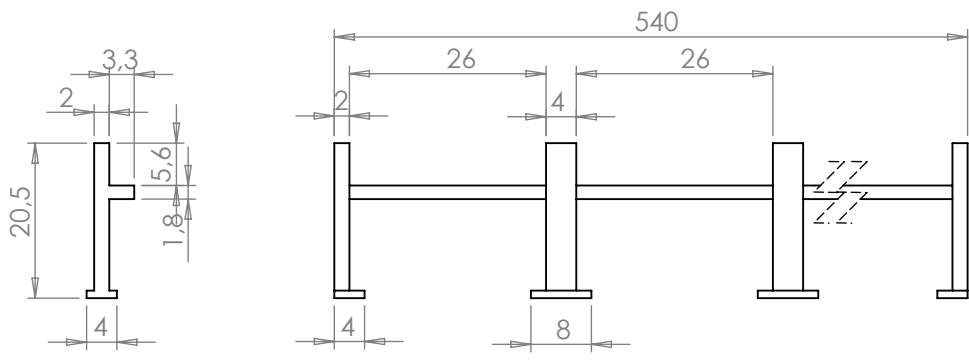
DRAWING NAME

**BRIDGEDECK**

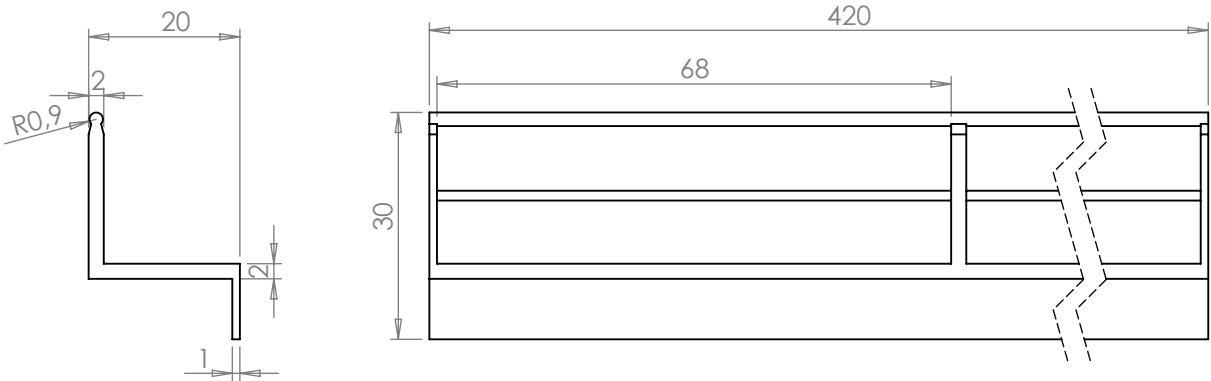
DMI	DRAWING NUMBER	INDEX	SHEET
	110-25485	A	

filename/path=110-25465\_railingsX:\Tasks\110\110-25465\Technical data\Drawings\

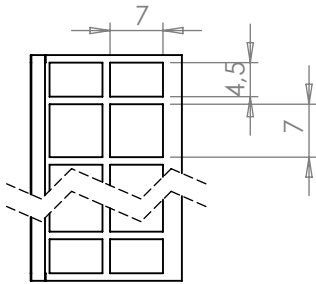
A  
B  
C  
D  
E  
F



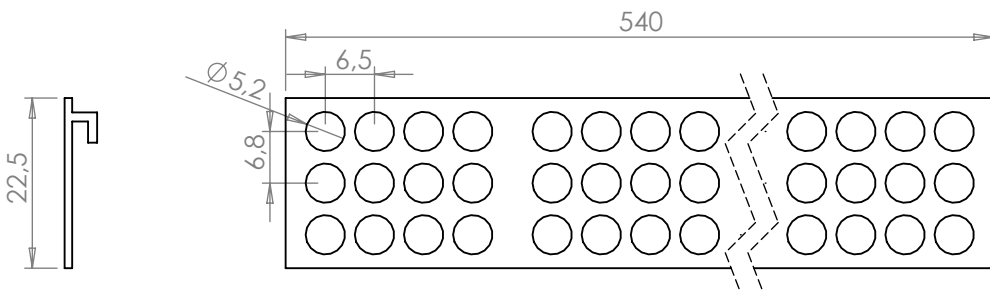
110-25465\_crash\_barrier




110-25465\_railway\_platform



110-25465\_safety\_screen\_22,5



DO NOT SCALE DRAWING	
	
DRAWN TER	DATE 09-06-2010
TITLE:	
DWG NO. 110-25465_railings	A4
SCALE:1:1	SHEET 1 OF 3

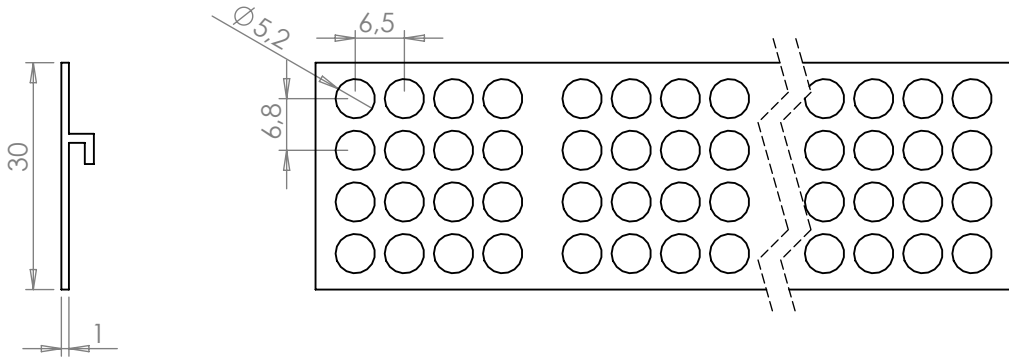
1

2

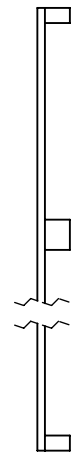
3

4

A



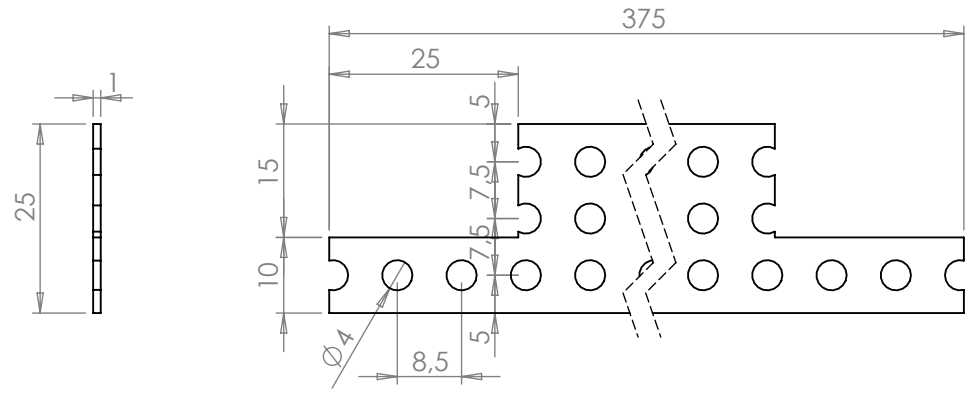
B



C

110-25465\_safety\_screen\_30


D



E

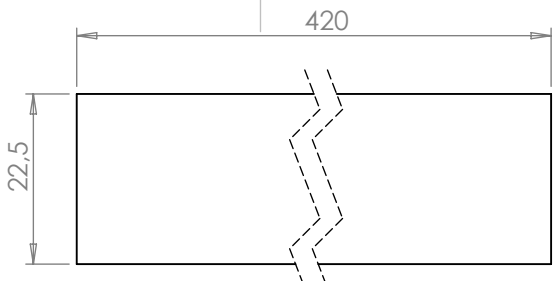
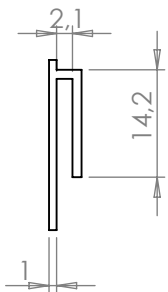
110-25465\_soffit\_plate

F

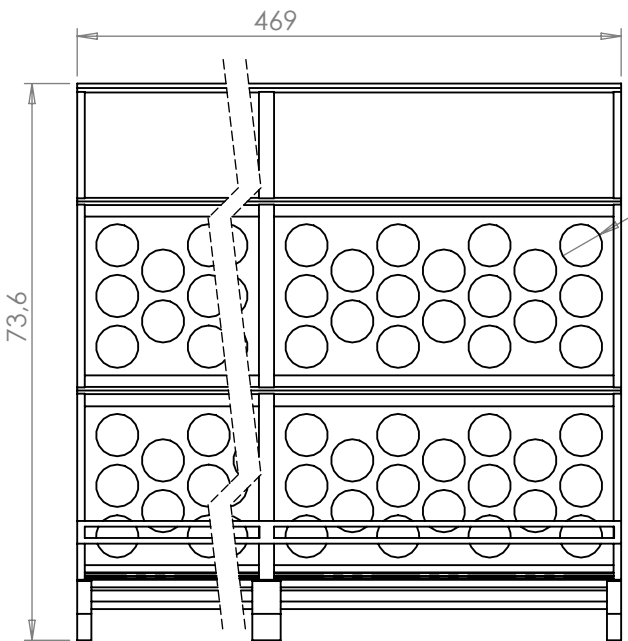
DO NOT SCALE DRAWING	
	
DRAWN	TER
DATE	09-06-2010
TITLE:	
DWG NO.	110-25465_railings
	A4
SCALE: 1:1	SHEET 2 OF 3

filename/path=110-25465\_railingsX:\Tasks\110\110-25465\Technical data\Drawings\

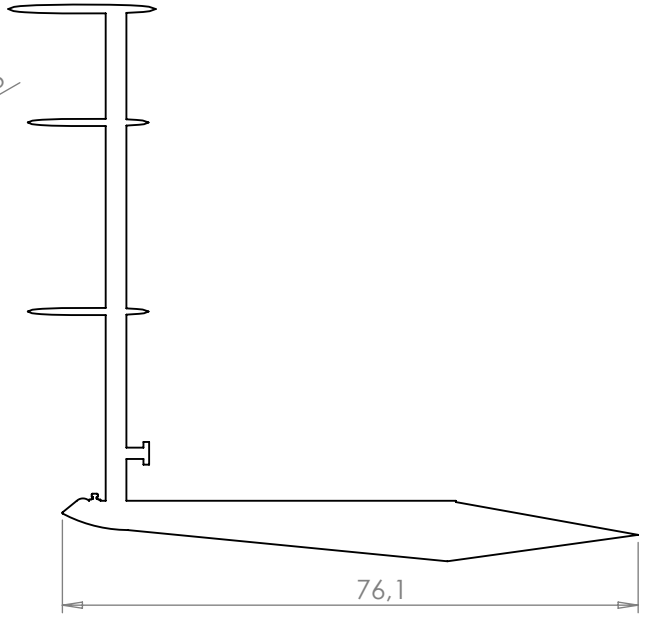
A  
B  
C  
D  
E  
F



110-25465\_solid\_fence

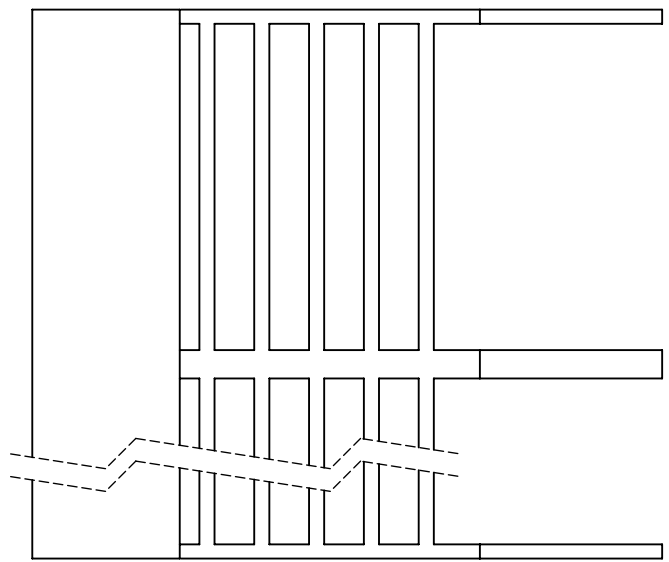


Ø5,6



76,1

110-25465\_windscreen



DO NOT SCALE DRAWING



DRAWN TER DATE 09-06-2010

TITLE:

DWG NO. 110-25465\_railings A4

SCALE: 1:1 SHEET 3 OF 3

## APPENDIX B

### The Boundary-Layer Wind Tunnel II

## Wind Tunnel II

FORCE Technology's 2.6 m wide x 1.8 m high x 21 m long Boundary-Layer Wind Tunnel II is used for variety of studies. This wind tunnel has maximum wind speed of 24 m/s when empty. The ceiling of the wind tunnel was adjusted so that it was horizontal throughout the length of the wind tunnel. A principle sketch of this wind tunnel is given in Figure 0.1.

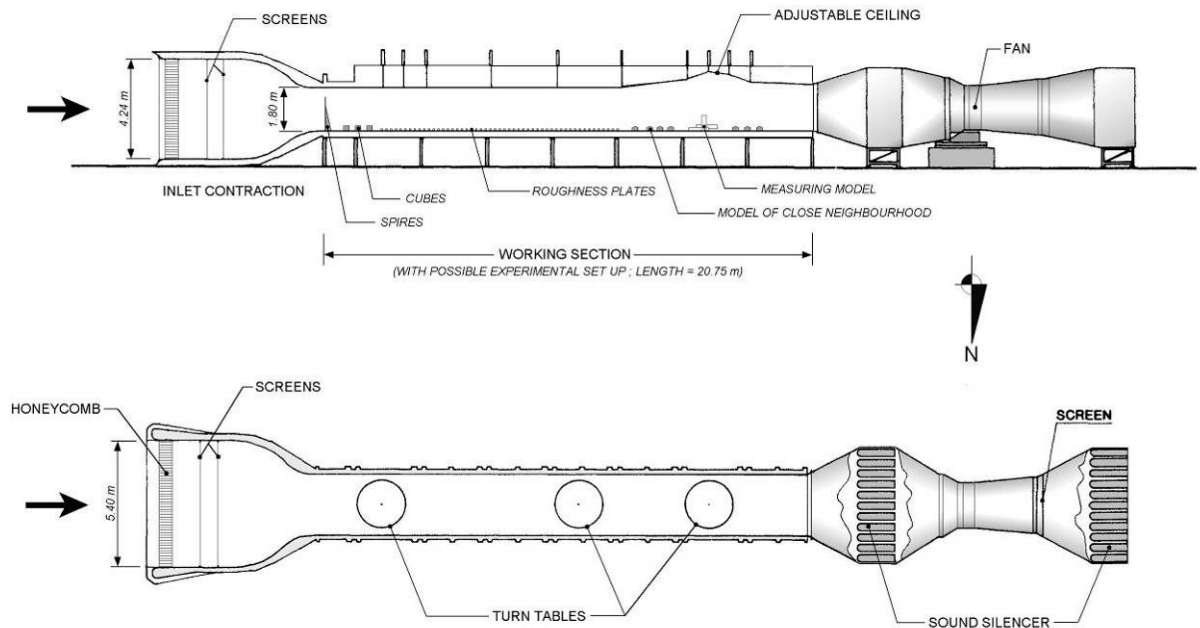


Figure 0.1. FORCE Technology's Boundary-Layer Wind Tunnel II.



Figure B.1. View along BLWT in Flow Direction.

The tunnel consists of an inlet section, a working section and a fan section. The air is sucked through the wind tunnel and returned through the building in which the wind tunnel is situated. In the inlet section, the air passes through a honeycomb, two fine-meshed nets and a contraction. Thus, a flow with uniform velocity and very little turbulence can be obtained. The working section has the following principal dimensions:

Length = 20.8 m  
 Width = 2.6 m  
 Height = 1.8 - 2.3 m (adjustable).

The long working section is necessary to build up a natural boundary-layer wind profile.

## APPENDIX C

### Damping Documentation



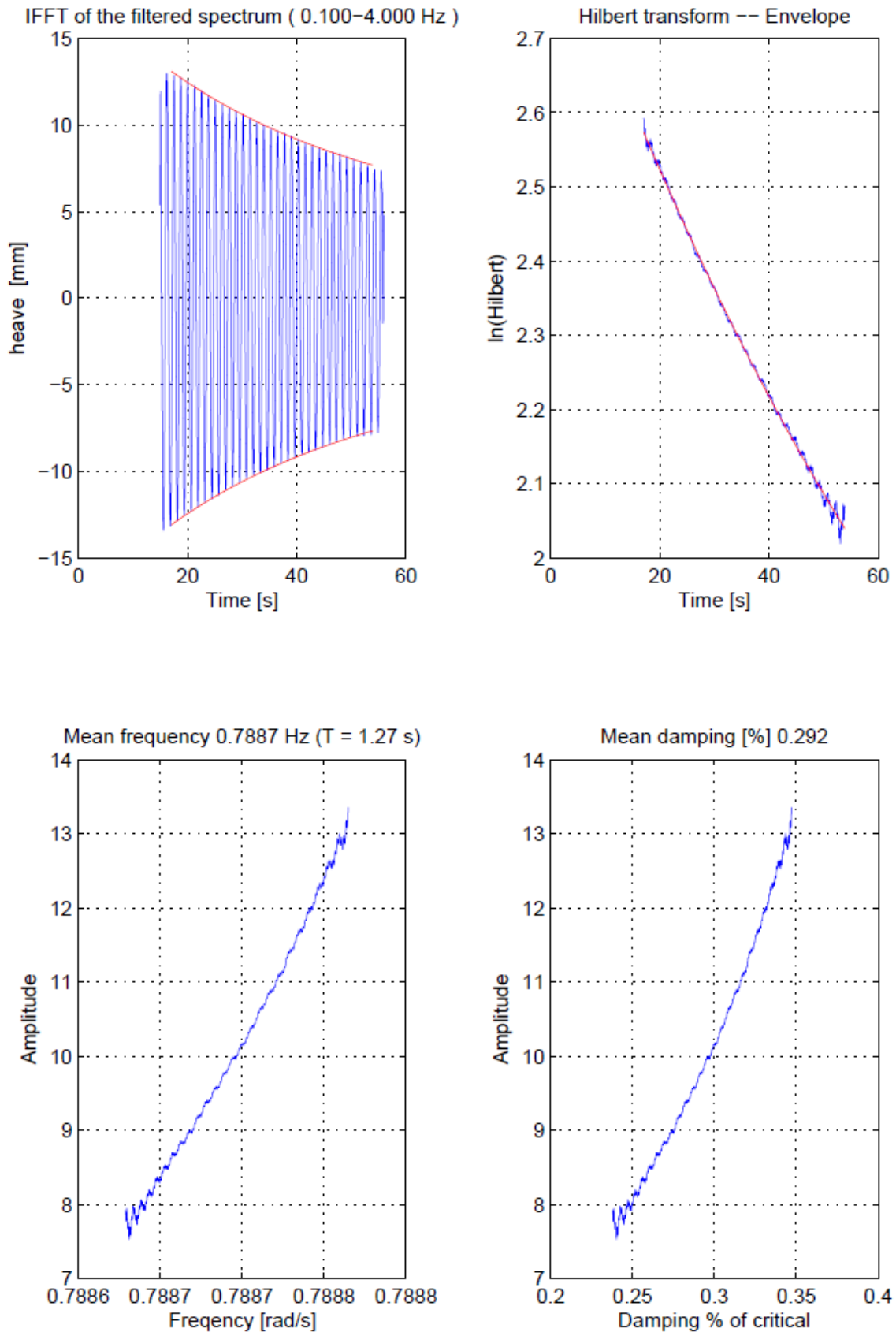


**Figure C.1. Stability tests – soft rig – heave damping**

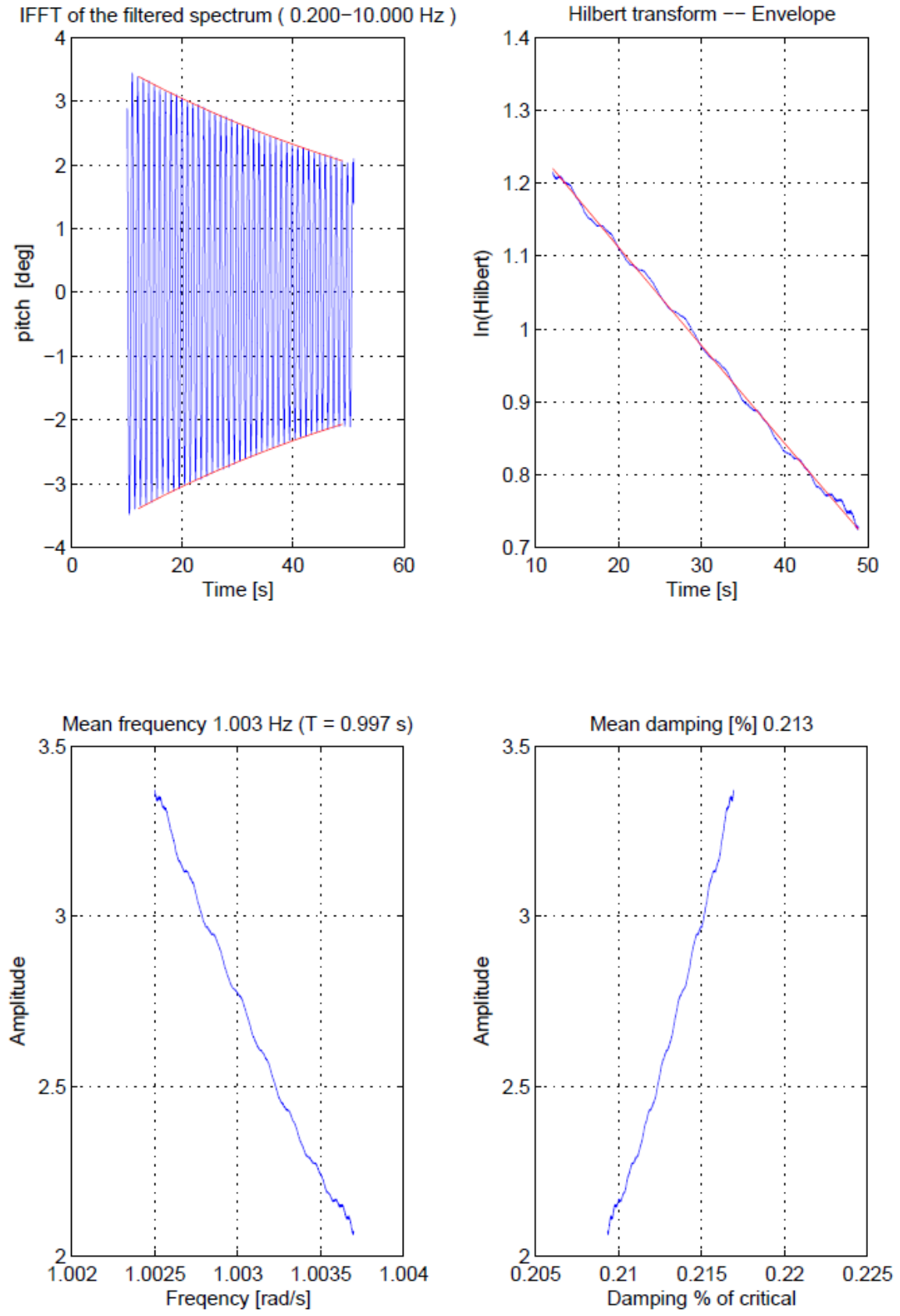


**Figure C.2. Stability tests – soft rig – pitch damping**

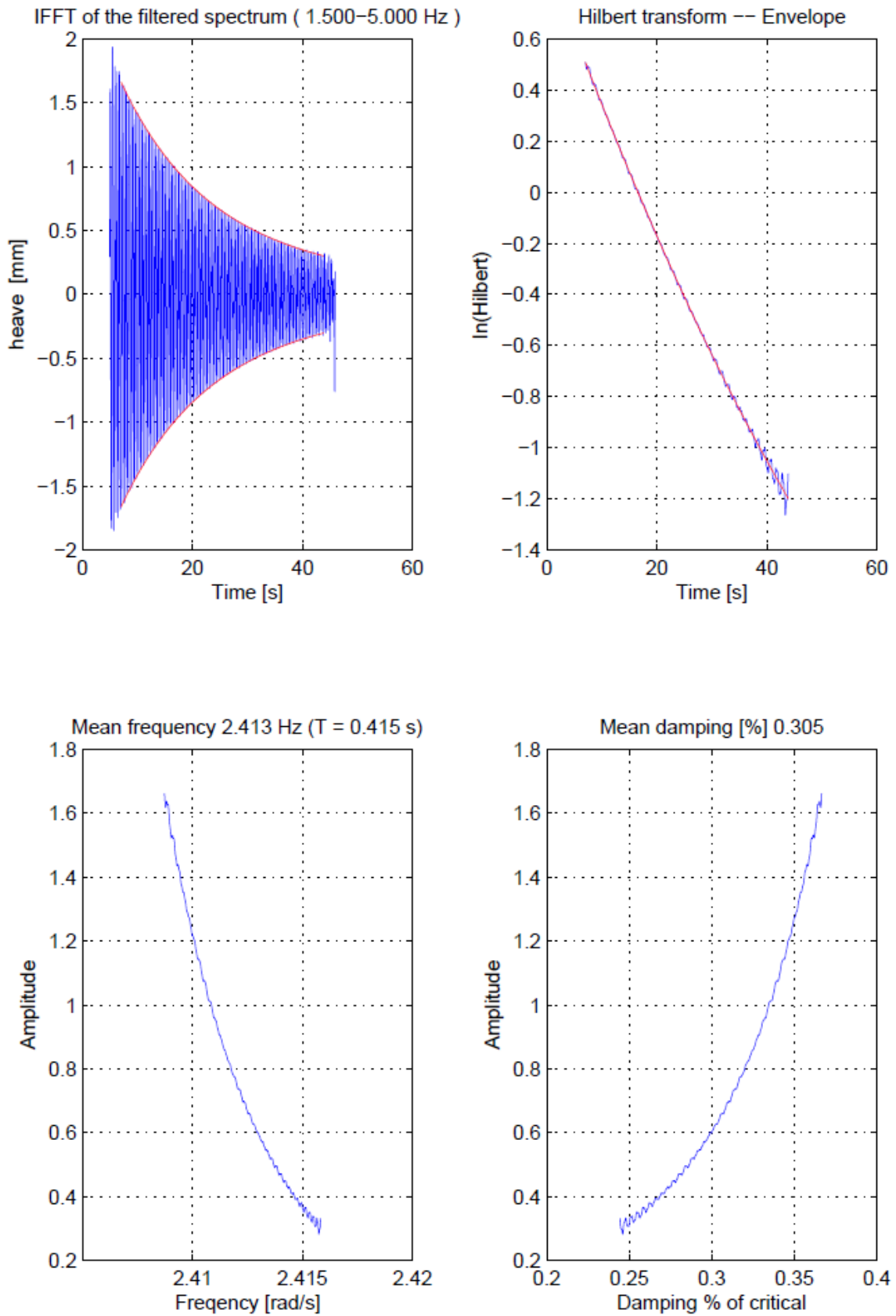


**Figure C.3. Vortex tests – stiff rig – heave damping**

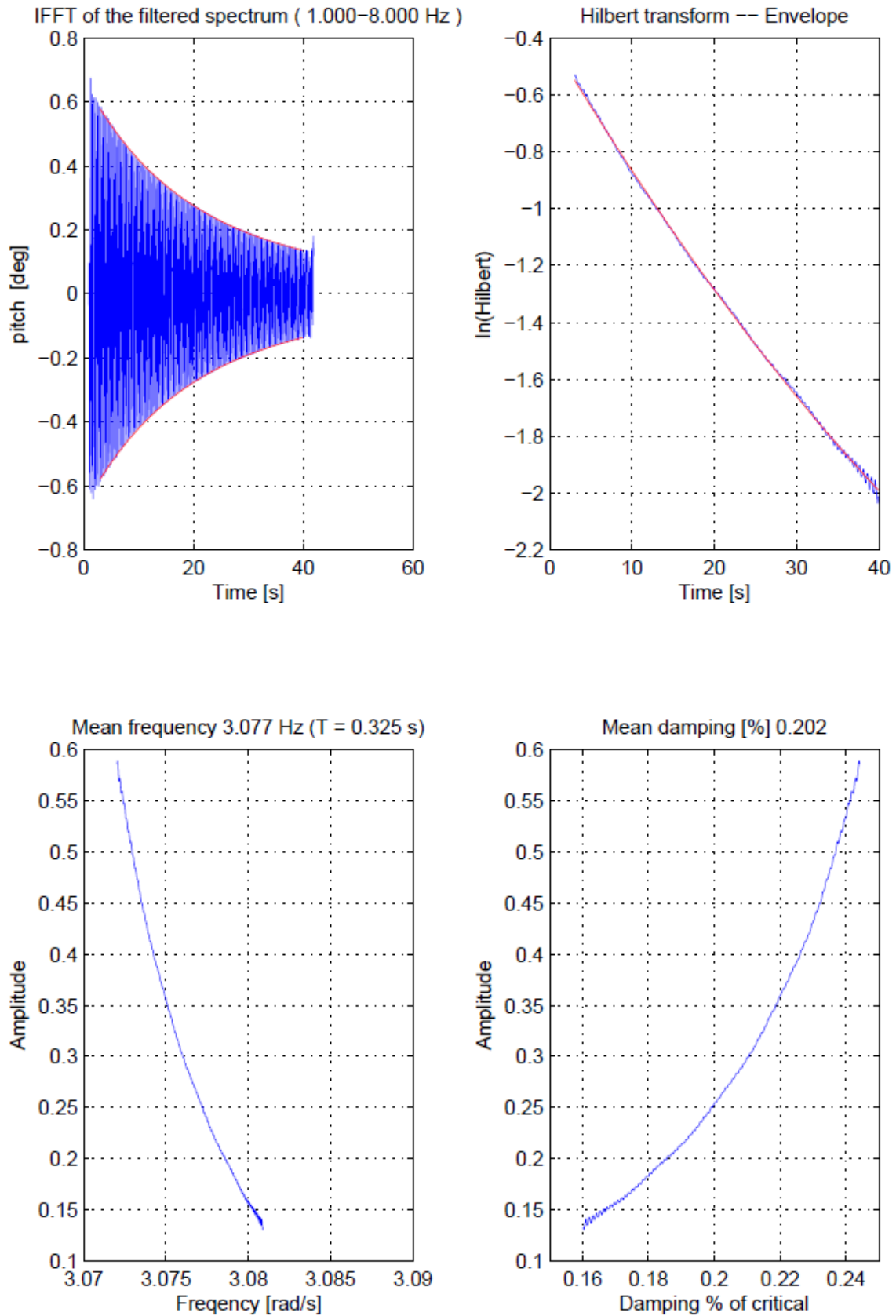
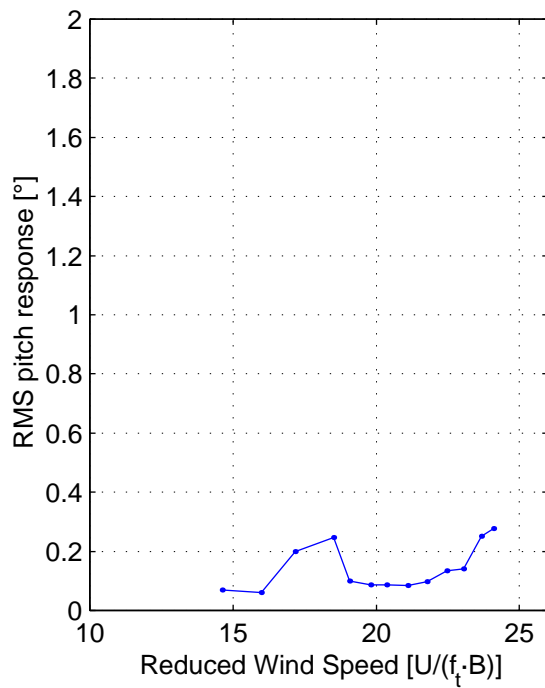
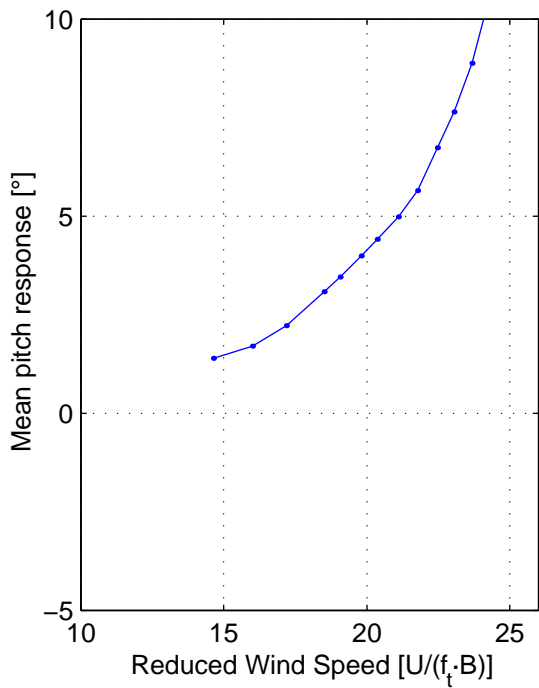
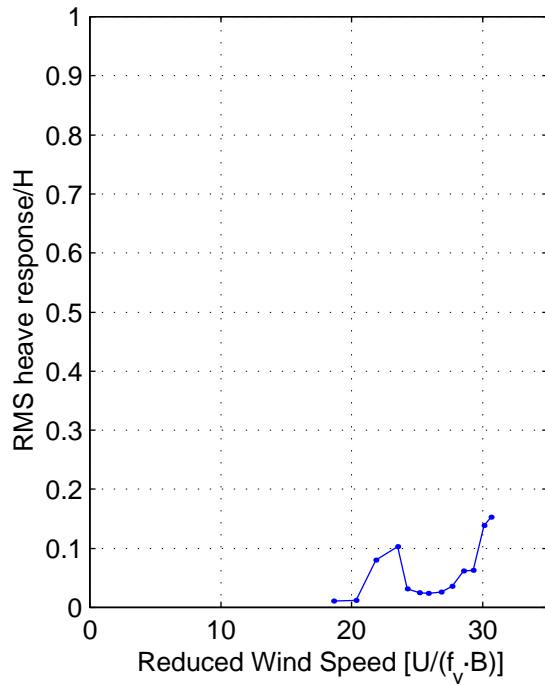
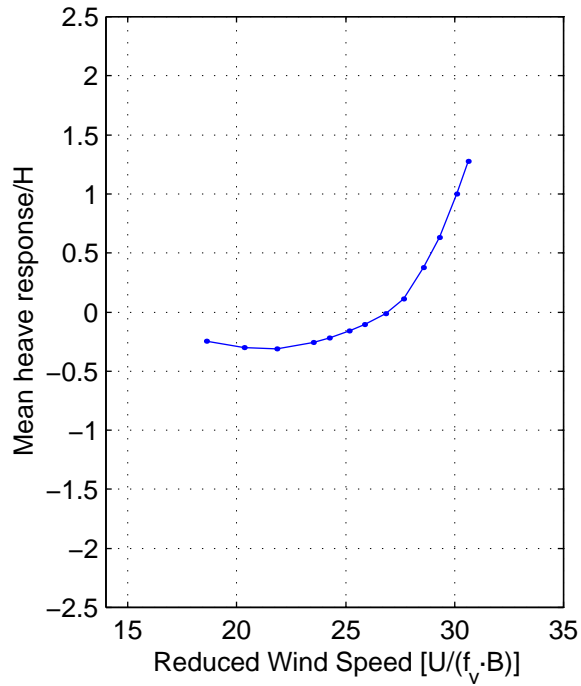


**Figure C.4. Vortex tests – stiff rig – pitch damping**

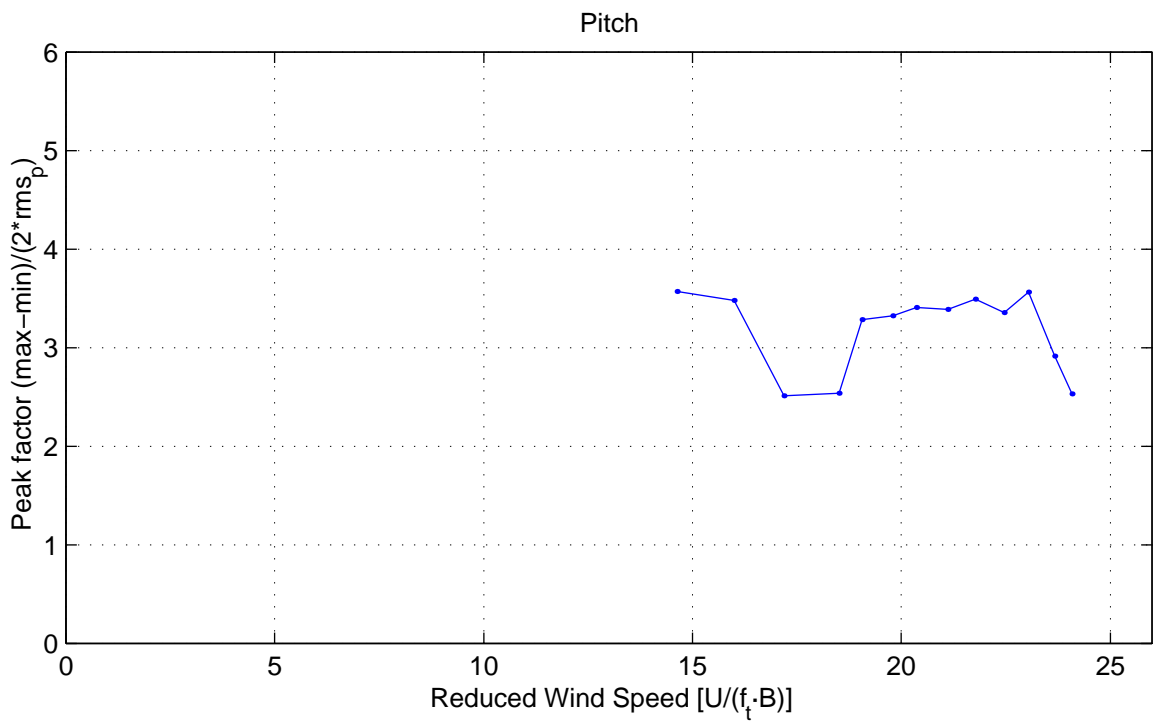
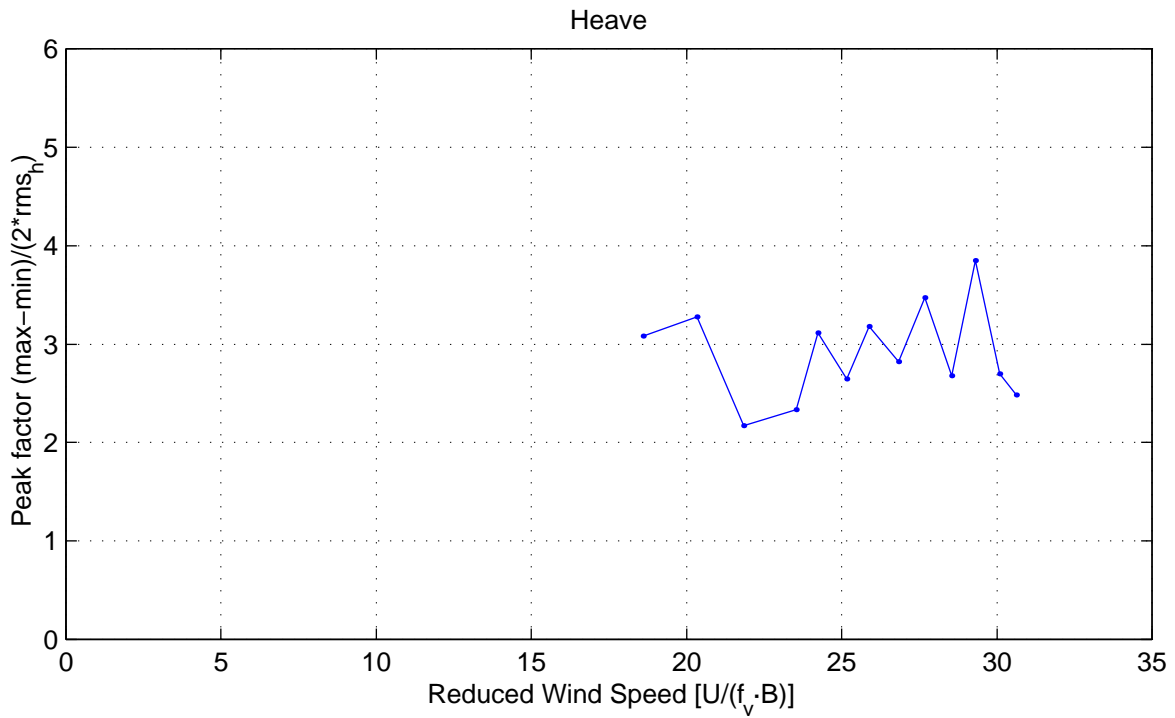
## APPENDIX D

### Stability Tests – Response Plots



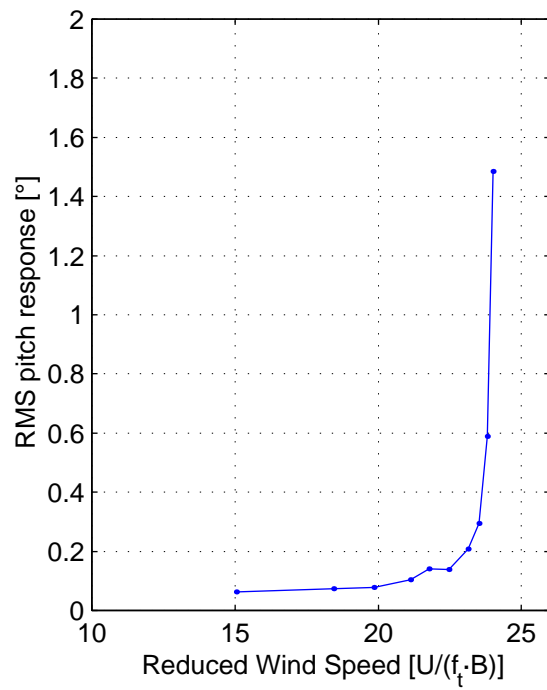
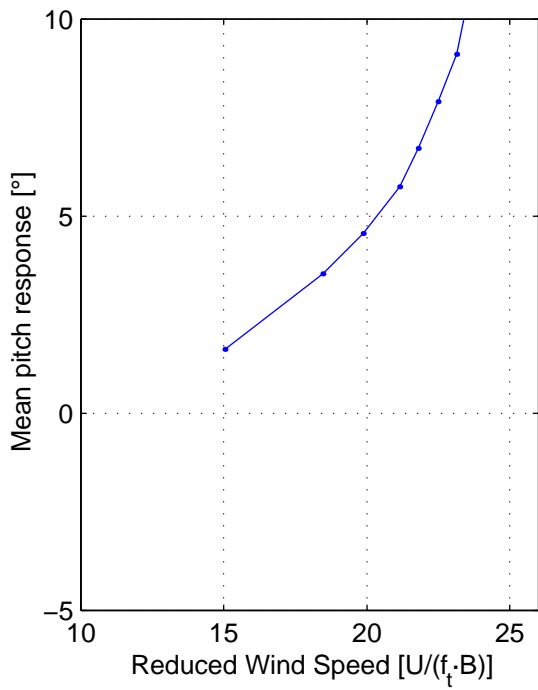
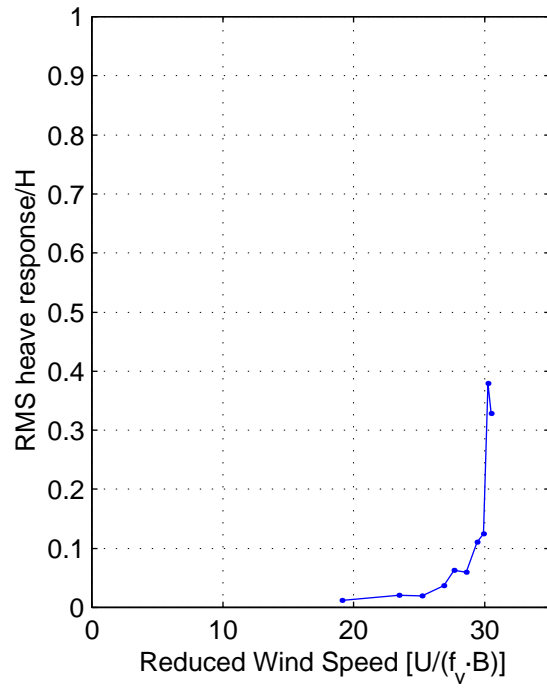
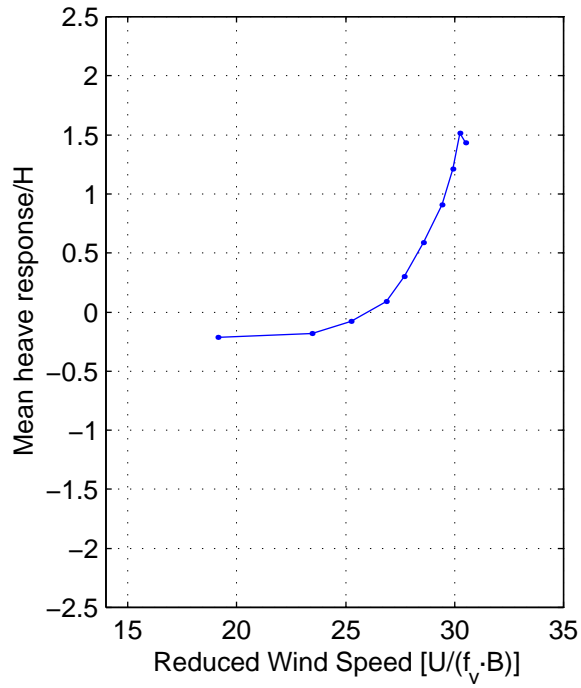
110-25465 Messina Strait Bridge  
 09-Jun-2010 /svl, stab.m  
 Mean and RMS Response

Stability Tests  
 Configuration C1  
 Smooth flow,  $\alpha = 0^\circ$

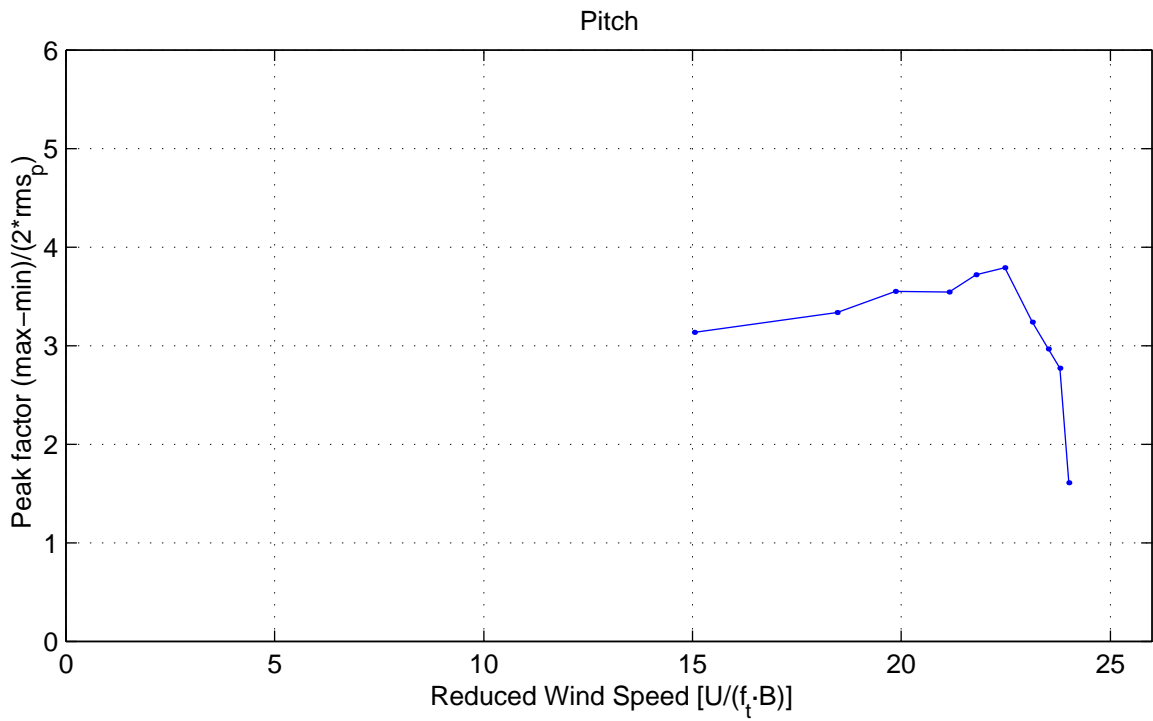
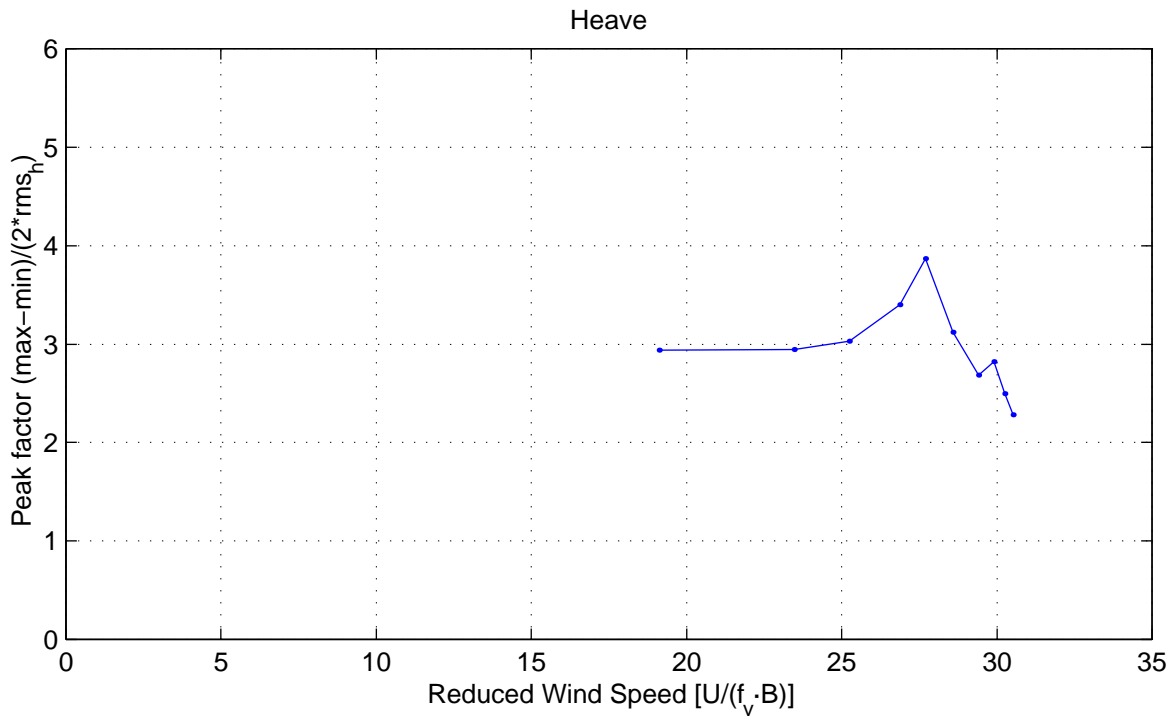


**110-25465 Messina Strait Bridge**  
 09-Jun-2010 /svl, stab.m  
 Peak factors

Stability Tests  
 Configuration C1  
 Smooth flow, α = 0°

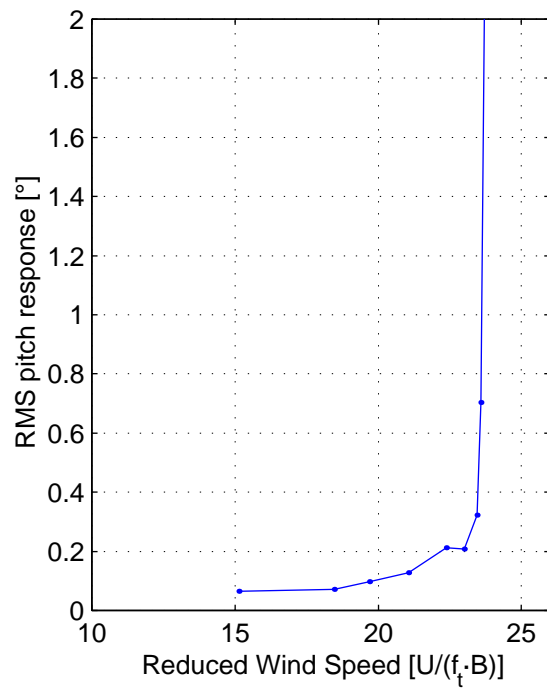
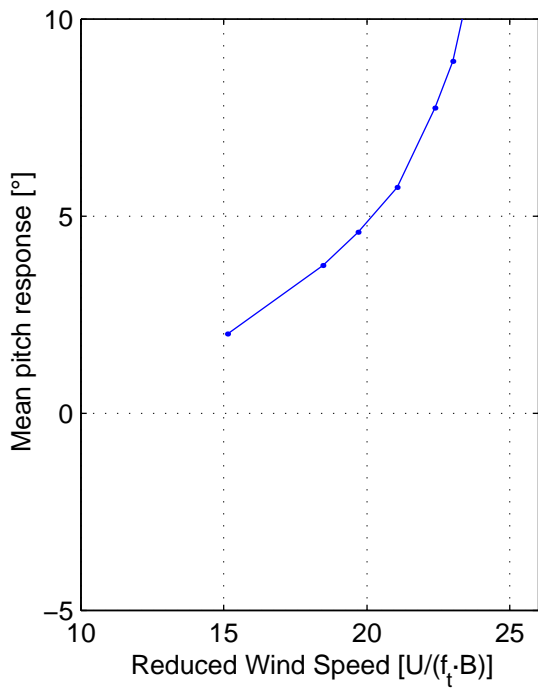
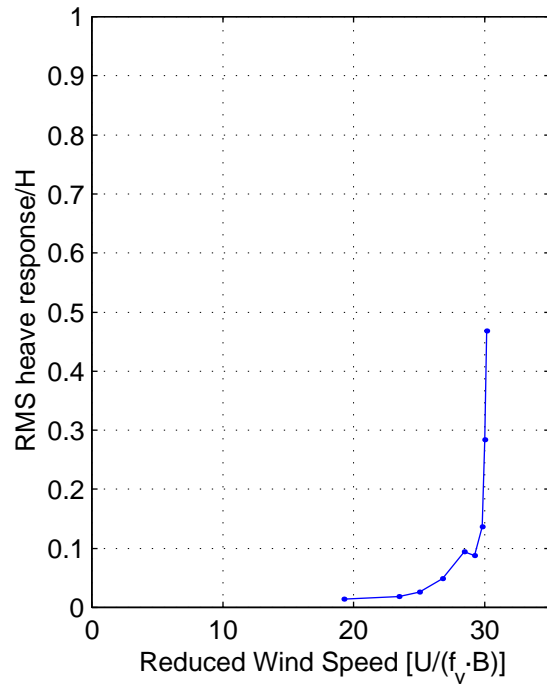
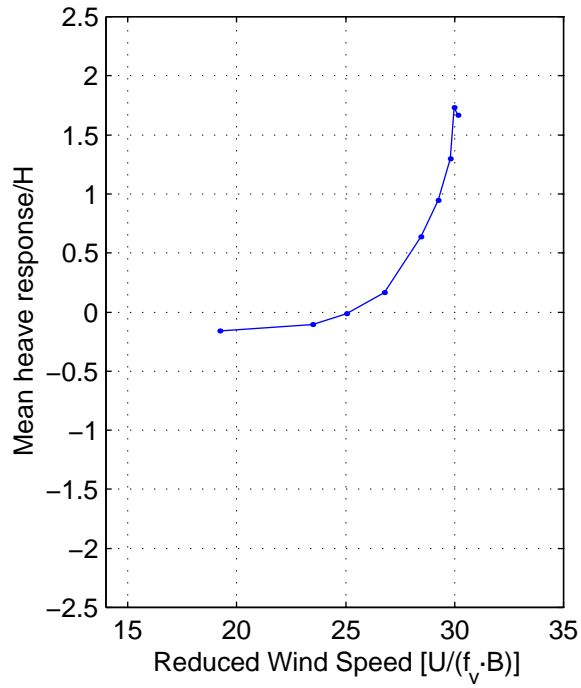






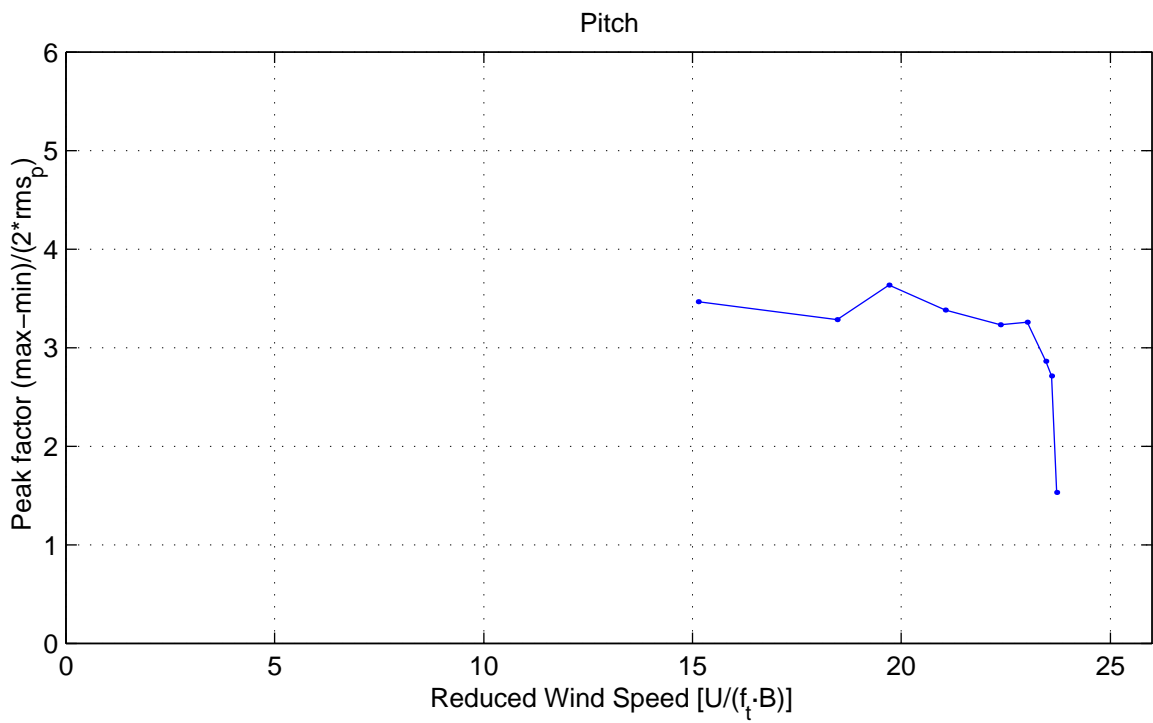
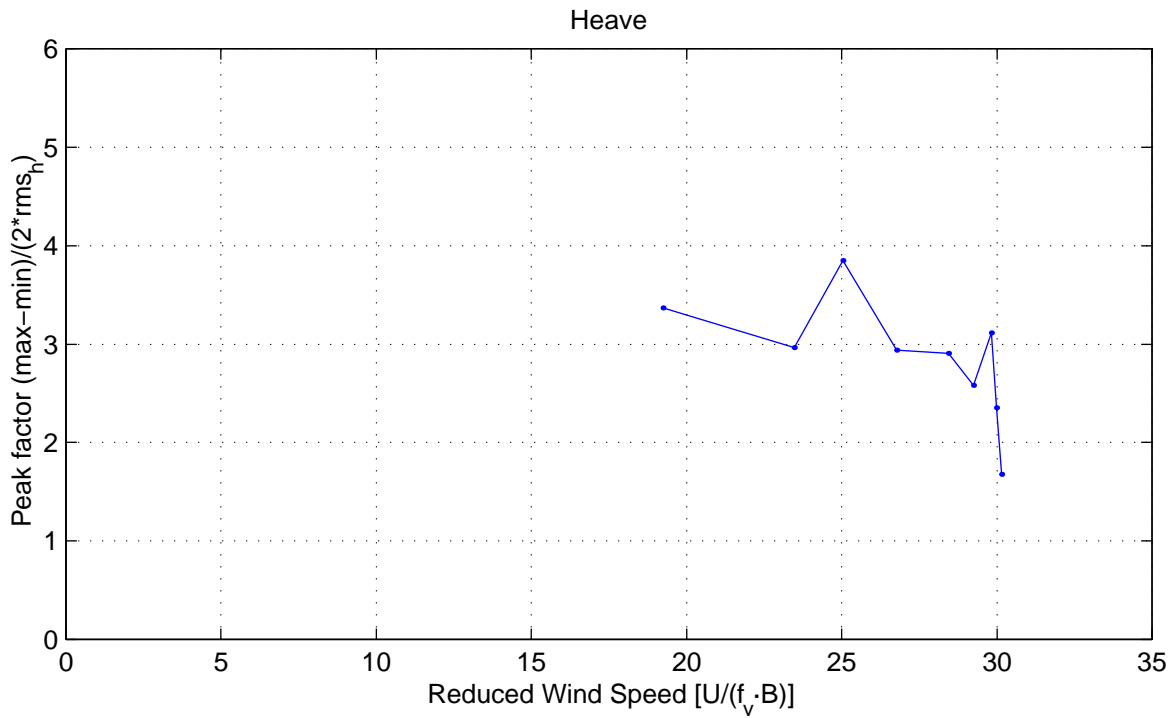
**110-25465 Messina Strait Bridge**  
 09-Jun-2010 /svl, stab.m  
 Peak factors

Stability Tests  
 Configuration C2  
 Smooth flow,  $\alpha = 0^\circ$



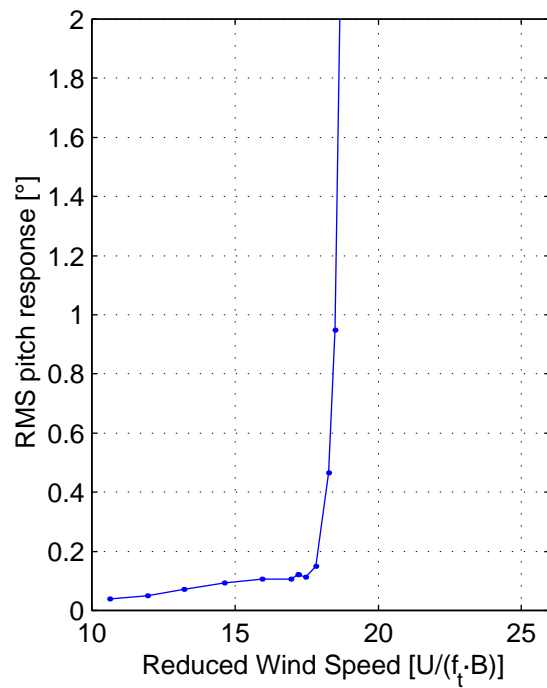
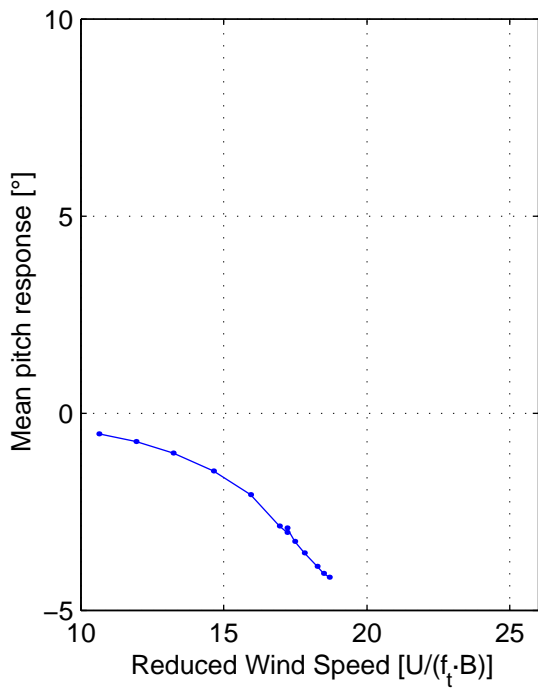
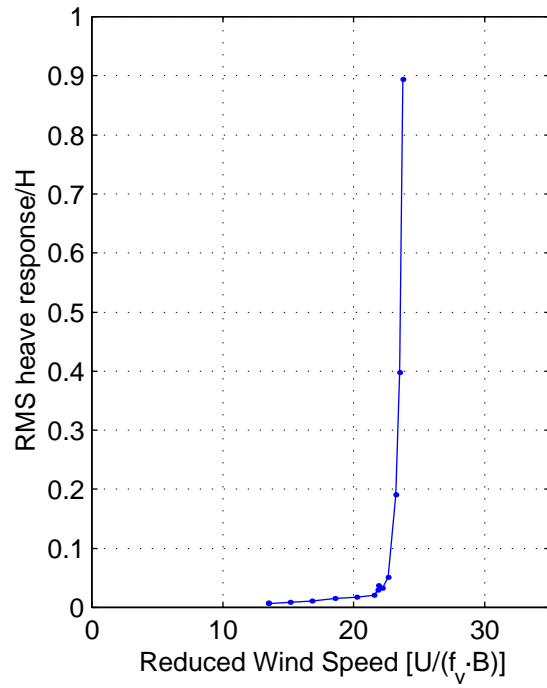
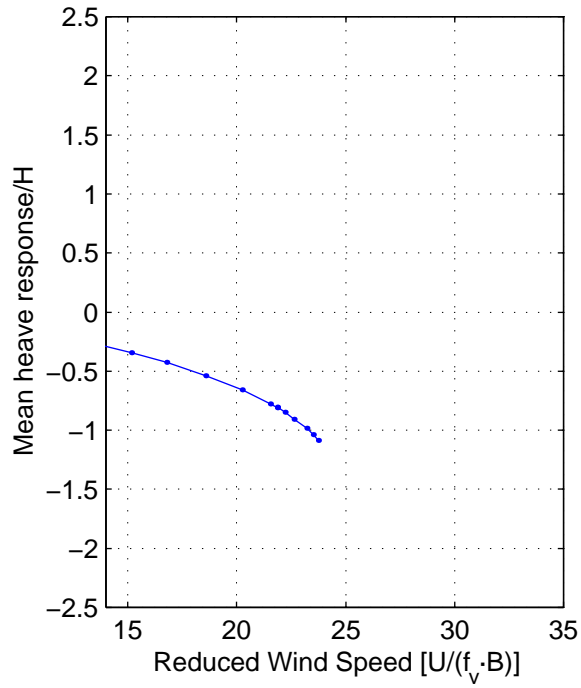
110-25465 Messina Strait Bridge  
 09-Jun-2010 /svl, stab.m  
 Mean and RMS Response

Stability Tests  
 Configuration C3  
 Smooth flow,  $\alpha = 0^\circ$



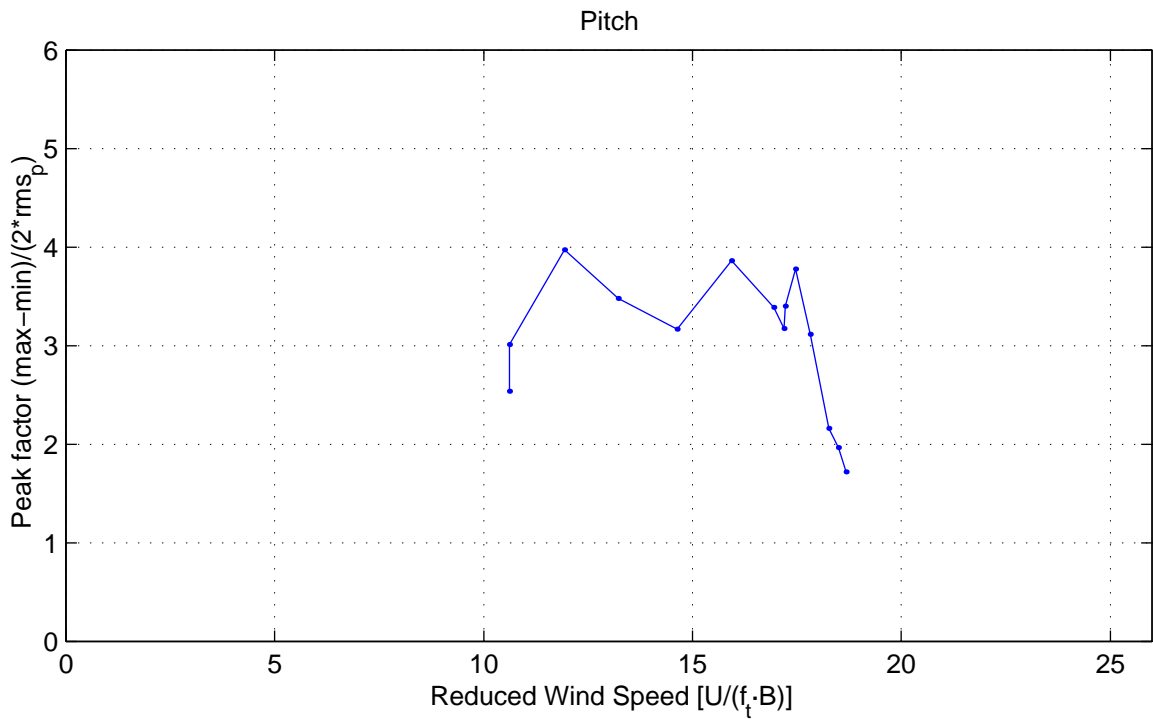
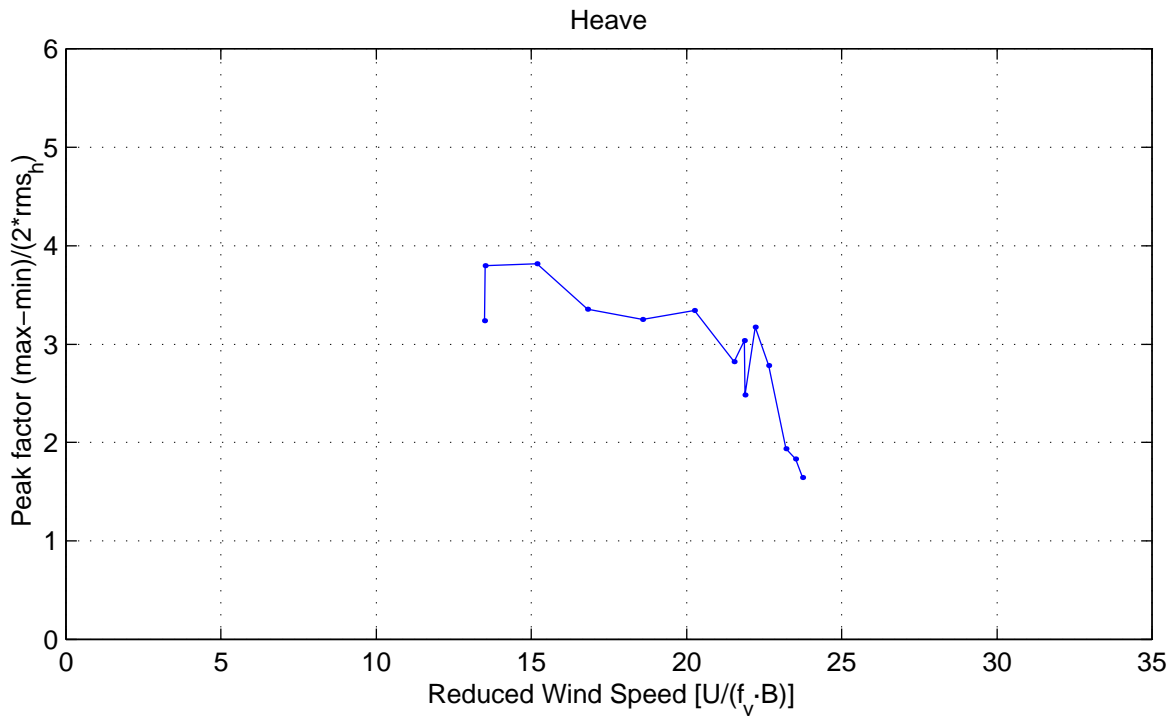
**110-25465 Messina Strait Bridge**  
 09-Jun-2010 /svl, stab.m  
 Peak factors

Stability Tests  
 Configuration C3  
 Smooth flow, α = 0°



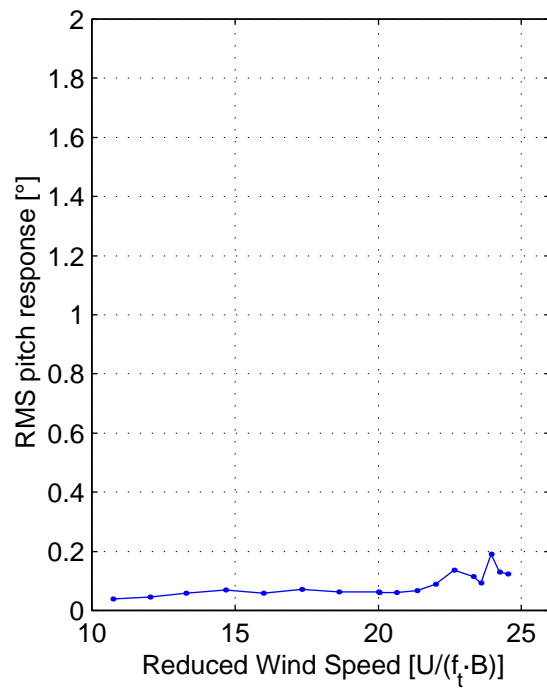
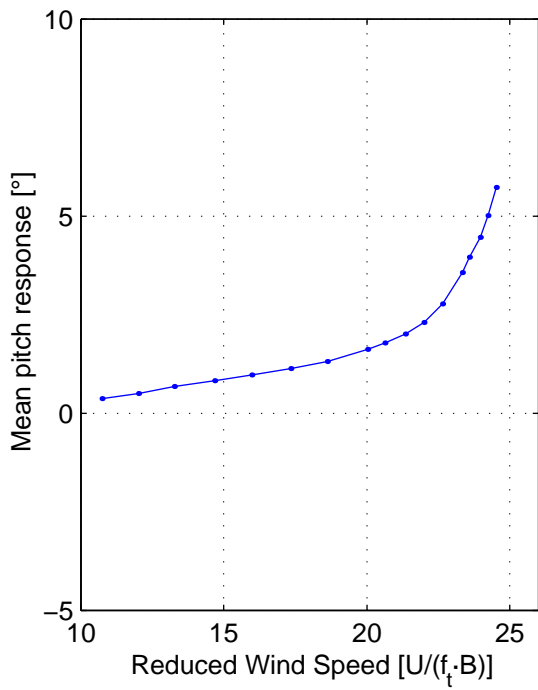
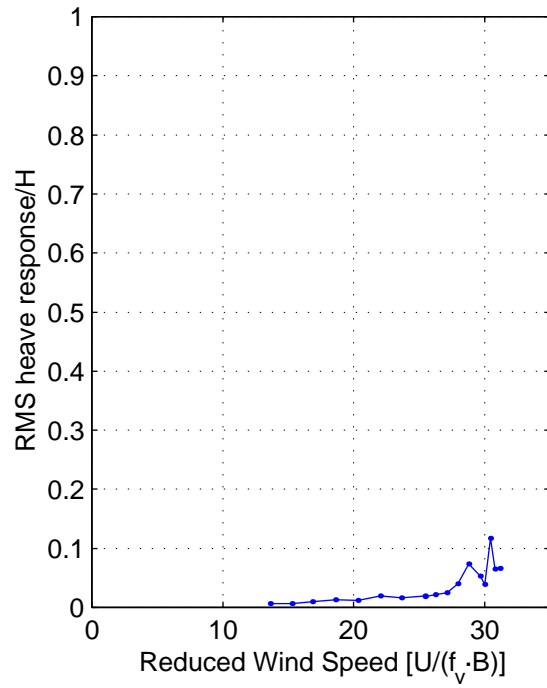
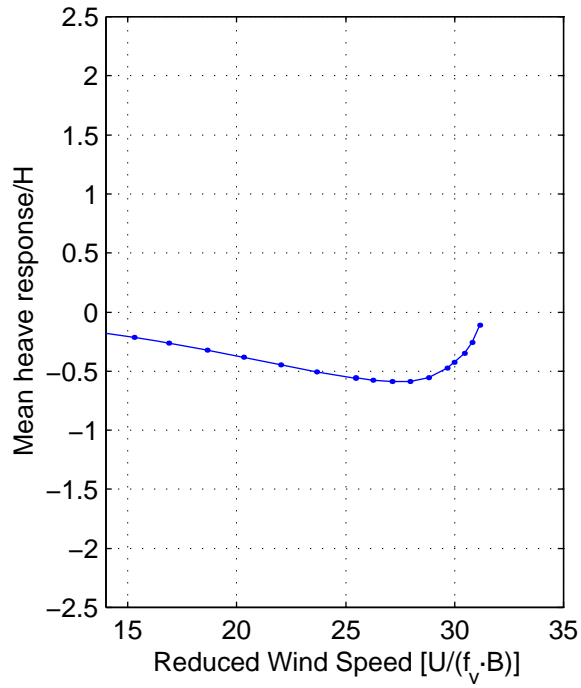
110-25465 Messina Strait Bridge  
 09-Jun-2010 /svl, stab.m  
 Mean and RMS Response

Stability Tests  
 Configuration C4  
 Smooth flow,  $\alpha = 0^\circ$



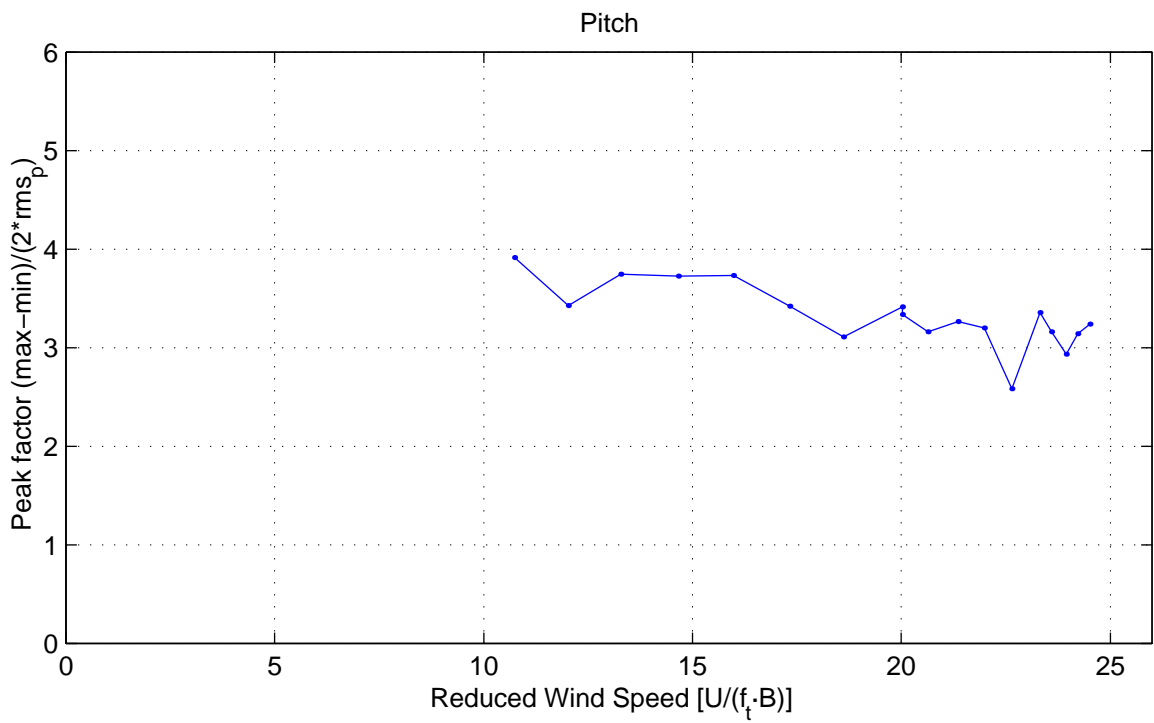
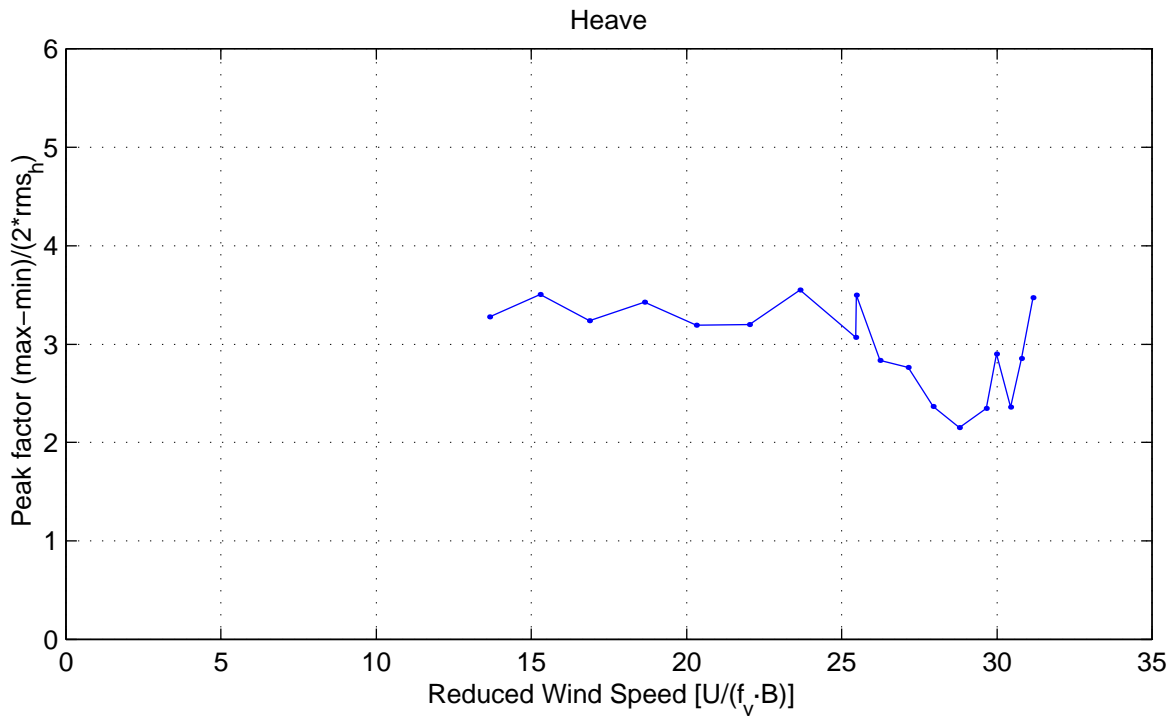
**110-25465 Messina Strait Bridge**  
 09-Jun-2010 /svl, stab.m  
 Peak factors

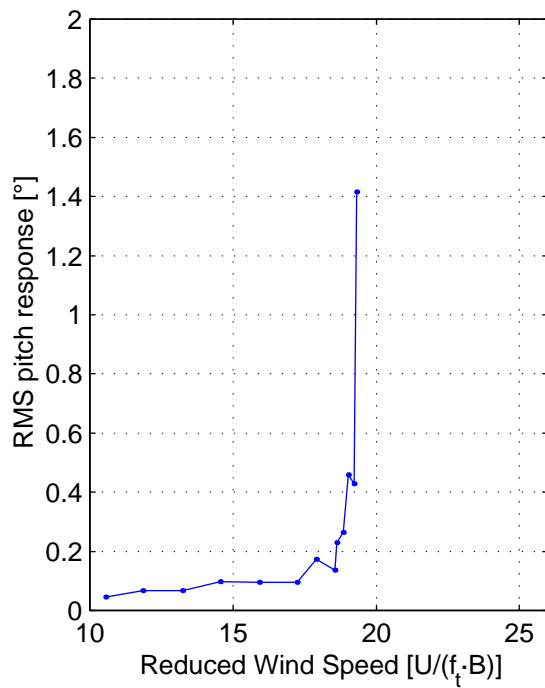
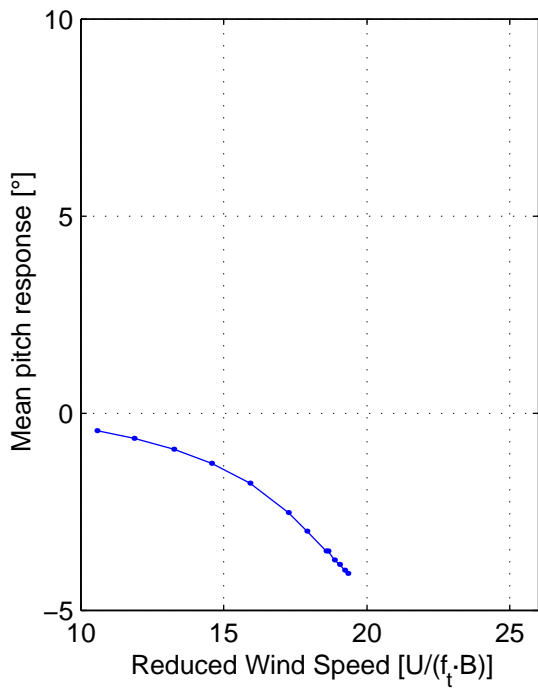
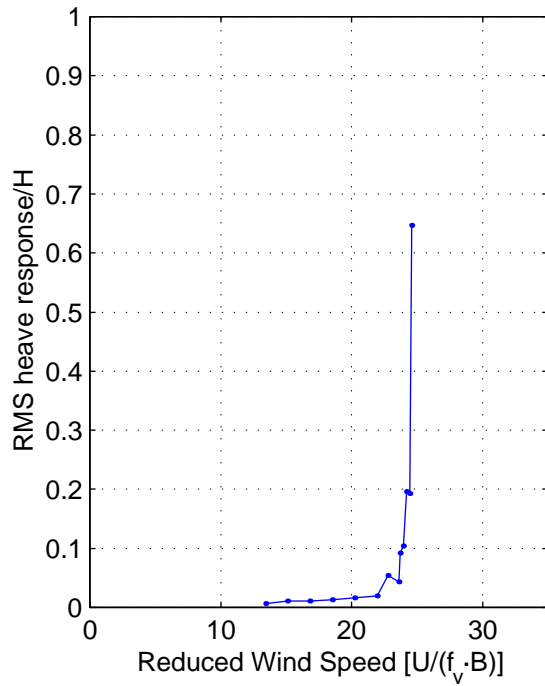
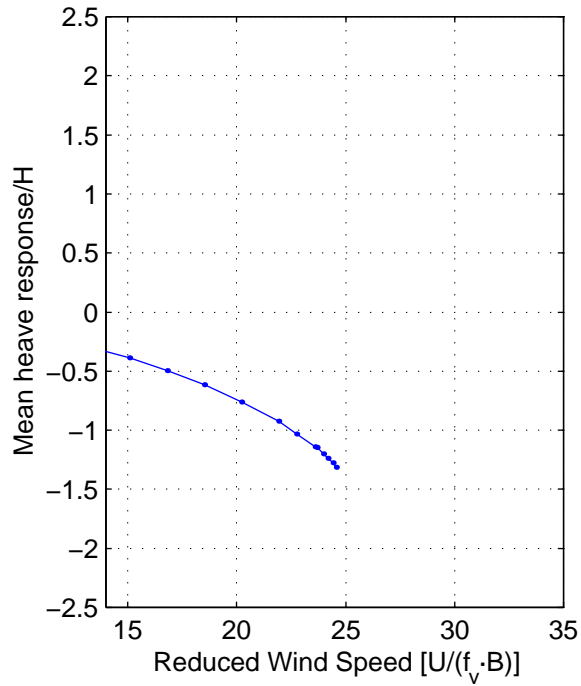
Stability Tests  
 Configuration C4  
 Smooth flow, α = 0°



110-25465 Messina Strait Bridge  
 09-Jun-2010 /svl, stab.m  
 Mean and RMS Response

Stability Tests  
 Configuration C5  
 Smooth flow,  $\alpha = 0^\circ$

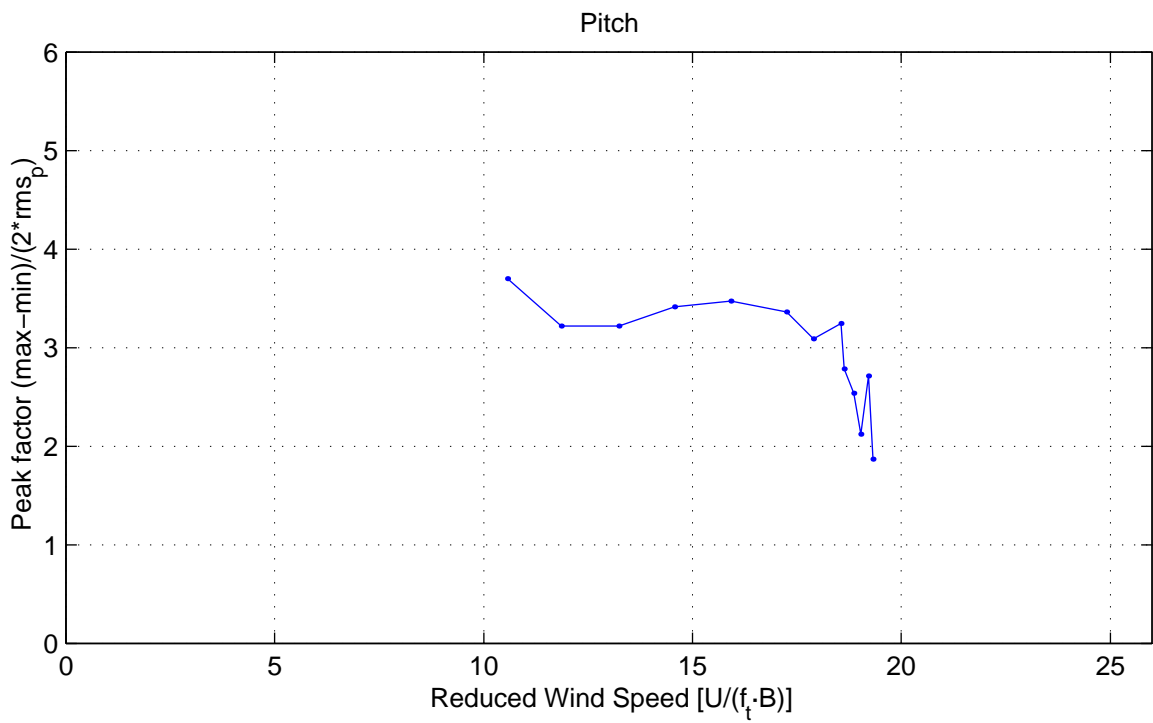
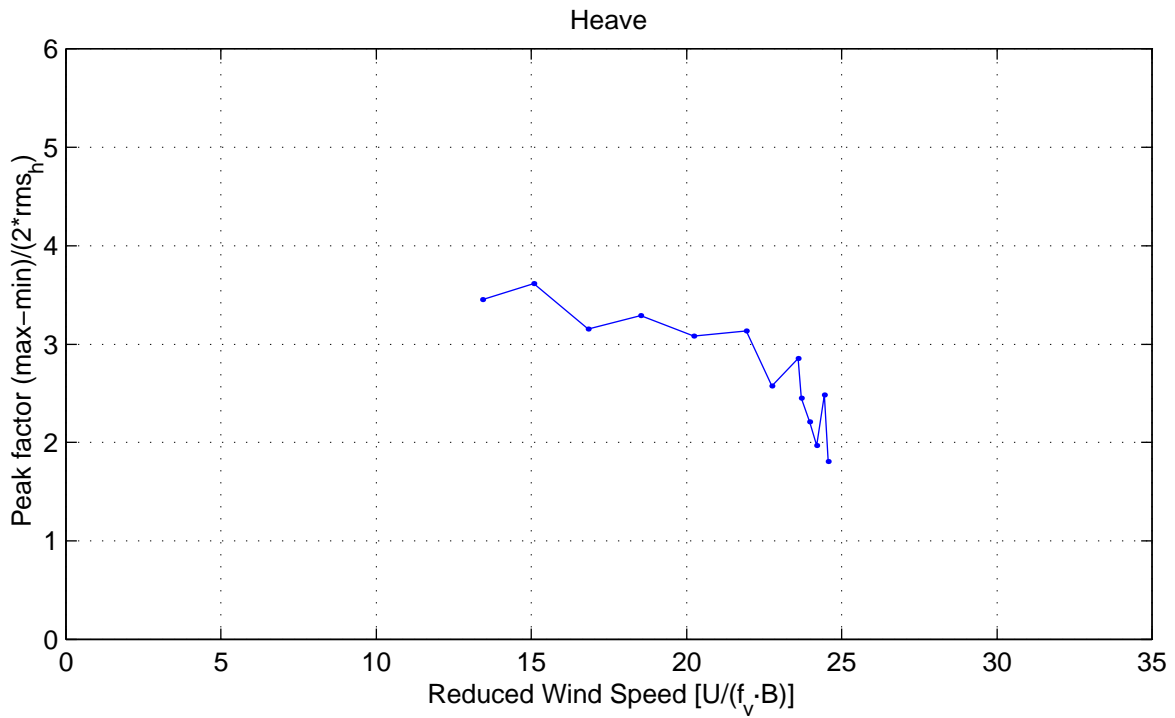




110-25465 Messina Strait Bridge  
 09-Jun-2010 /svl, stab.m  
 Mean and RMS Response

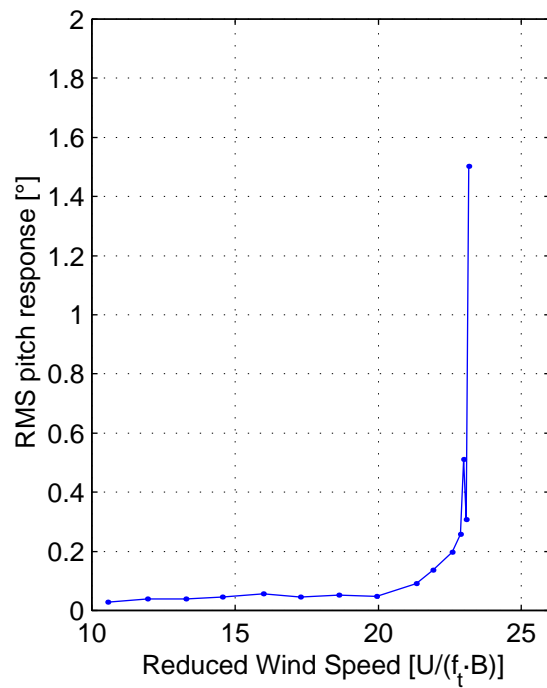
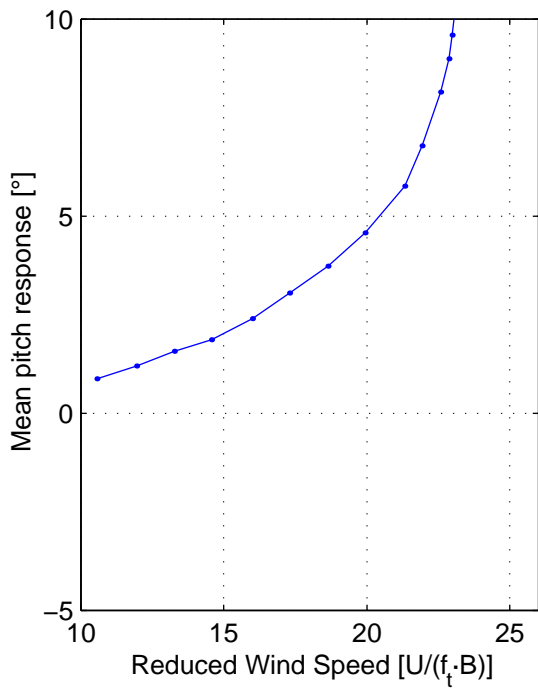
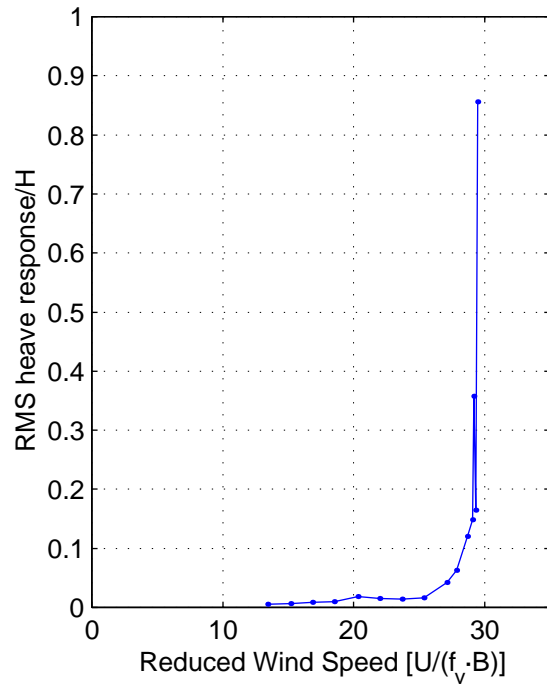
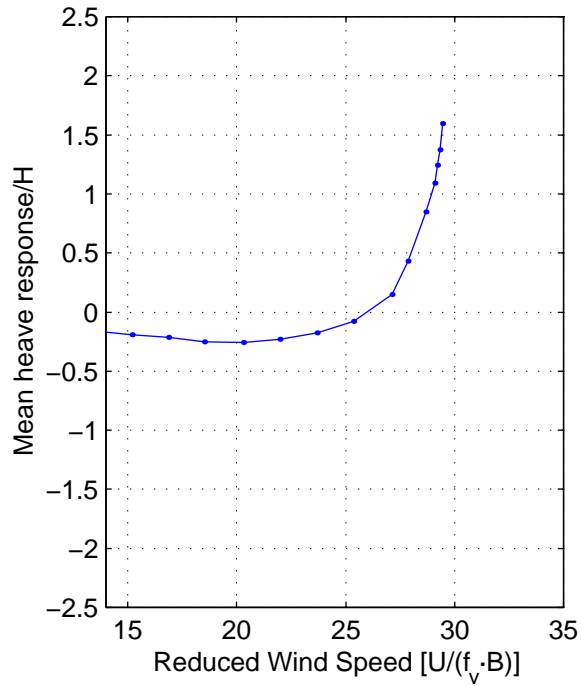
Stability Tests  
 Configuration C6  
 Smooth flow, α = 0°





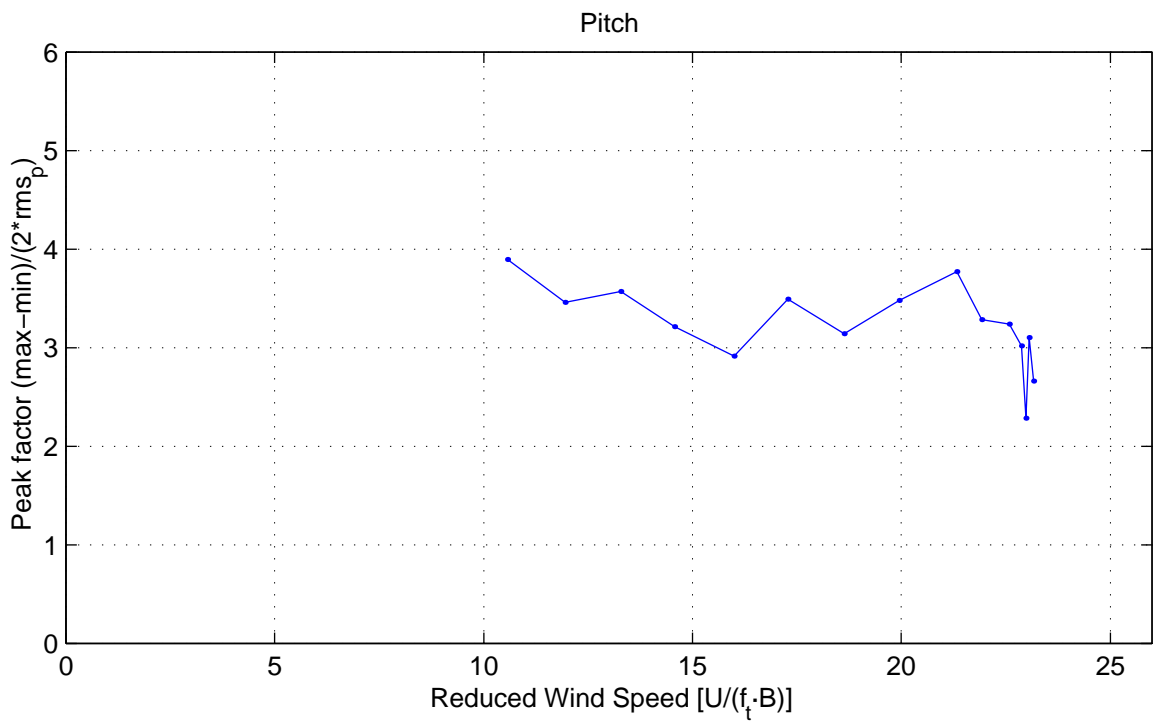
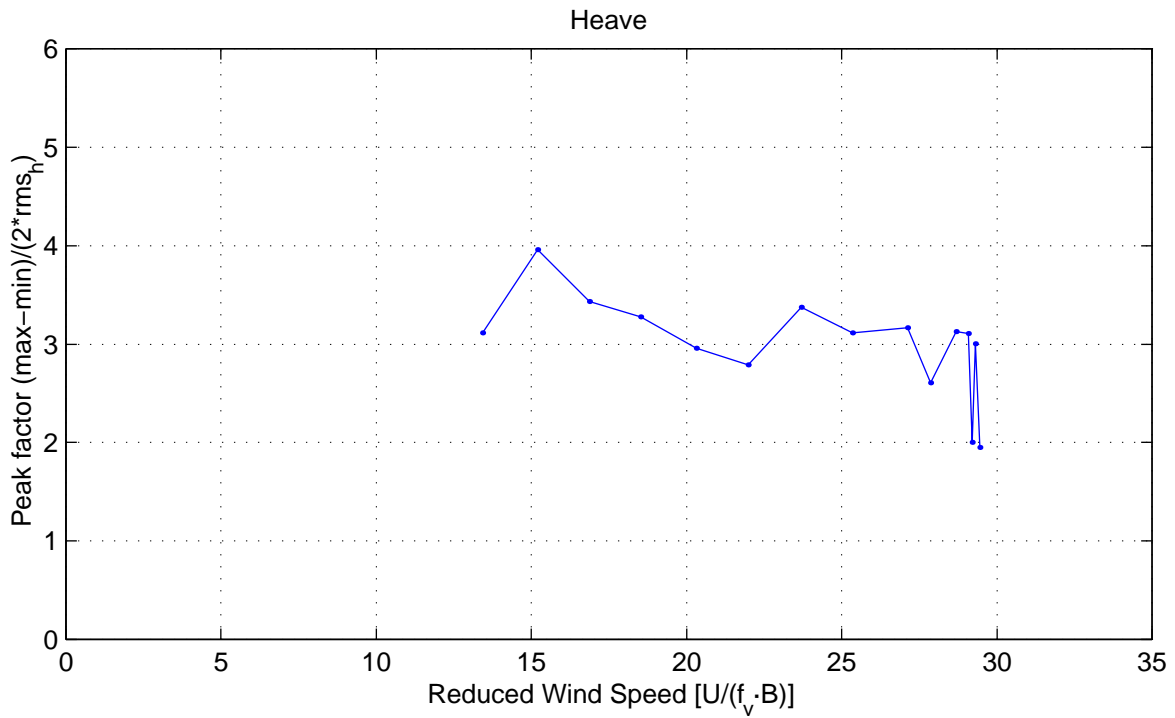
**110-25465 Messina Strait Bridge**  
 09-Jun-2010 /svl, stab.m  
 Peak factors

Stability Tests  
 Configuration C6  
 Smooth flow,  $\alpha = 0^\circ$



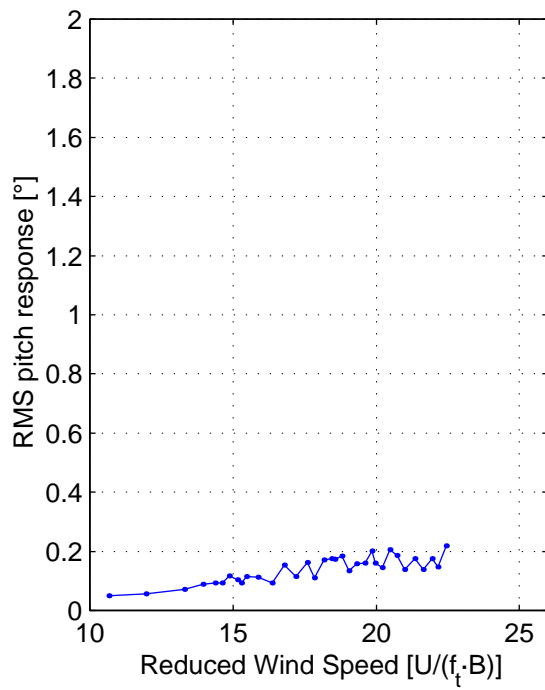
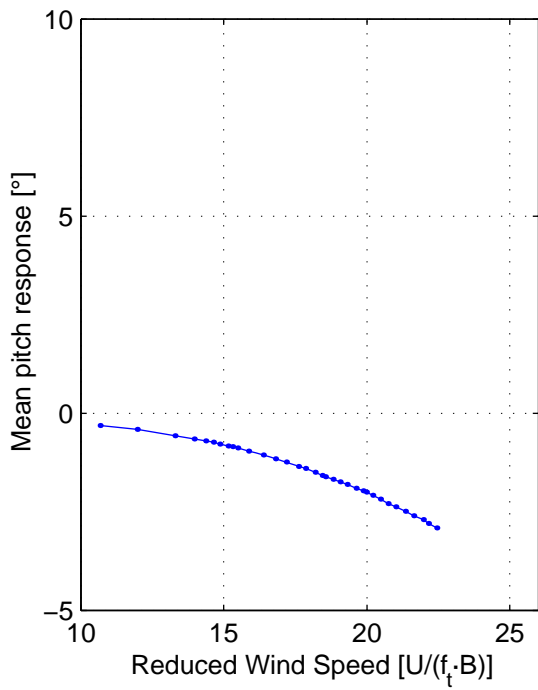
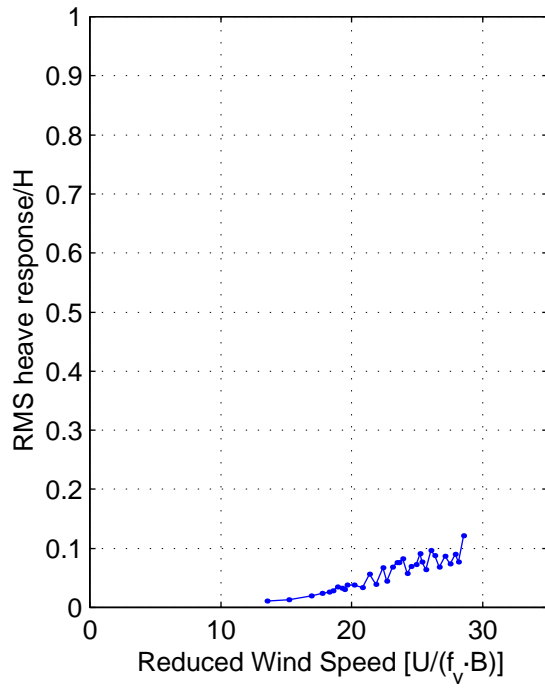
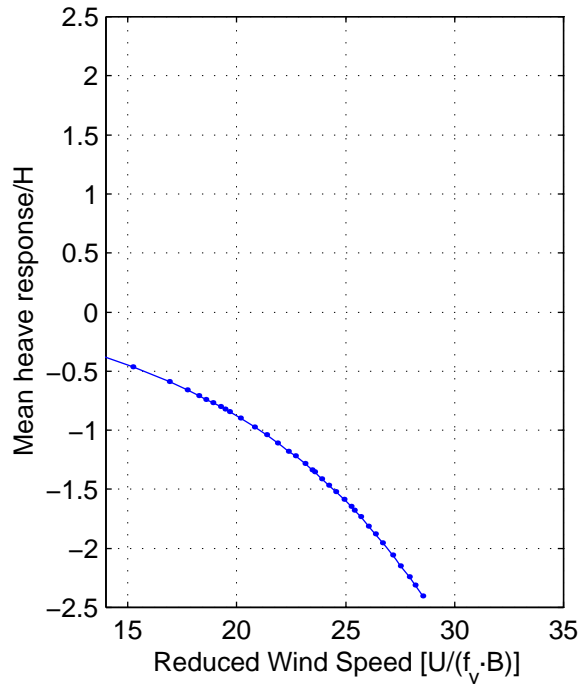
110-25465 Messina Strait Bridge  
 09-Jun-2010 /svl, stab.m  
 Mean and RMS Response

Stability Tests  
 Configuration C7  
 Smooth flow,  $\alpha = 0^\circ$



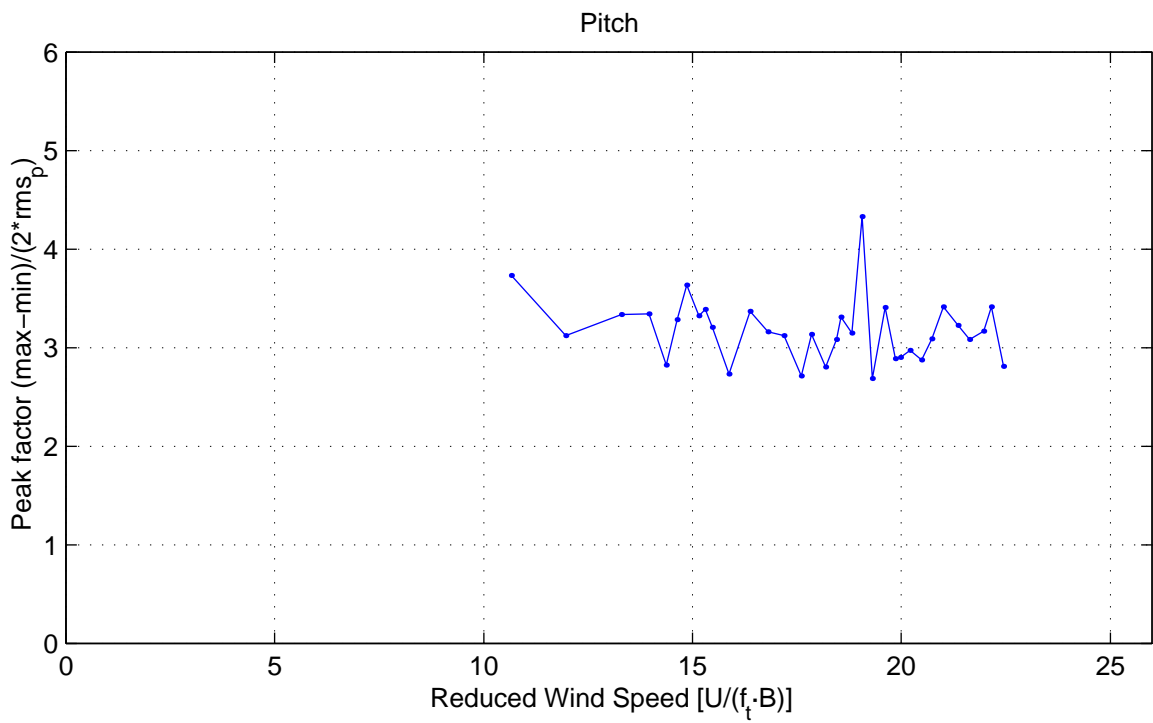
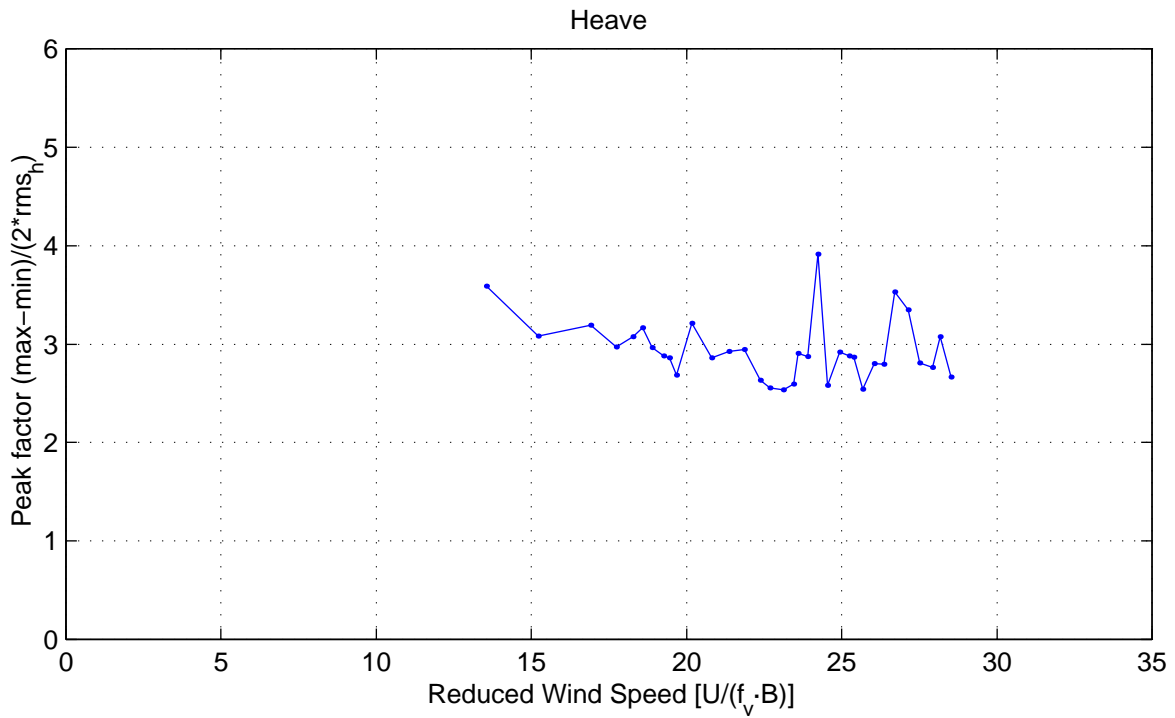
**110-25465 Messina Strait Bridge**  
 09-Jun-2010 /svl, stab.m  
 Peak factors

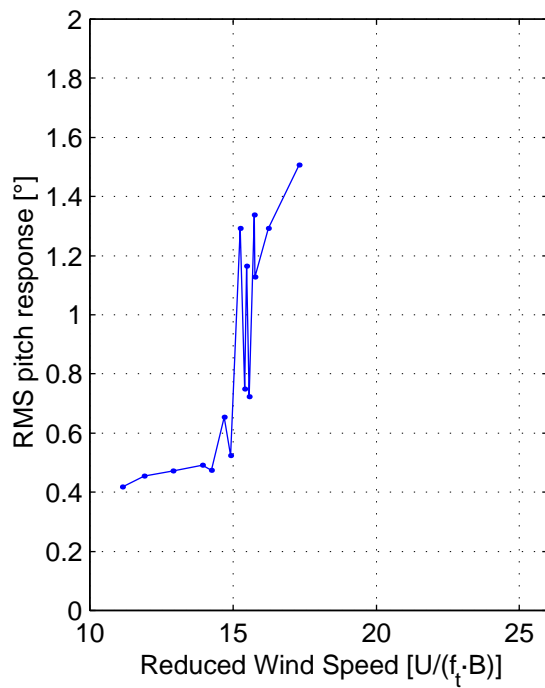
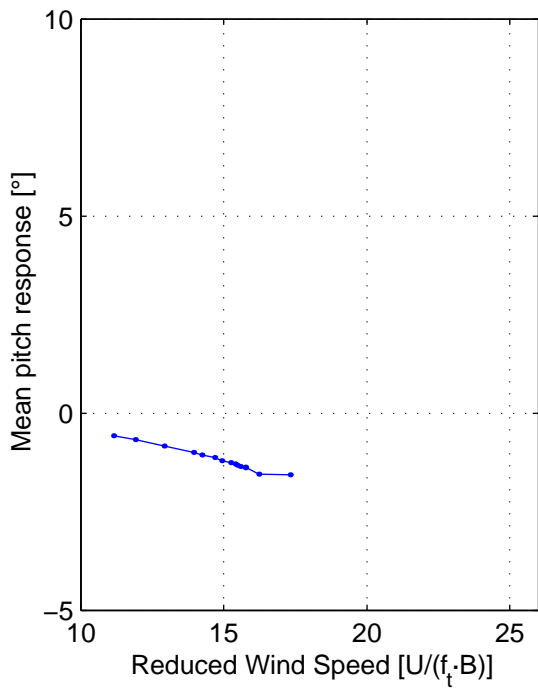
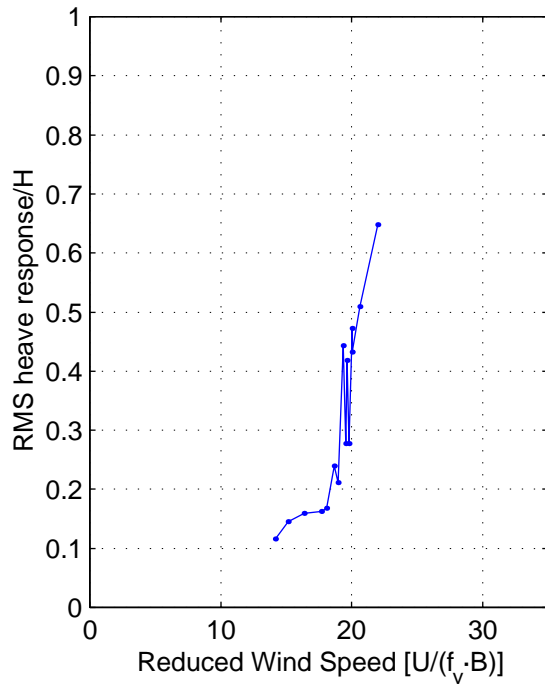
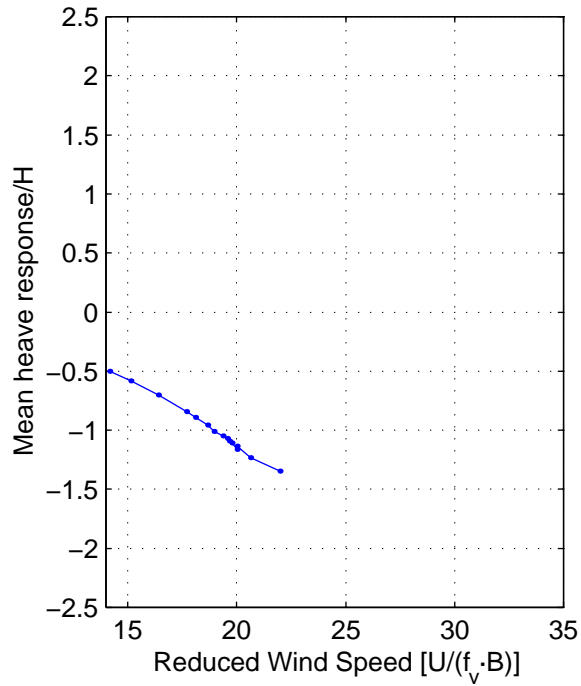
Stability Tests  
 Configuration C7  
 Smooth flow,  $\alpha = 0^\circ$



110-25465 Messina Strait Bridge  
 09-Jun-2010 /svl, stab.m  
 Mean and RMS Response

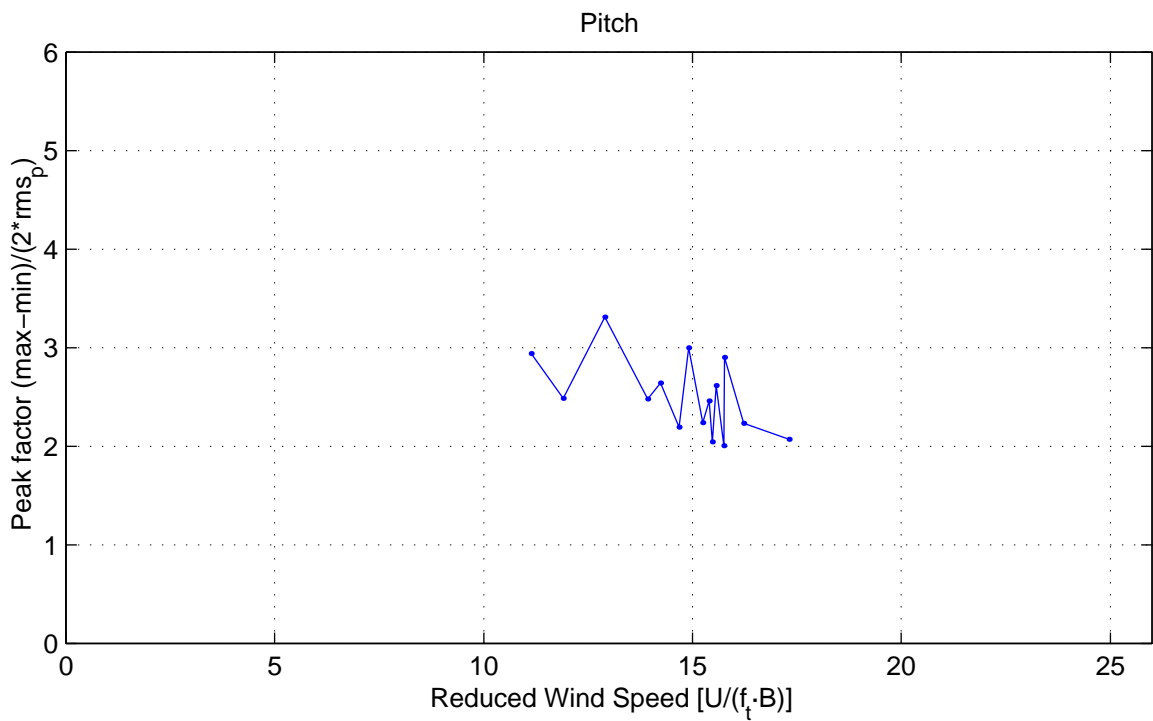
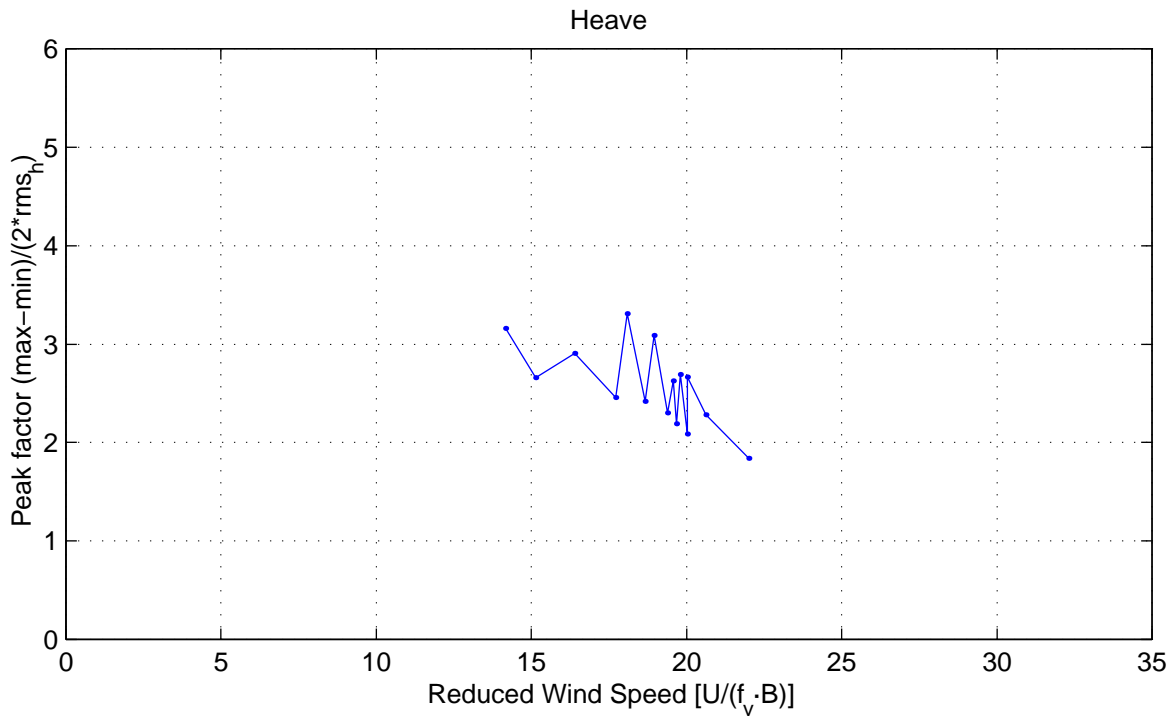
Stability Tests  
 Configuration C5  
 Smooth flow,  $\alpha = -4^\circ$





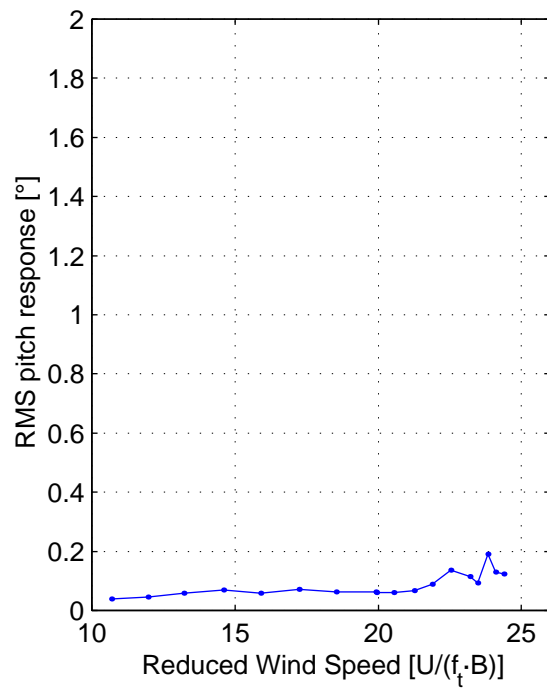
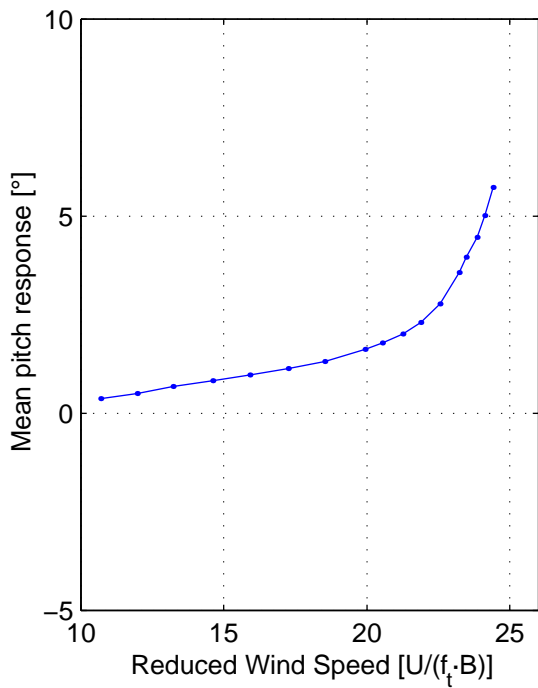
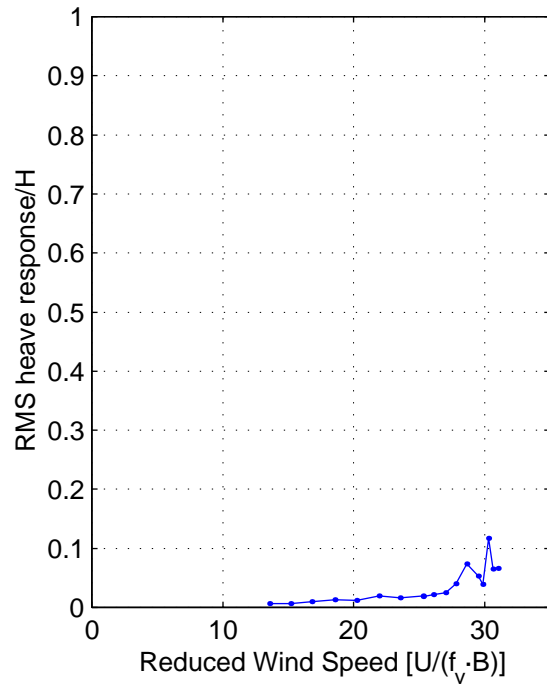
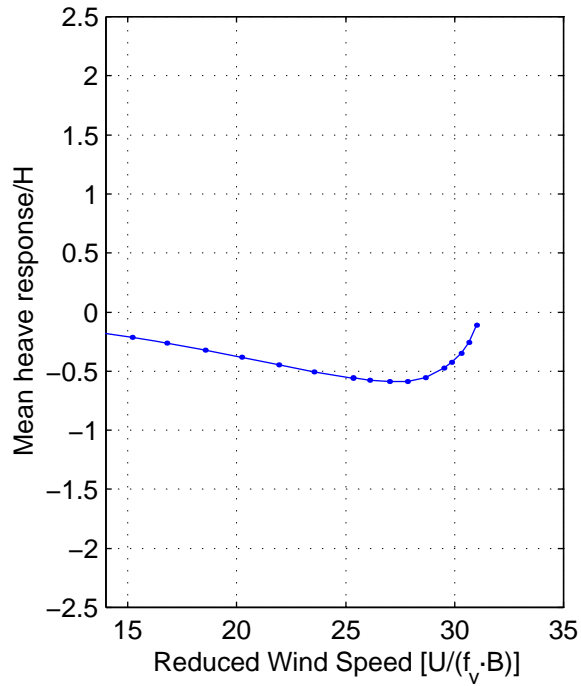
110-25465 Messina Strait Bridge  
 09-Jun-2010 /svl, stab.m  
 Mean and RMS Response

Stability Tests  
 Configuration C5  
 Turbulent flow,  $\alpha = -4^\circ$



**110-25465 Messina Strait Bridge**  
 09-Jun-2010 /svl, stab.m  
 Peak factors

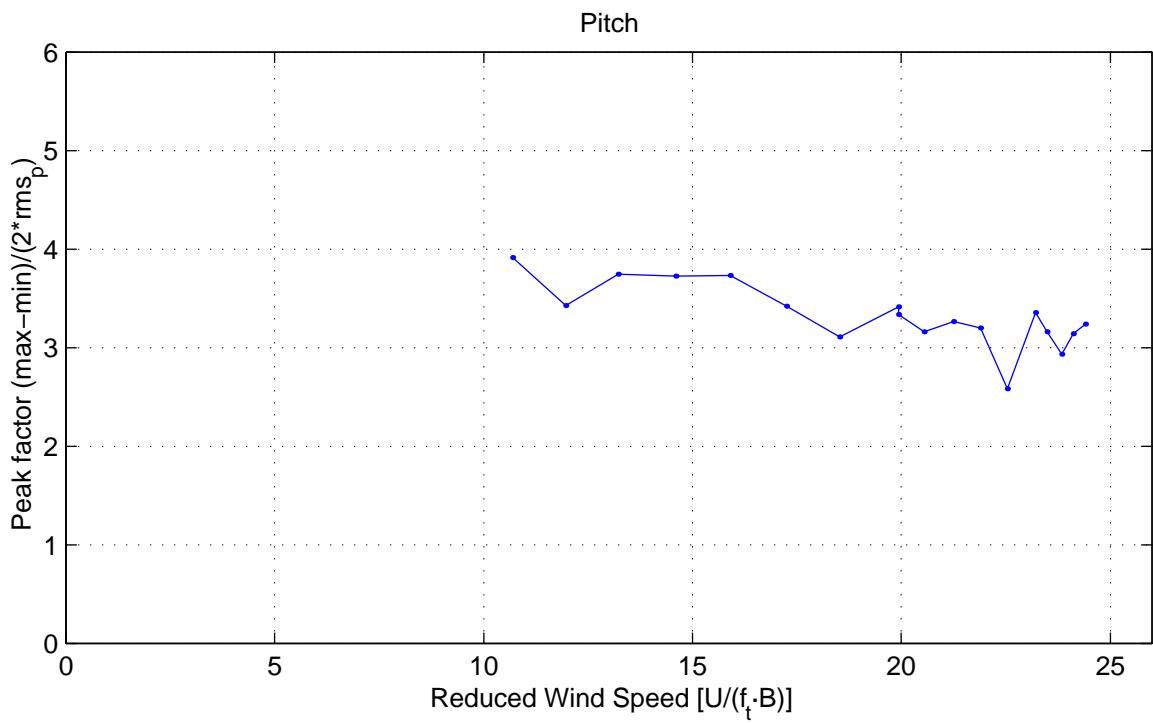
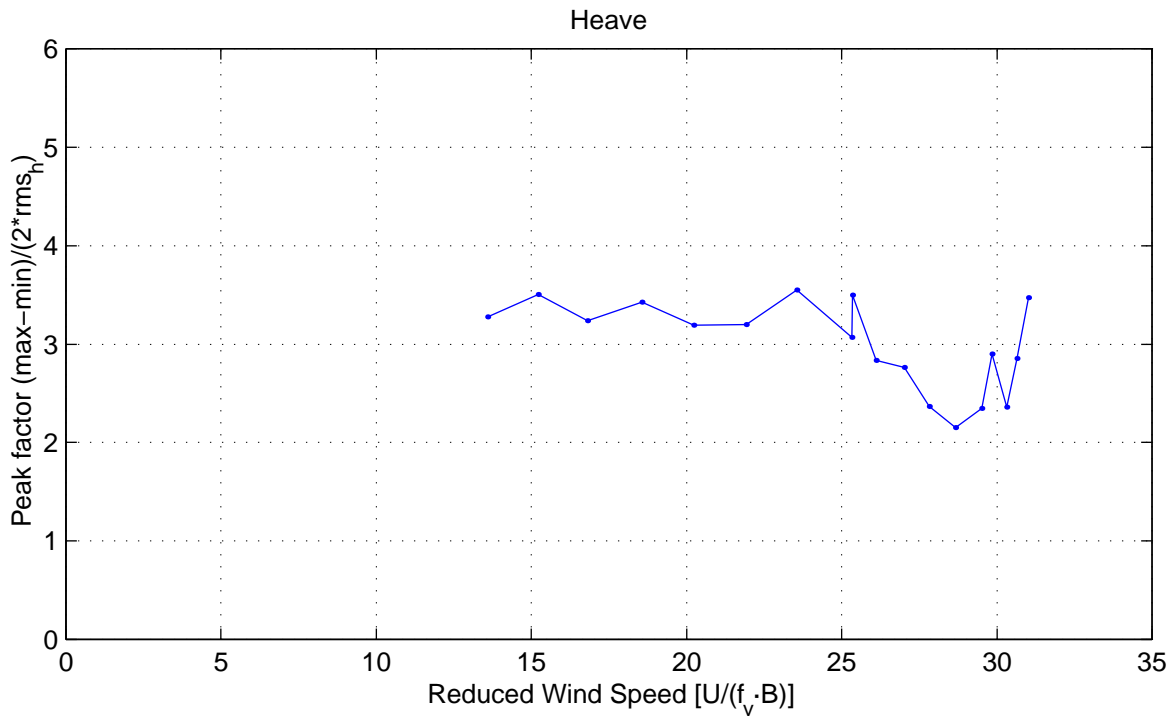
Stability Tests  
 Configuration C5  
 Turbulent flow,  $\alpha = -4^\circ$



110-25465 Messina Strait Bridge  
 09-Jun-2010 /svl, stab.m  
 Mean and RMS Response

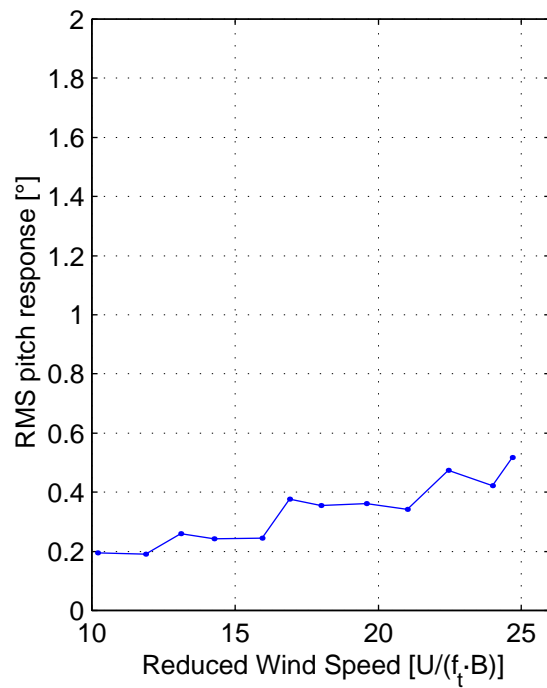
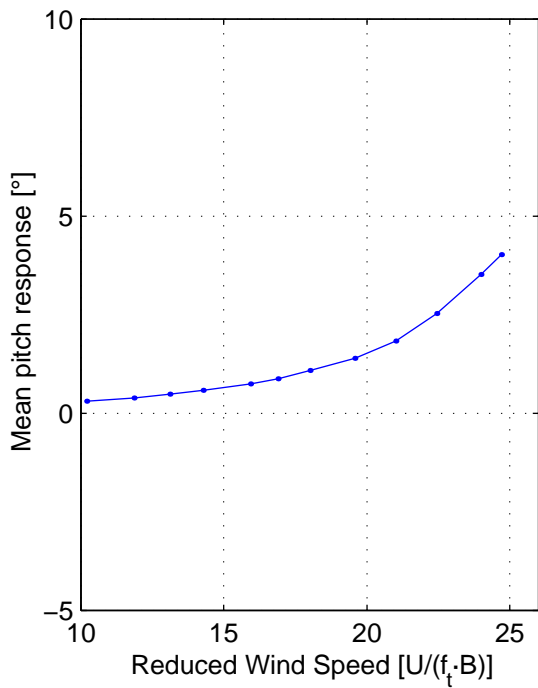
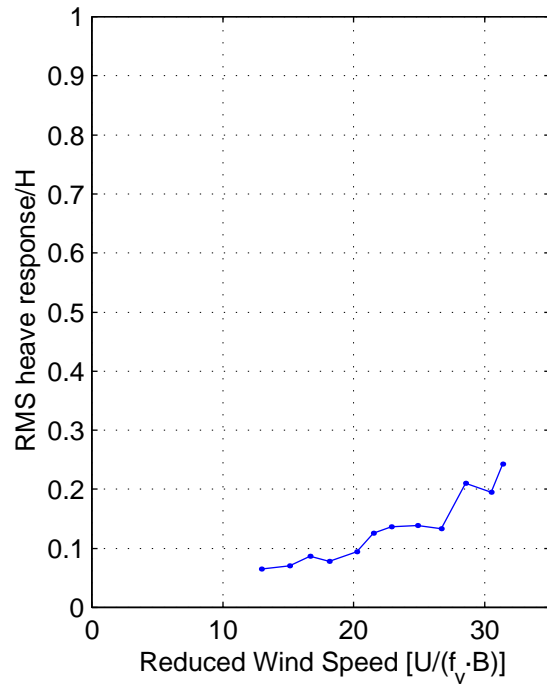
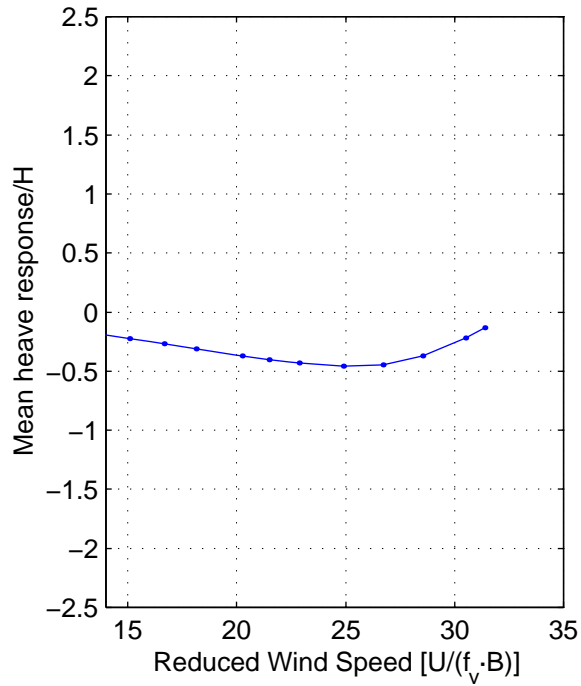
Stability Tests  
 Configuration C5  
 Smooth flow,  $\alpha = 0^\circ$

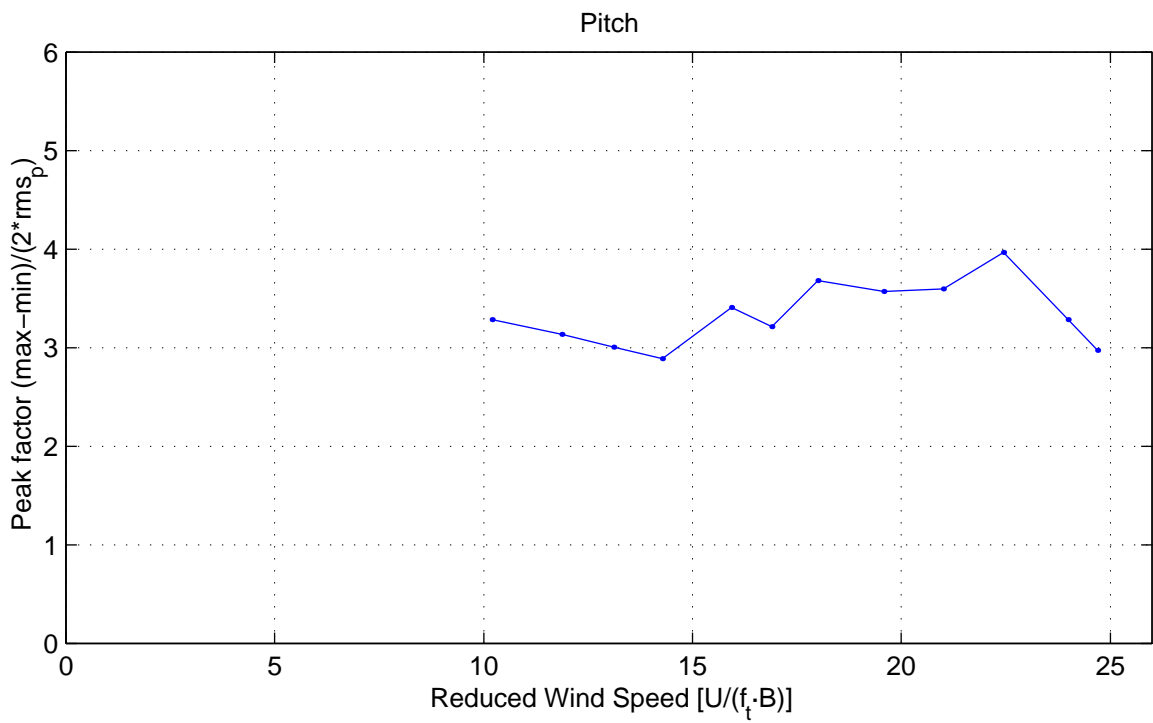
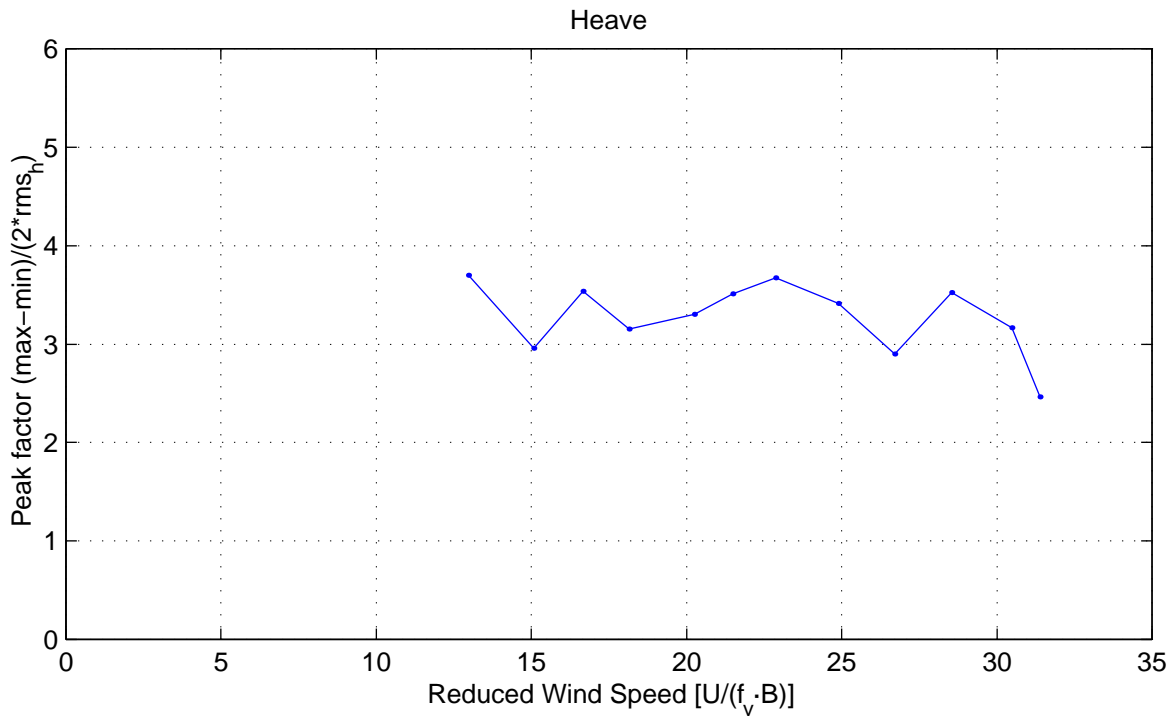




**110-25465 Messina Strait Bridge**  
 09-Jun-2010 /svl, stab.m  
 Peak factors

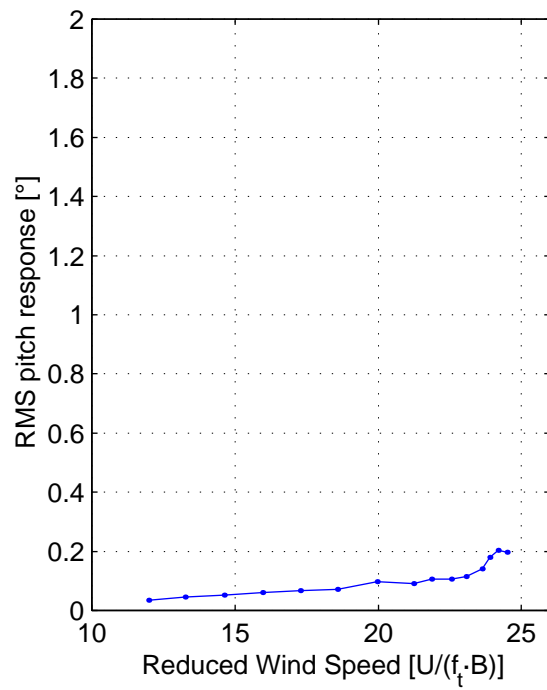
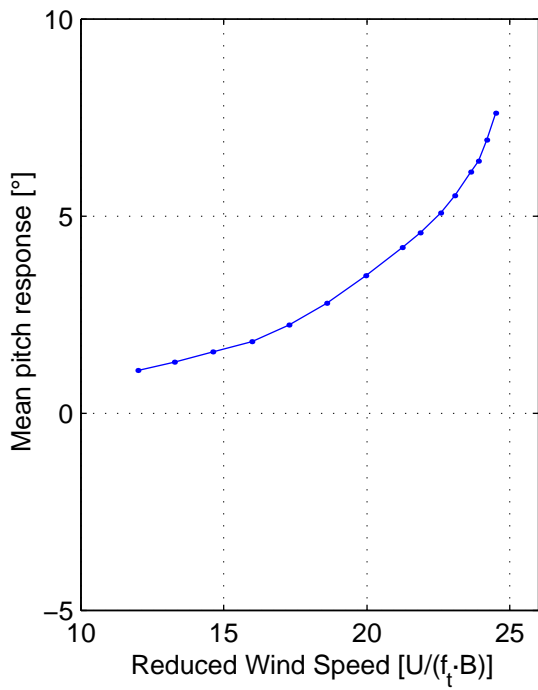
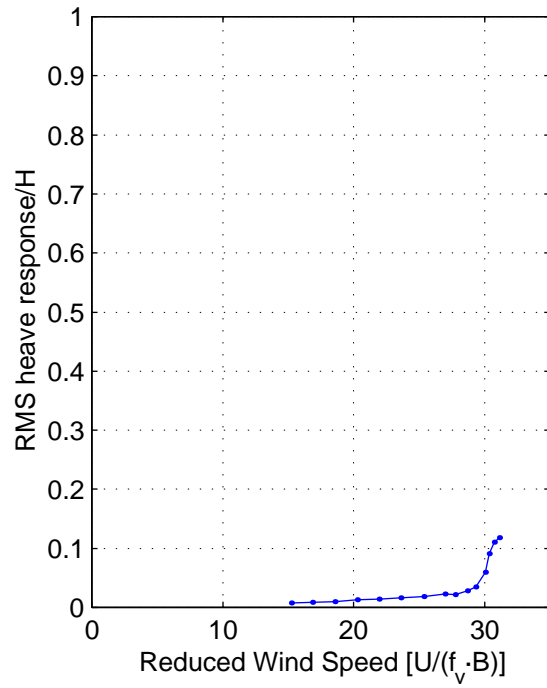
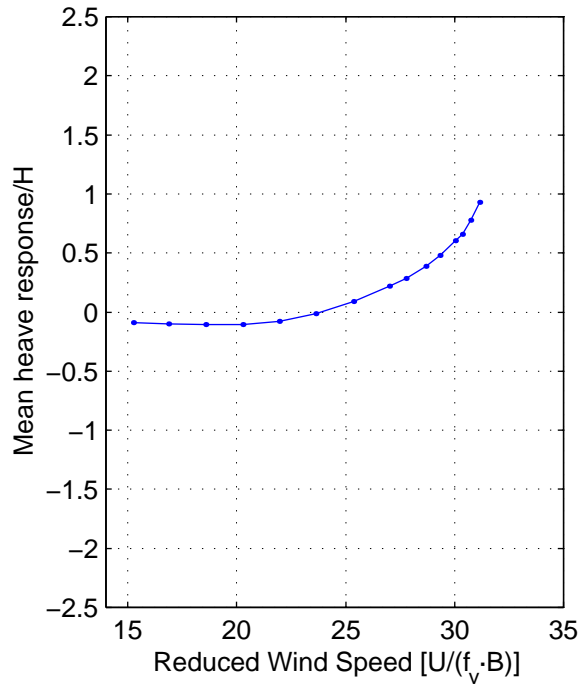
Stability Tests  
 Configuration C5  
 Smooth flow,  $\alpha = 0^\circ$





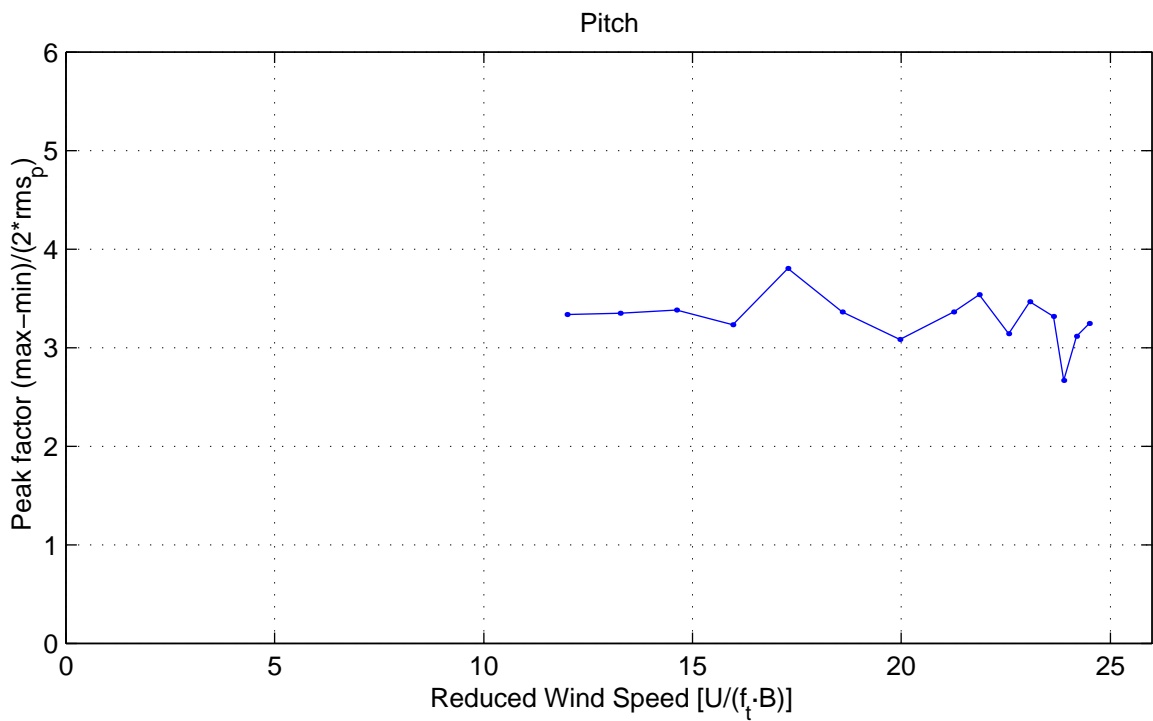
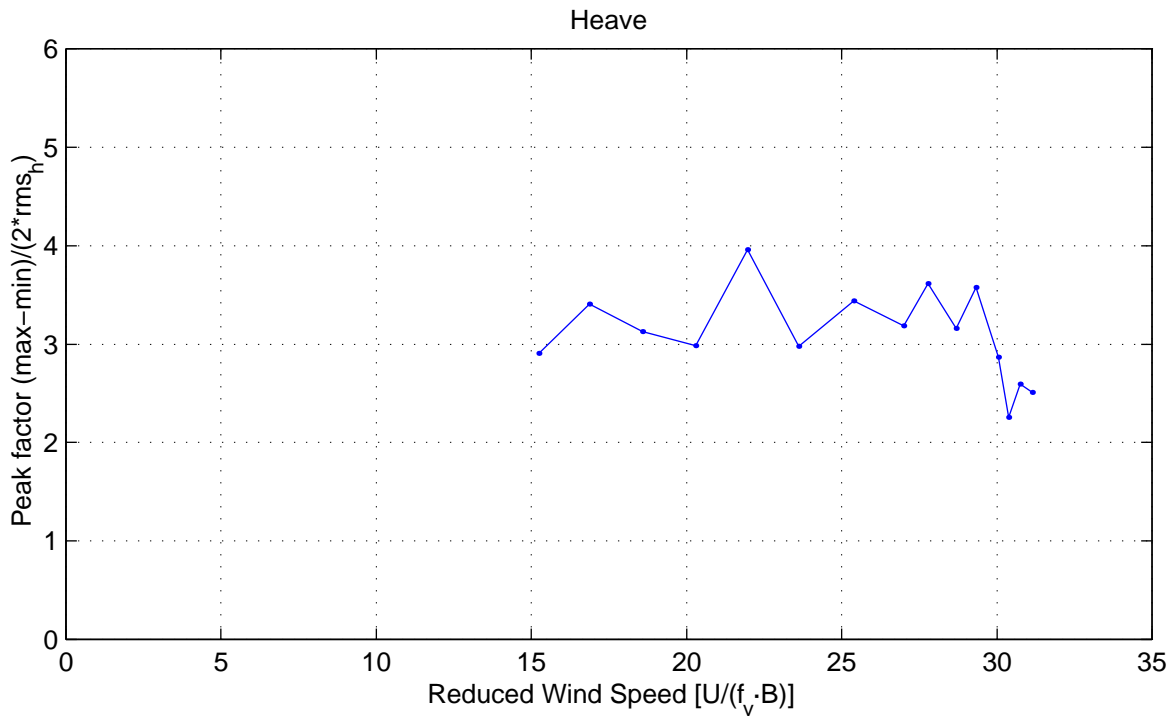
**110-25465 Messina Strait Bridge**  
 09-Jun-2010 /svl, stab.m  
 Peak factors

Stability Tests  
 Configuration C5  
 Turbulent flow,  $\alpha = 0^\circ$



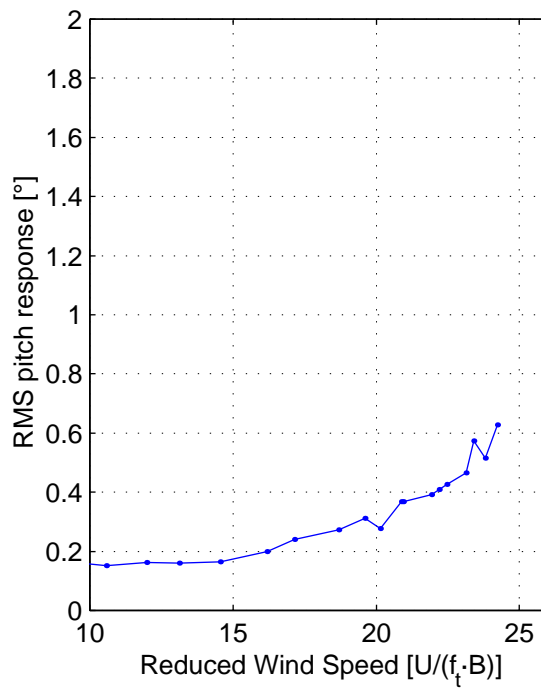
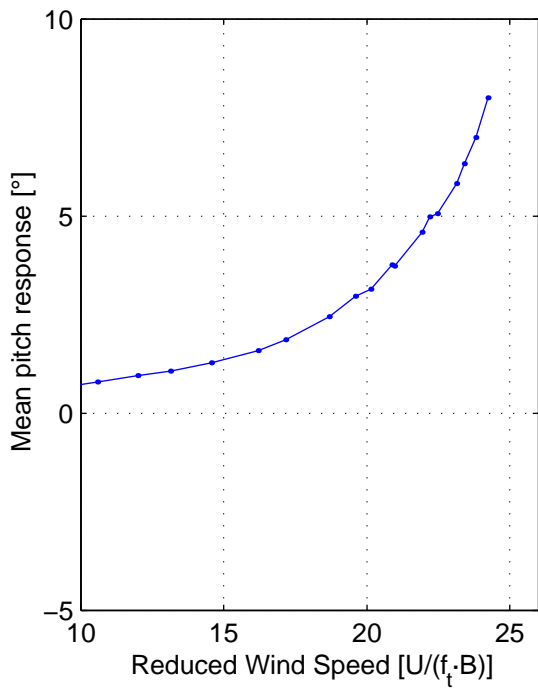
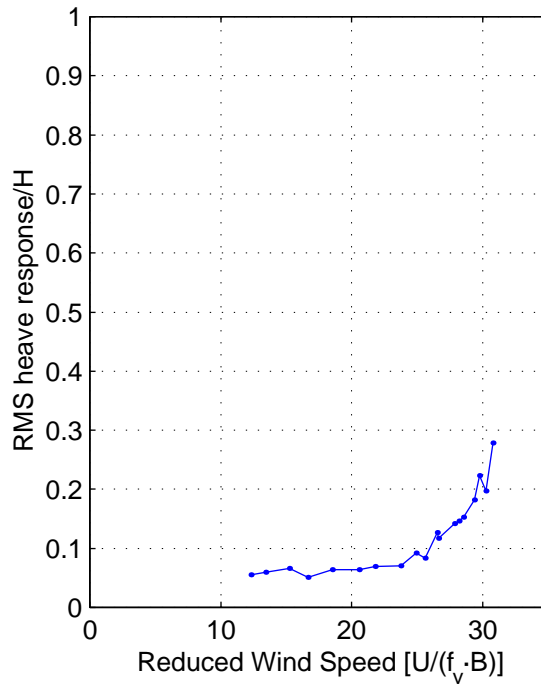
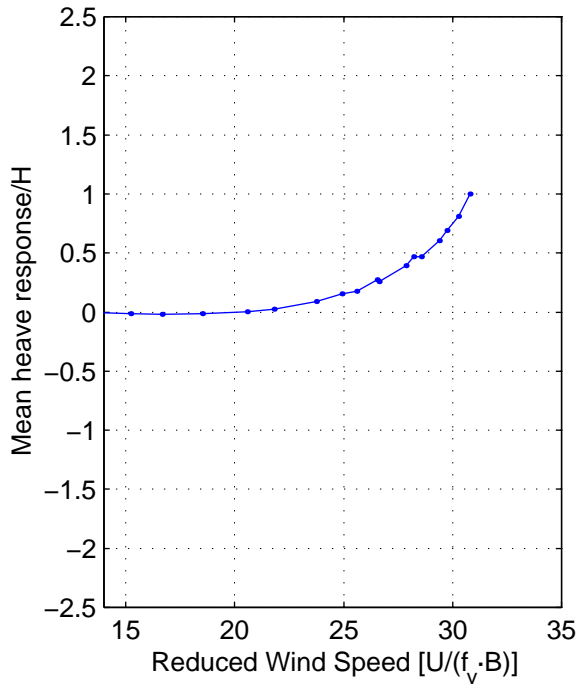
110-25465 Messina Strait Bridge  
 09-Jun-2010 /svl, stab.m  
 Mean and RMS Response

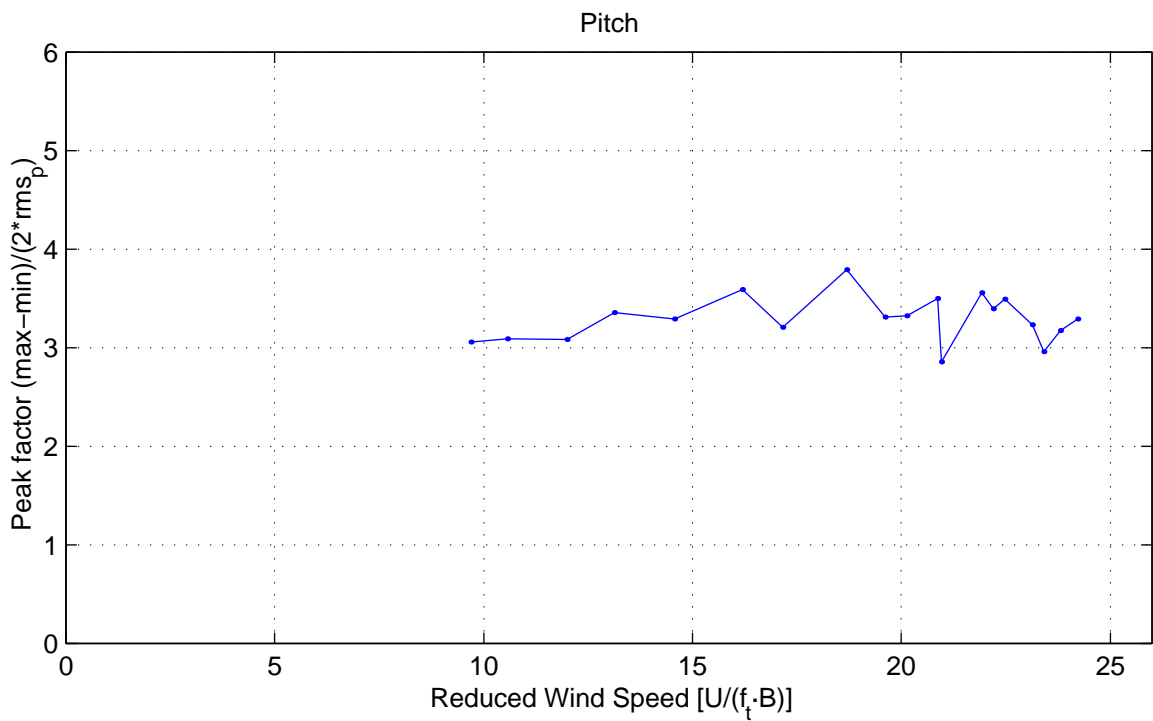
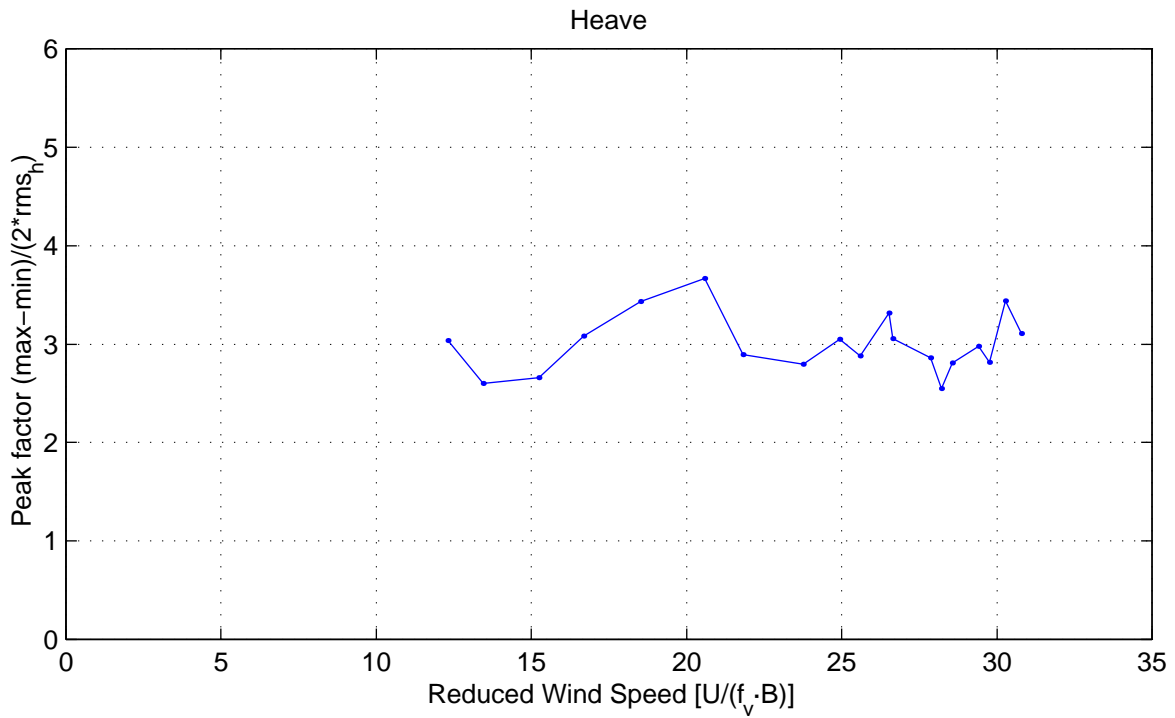
Stability Tests  
 Configuration C5  
 Smooth flow,  $\alpha = +4^\circ$



**110-25465 Messina Strait Bridge**  
 09-Jun-2010 /svl, stab.m  
 Peak factors

Stability Tests  
 Configuration C5  
 Smooth flow, α = +4°

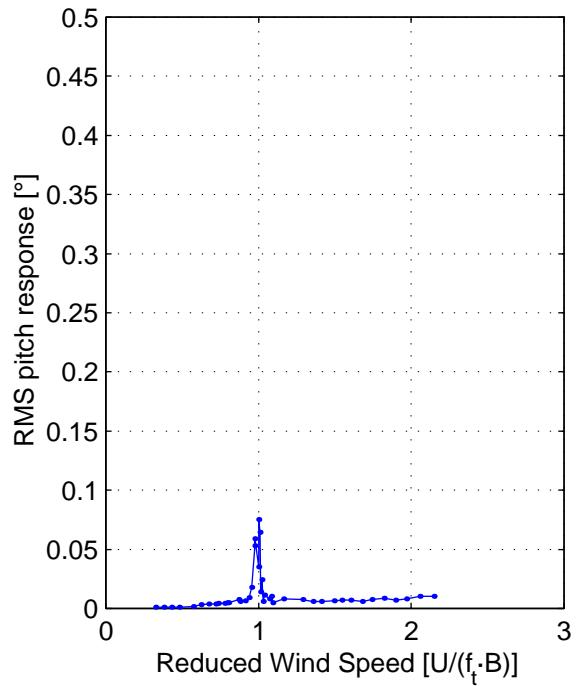
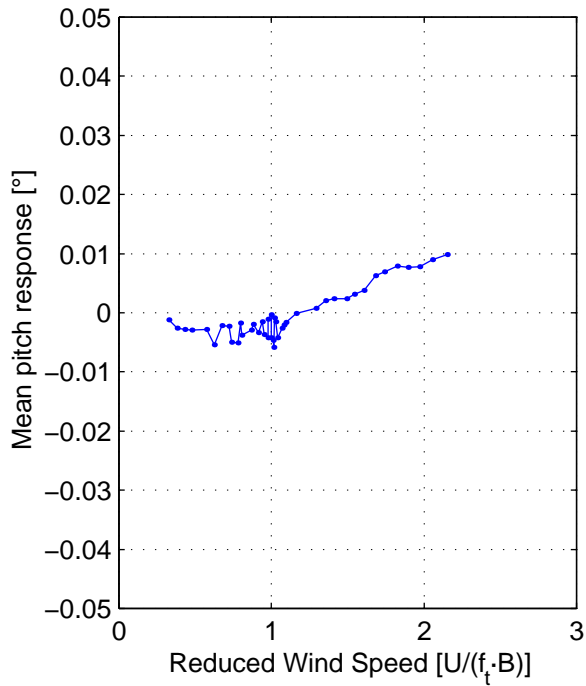
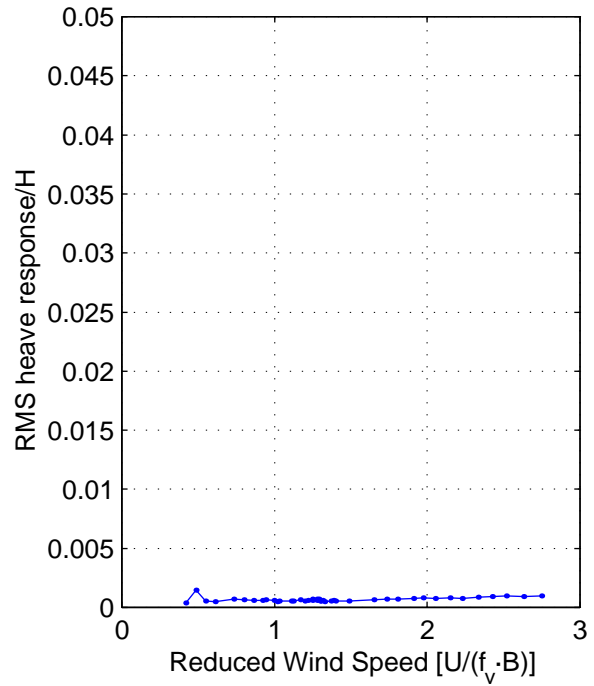
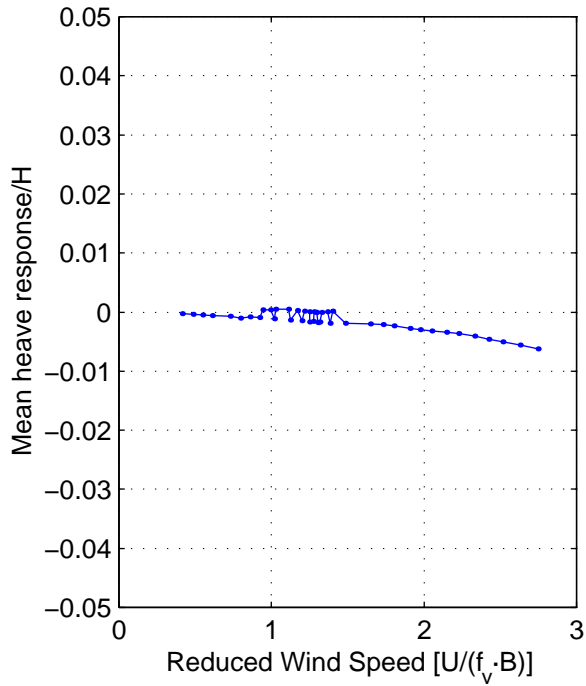




## APPENDIX E

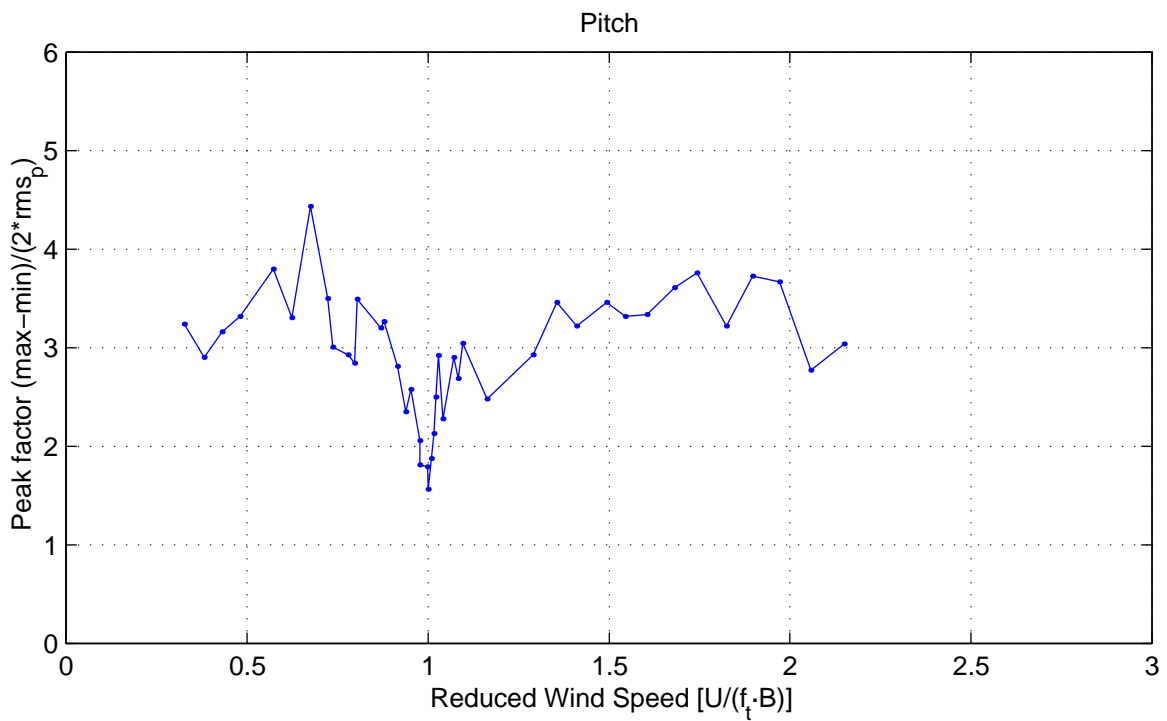
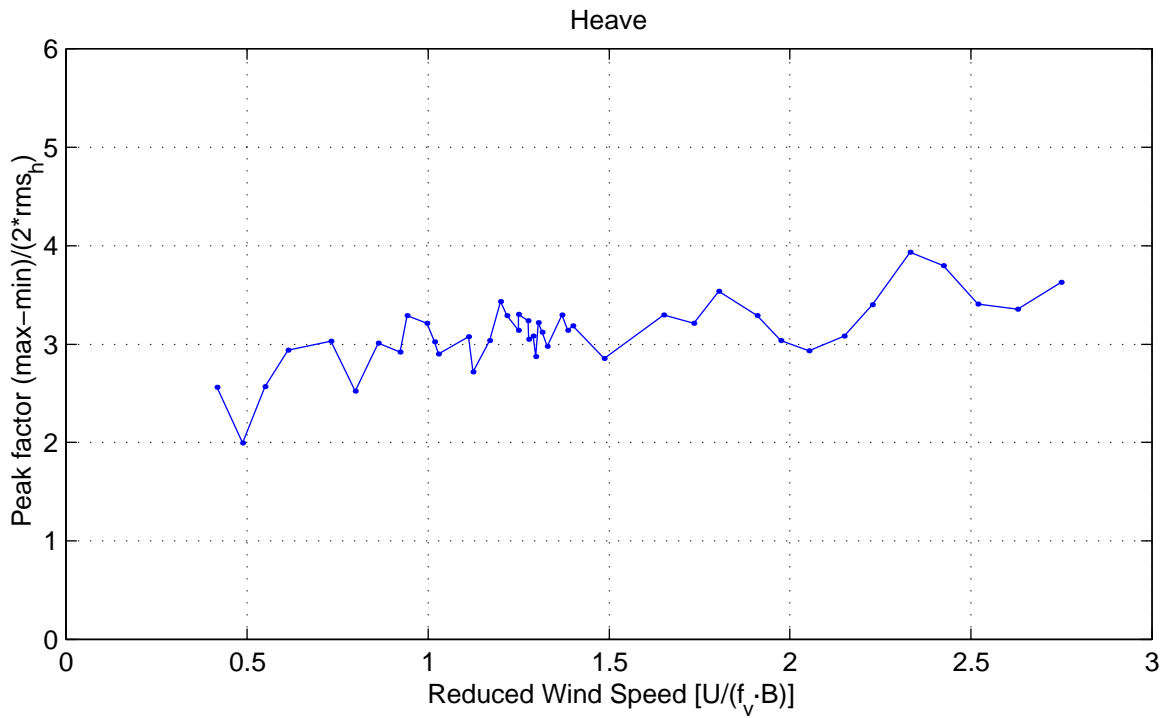
### Vortex Shedding Tests – Response Plots





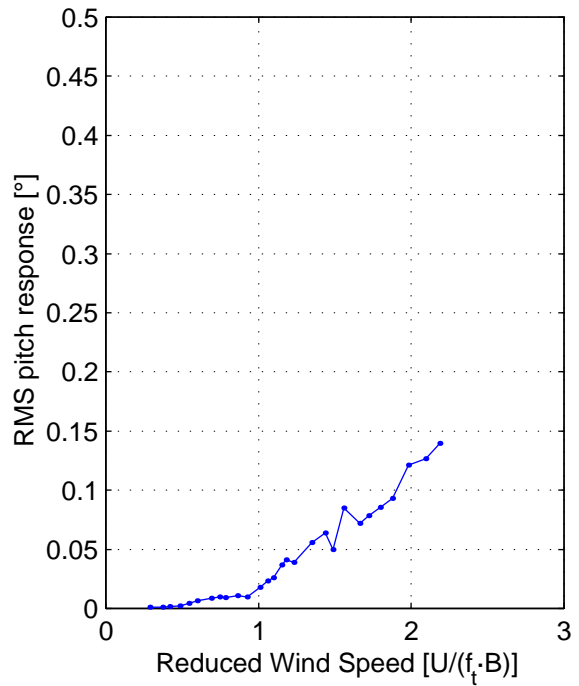
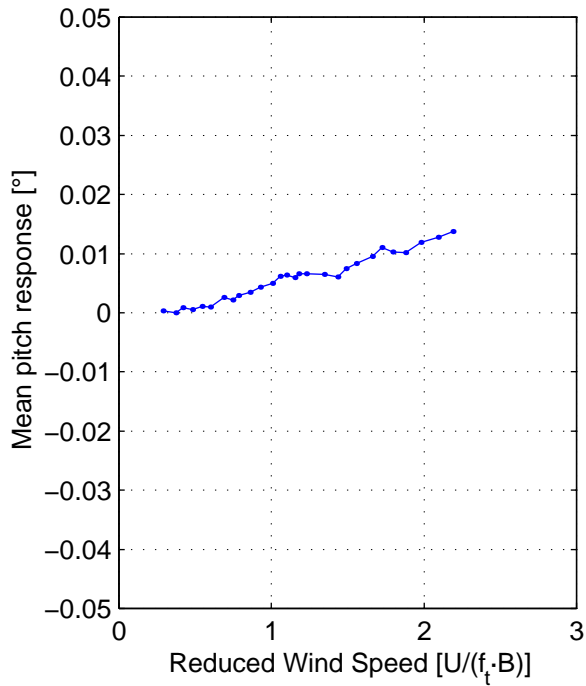
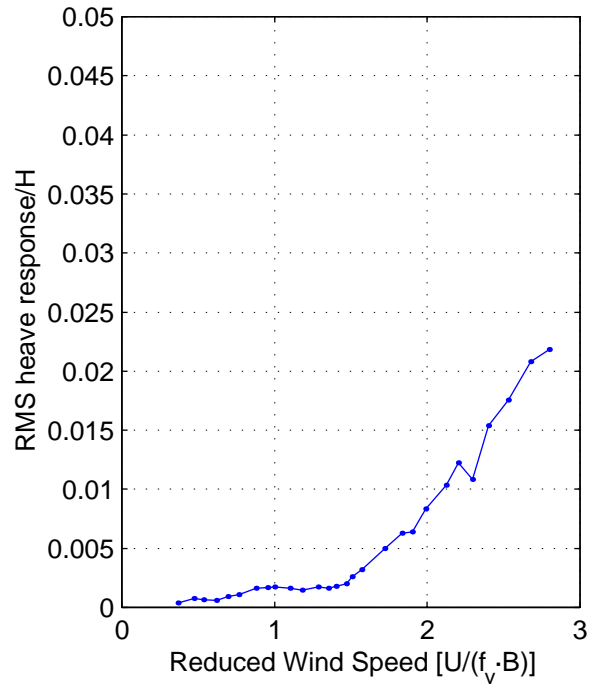
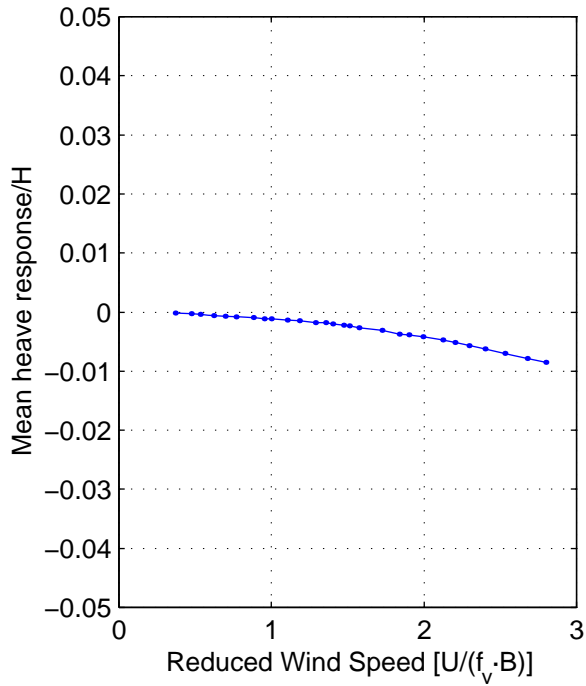
110-25465 Messina Strait Bridge  
 09-Jun-2010 /svl, vortex.m  
 Mean and RMS Response

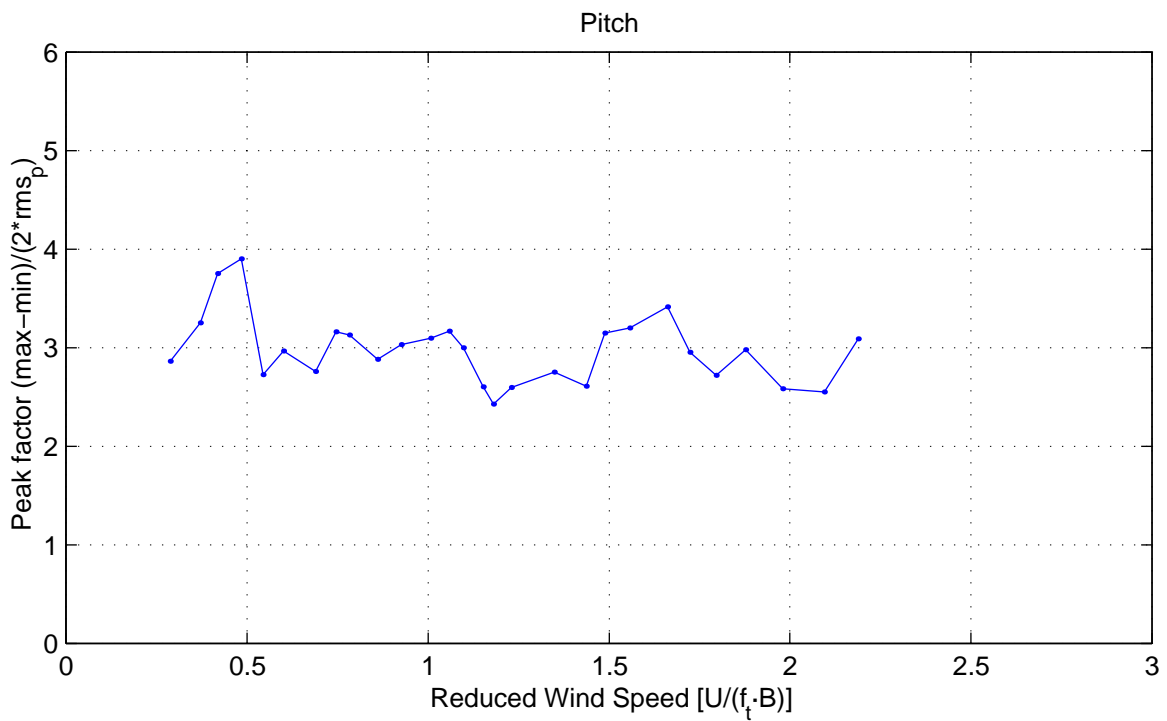
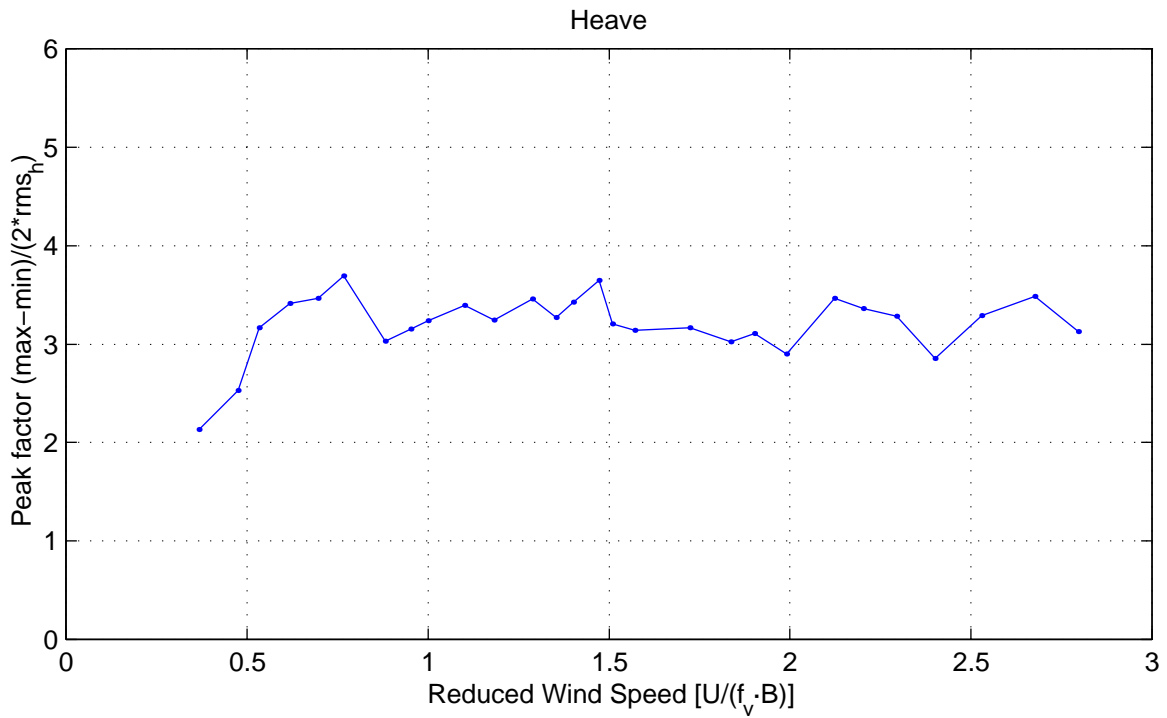
Vortex Tests  
 Configuration C5  
 Smooth flow,  $\alpha = 0^\circ$



110-25465 Messina Strait Bridge  
 09-Jun-2010 /svl, vortex.m  
 Peak factors

Vortex Tests  
 Configuration C5  
 Smooth flow,  $\alpha = 0^\circ$





110-25465 Messina Strait Bridge  
 09-Jun-2010 /svl, vortex.m  
 Peak factors

Vortex Tests  
 Configuration C5  
 Turbulent flow,  $\alpha = 0^\circ$



Copyright © FORCE Technology

---

FORCE Technology  
Division for Maritime Industry  
Hjortekærvej 99  
2800 Kgs. Lyngby, Denmark  
Tel. +45 72 15 77 00  
Fax +45 72 15 77 01  
force@force.dk  
www.force.dk

FORCE Technology  
Headquarters  
Park Allé 345  
2605 Brøndby, Denmark  
Tel. +45 43 26 70 00  
Fax +45 43 26 70 11  
force@force.dk  
www.force.dk

